Extracellular space diffusion parameters and metabolism in the rat somatosensory cortex during recovery from transient global ischemia and hypoxia

Dr.med. Norbert Zoremba

PhD-Thesis

Prague 2009

Content

1. Introduction:

The extracellular space (ECS) represents the microenvironment of nerve cells and serves as an important communication channel (Nicholson, 1979; Syková, 1992). The diffusion of neuroactive substances through the ECS of the CNS is the underlying mechanism of extrasynaptic or "volume" transmission, which is an important mode of interactions among neurons, axons and glia cells (Fuxe and Agnati, 1991; Angati et. al., 1995; Zoli et al., 1999; Nicholson and Syková, 1998; Syková, 2004, Syková and Nicholson, 2008). Besides extrasynaptic transmission, the ECS of the brain enables stable electrical signalling by providing a reservoir of extracellular ions sufficient to maintain resting, synaptic and action potentials and forms a conduit for essential substances to move between blood vessels and cells by diffusion (Syková and Nicholson, 2008).

1.1. Diffusion in the extracellular space

The extracellular space of the brain is comparable to a porous medium containing an interstitial fluid. Many experimental studies have established the labyrinthine nature of the ECS, and substances that do not cross cellular boundaries follow defined physical rules. Within the ECS, the dominant mechanism of molecular transport is diffusion constrained by the geometry of this compartment (Sykova and Nicholson, 2008). The diffusion of neurotransmitters, substrates and metabolites in the ECS is influenced by the size of the extracellular clefts, the presence of membranes, fine neuronal and glial processes, macromolecules of the extracellular matrix, charged molecules and cellular uptake (Syková et al., 2000; Syková, 2004).

The distribution of substances in the ECS is modified by the loss of molecules through removal across the blood-brain barrier, uptake into cells, or binding to receptors. In contrast to a free medium, diffusion in the ECS can be satisfactorily described by a modified version of Fick´s law, if volume fraction α, tortuosity λ, and non-specific uptake k' are taken into account (Nicholson and Phillips, 1981; Nicholson, 1992).

1.1.1 Extracellular space volume fraction

The extracellular space of the brain has been described as being similar to the water phase within a foam, where the gaseous phase corresponds to the cells of the brain (Kuffler and Potter, 1964; Sykova and Nicholson 2008). The volume fraction is the proportion of the tissue volume occupied by the ECS. It is denoted by α and can be defined as

$$\alpha = V_{ESC}/V_{Total} \qquad (1)$$

where V_{ESC} denotes the extracellular volume and V_{Total} the total volume of the tissue. The values of the extracellular volume fraction α are written as a decimal. In a free medium, such as an aqueous solution or diluted agar gel, the value of α is 1. It is well established that in healthy CNS tissue, the ECS occupies about 20% of the total tissue volume (Nicholson and Phillips, 1981; Lehmenkühler et al., 1993; Sykova, 2007; Syková and Nicholson, 2008), thus the ECS volume fraction α is about 0.20. The concentrations of substances in the ECS are related to the extracellular volume fraction if simple diffusion occurs. If the substances are liquid soluable, or when cells actively transport or

accumulate them, their concentration in the ECS can not be easily calculated because this process is more complex. In these cases, it is more appropriate to refer to the "distribution space" of the substances.

1.1.2. Diffusion hinderances and tortuosity

Diffusion in the extracellular space can be influenced by increased diffusion pathways, dead space microdomains, obstruction by macromolecules, transient receptor binding and non-specific interactions with fixed charges. Small molecules can diffuse through the ECS with an effective diffusion coefficient D^* that is two or three times less than the free diffusion coefficient D (Levin et al., 1970; Syková and Nicholson, 2008). The hinderance in extracellular diffusion compared with a free medium can be characterized by the tortuosity λ. It is defined as

$$\lambda = \sqrt{D / D^*} \qquad D^* = \frac{D}{\lambda^2} \qquad (2)$$

One factor that could increase λ can be an increase in geometric path length, representing the necessity for molecules in the brain ECS to travel a more circuitous path around cellular obstructions to arrive at their destination, compared with the path in a free medium (Syková and Nicholson, 2008). Another factor is the transient trapping of molecules in local dead-space microdomains in the ECS, which transiently delay the diffusion of these molecules (Hrabetova and Nicholson, 2000; Hrabetova et al., 2003). Additional factors that can influence tortuosity λ are increased interstitial viscous drag by macromolecules, transient binding to receptors and non-specific interactions with fixed negative charges (Maroudas et al., 1988; Johnson et al., 1996;

Rusakov and Kullmann, 1998; Novak and Kaye, 2000). In the adult brain, a tortuosity λ of between 1.4 and 1.7 has been found (Nicholson and Phillips, 1981; Lehmenkühler et al. 1993; Voříšek and Syková, 1997; Syková, 1997).

1.1.3. Uptake of substances

During diffusion some molecules are lost irreversibly from the ECS by diffusion across the blood-brain-barrier or by entering cells through active or passive transport (Patlak and Fenstermacher, 1975; Nicholson, 1992). Usually the loss of substances is proportional to their concentration and can be described as

$$\text{uptake} = k'C \qquad (3)$$

where k' is a rate constant and C the concentration in the ECS. In the absence of diffusion, the decrease in concentration as a function of time would be represented by an exponential curve governed by k' (Nicholson, 1992; Syková and Nicholson, 2008).

1.1.4. Anisotropic diffusion

Anisotropic diffusion might preferentially channel the movement of neuroactive substances in the ECS, and therefore it may be responsible for some specificity in extrasynaptic transmission. In many brain regions, e.g. the cerebellum, the effective diffusion coefficient D^*, and hence the values of λ, varies along the different axes in the tissue as a consequence of the local anatomic structure. Substances usually diffuse more readily along an axon bundle than across it. The volume fraction α is always a scalar with a single

value, but in anisotropic tissue, it is not possible to correctly estimate α with the real-time iontophoretic method unless all components of λ are determined (Syková and Nicholson, 2008). If the effective diffusion coefficient D^* and λ are the same when measured in any direction, then the tissue is said to be isotropic. It was shown in several studies that in the cortex, isotropic diffusion is present (Nicholson and Phillips, 1981; Syková, 2004).

1.2. Measurement of the extracellular space diffusion parameters

In the extracellular space of the brain, diffusion is the dominant mechanism of transport, constrained by the geometry of this compartment. Early studies with radiotracers, impedance measurements and electron microscopy led to contradictory results regarding the dimension of the extracellular space. In the first study with electron microscopy it was suggested, that no extracellular space was present (Wykoff and Young, 1956). In contrast to this finding, subsequent studies showed an extracellular space volume fraction of about 5% (Horstmann and Meves, 1959; Villegas and Fernandez, 1966). The development of novel tissue preparation methods for electron microscopy, based on rapid freezing and the freeze substitution of fixatives, enabled researchers to determine an extracellular space volume fraction of 15-20% (Van Harreveld et al., 1972). A relation between impedance and ECS volume fraction has been found in many studies (Ranck, 1963; Hossmann, 1971), although frequently there was an implicit assumption that tortuosity remained unchanged during any alteration in volume fraction (Syková and Nicholson, 2008).

The concept underlying other methods of direct diffusion measurements is to introduce a detectable substance into the ECS and to measure its time-dependend concentration distribution in the extracellular space. One possibility is to use radiotracers to detect the size of the extracellular space. Radiotracer studies of the extracellular volume fraction were made using different ECS markers, but only studies used "good" markers such as Ca-EDTA, Cr-EDTA or sucrose yielded reliable results for the size of the extracellular volume fraction (Sykova and Nicholson, 2008). The values of α obtained with the ECS radiotracer method were about 15 % (Fenstermacher and Kaye, 1988), i.e. somewhat less than the values obtained with newer methods.

More reliable methods are the real-time iontophoretic method and diffusion-weighted MRI. A major advantage of these two methods is their ability to not only determine the size of the extracellular space, but also to describe the diffusion properties of the tissue. The difference between the two methods lies in their invasivity and the values that can be determined by their use. With the TMA method the absolute values of α, λ and k' can be determined very exactly, but it is an invasive technique and thus only suitable for animal experiments. DW-MRI is a non-invasive technique and thus can be used in humans, but it can only determine λ and the diffusion coefficient of water. Beside these techniques, the size of the extracellular space can be determined satisfactorily by the Integrative Optical Imaging (IOI) technique, in which macromolecules carrying a fluorescent label are used as an extracellular marker. This technique enables the description of diffusion processes for large molecules in the brain.

1.2.1. Real-time iontophoresis

The diffusion parameters of the ECS and their dynamic changes can be determined using the real-time iontophoretic method. The underlying concept of this direct diffusion measurement method is to introduce a detectable substance into the ECS and subsequently to measure its concentration distribution over space and time. Based on microelectrodes for both delivering the molecules and sensing them, tetramethylammonium (TMA^+) - a substance to which cell membranes are relatively impermeable - is released by iontophoresis and its local concentration is measured with a TMA-selective microelectrode located about 100-150 µm from the release site. The behaviour of a large ensemble of random walks can be described by the classical macroscopic diffusion equation formulated largely by Fick in 1855 (Fick, 1995; English translation). The three-dimensional diffusion can be described by Fick´s second law as:

$$\frac{\delta c}{\delta t} = \nabla * (D \nabla c) \qquad (4)$$

The concentration of the substance is denoted by C, which is a function of time t and position. D represents the free diffusion coefficient of the substance and ∇ is the Nabla-operator for the description of the diffusion in a three-dimensional cartesian coordinate system.

The diffusion described by Fick´s law applies to molecules moving in a free medium such as water. In a complex environment like the ECS of the brain the diffusion equation must be modified. Based on the original diffusion equation, Nicholson and Phillips made an approach to describe the diffusion in a porous medium taking the averaged properties of the medium into account

through the volume fraction α and tortuosity λ. In the brain, diffusion can be described by the following equation (Nicholson and Phillips, 1981; Nicholson and Syková, 1988; Nicholson, 2001; Syková and Nicholson, 2008):

$$\frac{\delta C}{\delta t} = \frac{D}{\lambda^2}\nabla^2 C + \frac{Q}{\alpha} - v^* \nabla C - \frac{f(C)}{\alpha} \qquad (5)$$

The actual concentration in the interstitial space is represented by C, a function of time t and position. The symbols ∇ and ∇^2 symbolize the first and second derivates. The first term on the right of the equals sign, tortuosity λ enters the equation in the form of a reduction in the free diffusion coefficient D to yield the effective diffusion coefficient D* ($D^*=D/\lambda^2$). The next term is a source term Q, which is divided by the volume fraction α, reflecting the fact that the molecules released into the ECS are restricted to a smaller volume than if they had access to the entire brain tissue (Nicholson and Phillips, 1981; Sykova and Nicholson, 2008). The third term represents the distribution of bulk flow as a scalar product of the velocity vector v and the concentration gradient ∇C. In short distance diffusion such as that measured by the real-time iontophoresis method, bulk flow has only a very small influence and can be neglected. The final term represents the loss of substances by uptake into a cell, clearance over the blood-brain barrier, enzymatic degradation or other processes. The loss is often proportional to the local concentration and can be described as $f(C) = - k'\alpha C$. Based on the equation for diffusion in the ECS, the TMA^+ real-time iontophoretic

method was developed. A micropipette released TMA^+ by iontophoresis with a constant source strength Q into the brain tissue or an agarose gel. An ionselective microelectrode located about 100 µm from the release point measures the rising concentration of TMA^+ during and after the iontophoretic application. The recorded concentration-time profiles of TMA^+ in the extracellular space during and after an iontophoretic pulse can be fitted to a modified radial diffusion equation to yield the extracellular volume fraction α, tortuosity λ and non-specific uptake k´ (Nicholson and Phillips, 1981; Nicholson and Syková, 1998). Based on the knowledge, that in cortical tissue no anisotropy is present, the diffusion can be described as:

$$C(t) = \frac{Q\lambda^2}{8\pi D\alpha r}\left[\begin{array}{l} erfc\left(\frac{r\lambda}{2\sqrt{Dt}} + \sqrt{k't}\right)\exp\left(r\lambda\sqrt{\frac{k'}{D}}\right) \\ + erfc\left(\frac{r\lambda}{2\sqrt{Dt}} - \sqrt{k't}\right)\exp\left(-r\lambda\sqrt{\frac{k'}{D}}\right) \end{array}\right] \qquad (6)$$

The concentration C in dependence on time is recorded at a distance r from the origin where the source Q is located. The free diffusion coefficient is represented by D and the first-order kinetic constant *k´* describes the loss of probe ions from the ECS. During the iontophoretic application of the probe ions, the source is defined by $Q = In_t/zF$, where I is the current applied to the iontophoresis pipette, n_t is the transport number for the ion and the electrode, F is Faraday´s electrochemical equivalent, and z is the ion valency. The transport number n_t represents the fraction of the applied current that actually expels the

ion, and it is determined from iontophoretic measurements in agarose gel. During diffusion in an agarose gel, the diffusion values $\alpha=1$, $\lambda=1$ *and* $k'=0$ are set by definition. Based on these settings and equation (6), the iontophoretic application in an agarose gel can be described as:

$$C(t) = \frac{Q}{4\pi Dr} erfc\left(\frac{r}{2\sqrt{Dt}}\right) \qquad (7)$$

A value for D is also determined in agarose by curve fitting, although it is usually taken as a known constant for a given temperature. During the whole measurement period a small forward bias current is applied continually to the iontophoresis electrode to expel the ions at all times and to maintain both a constant value of n_t and a finite baseline concentration value (Syková and Nicholson, 2008).

1.2.2. Integrative Optical Imaging

The limitation of the real-time iontophoretic technique is that only a restricted set of ions can be used for exploring the geometrical structure of the ECS. Diffusion in the brain is not only dependent on small ions. Proteins and various macromolecules form part of the traffic within the ECS and are increasingly candidates for new drug vectors, so their diffusion behaviour is important (Syková and Nicholson, 2008). To improve the tools available to study the diffusion of large molecules in the brain, the method of integrative optical imaging (IOI) was developed (Nicholson and Tao, 1993). In the IOI method macromolecules with a fluorescent label are released from a micropipette by a

pressure pulse. The distribution of the fluorescent extracellular marker is registered with high-resolution, charge-coupled device cameras. Based of the intensity of the fluorescence around the point source and dependent on time, the extracellular diffusion parameters can be calculated based on the diffusion equation. Initially the IOI technique was used in brain slices, but now it is also employed for *in vivo* measurements (Nicholson and Tao, 1993; Thorne and Nicholson, 2006). There are many different fluorescent macromolecules available, but dextrans are very often used with this method. Dextrans have a large range of relative molecular masses between 3.000 – 70.000 Da and above and thus allow researchers to study the diffusion of many varieties of molecules. The IOI method is usually limited to the most superficial 200 µm of the gray matter or in brain slices where an epiflorescent image can be obtained without appreciable light-scattering. The major advantage of the IOI method is that it permits studying the diffusion of macromolecules of different sizes.

1.2.3. Diffusion-weighted MRI (DW-MRI)

Diffusion-weighted imaging (DW-MRI) is a non-invasive method that allows the in situ measurement of water diffusion predominantly within the interstitial space by determining the apparent diffusion coefficient of water (Le Bihan, et al., 1986). The MRI technique relies on applying magnetic field gradients as a pair of pulses separated by a defined time interval, so that the first pulse encodes the positions of the probe molecules into the phase of the nuclear spin magnetization and the second pulse reverses the effect of the first to rephrase the magnetization. It has been used to demonstrate a shift of water between the intra- and extracellular compartments following various types of

brain injury in animals as well as in humans (Le Bihan and Basser, 1995; Clough et al., 2007). In all these studies, changes in the later postischemic period were evaluated. However, up to now no study has investigated the diffusion changes in the first hours after reoygenation and reperfusion and compared them with the results from DW-MRI. This allowed for the analysis of the relationship between the dynamic changes in the diffusion properties of the complete brain cortex measured by MRI and the extracellular diffusion properties measured by the real-time iontophoretic method.

In this work an evaluation of the postischemic and posthypoxic changes in diffusion parameters, ADC_w and metabolite concentrations and their dependency on the severity of hypoxia/ischemia were studied. The combination of real-time ECS diffusion measurements, microdialysis, MRI, DC-potentials and extracellular potassium concentrations provides extensive data about the behaviour of postischemic and posthypoxic brain tissue. The extracellular diffusion parameters describe the properties of the extracellular compartment and affect the extracellular concentrations of substrates and metabolites. Therefore, changes in extracellular substrate and metabolite levels cannot be explored separately. The evaluation of extracellular metabolite and substrate concentrations and measurements of water diffusion allow the description of the redox state of the brain tissue and identify whether a brain edema is of vasogenic or cytogenic origin.

1.3. Microdialysis

Diffusion in the ECS is also essential for the delivery of oxygen and glucose from the vascular system to brain cells and the clearance of metabolites produced by neuronal cells (Nicholson, 2001). Normal brain function depends on a continuous supply of substrates, e.g. oxygen and glucose, to maintain the extracellular/intracellular ionic distribution and to enable synaptic as well as extrasynaptic transmission. Even short periods of ischemia or hypoxia result in a loss of function, breakdown of membrane potentials and in changes in substrate and metabolite concentrations in the brain microenvironment. Besides the knowledge of ECS diffusion parameters, the concentration of extracellular substrate and metabolite levels are very important to describe the changes during and after hypoxia/ischemia.

Intracerebral microdialysis is a highly sensitive technique to monitor cerebral energy metabolism. It allows the determination of brain metabolite and substrate levels in the extracellular fluid (ECF) and the measurement of regional metabolic tissue concentrations (Ungerstedt, 1991). In many studies, lactate has been interpreted as one of the markers of anaerobic metabolism, accumulating as the end product of glycolysis, if an imbalance arises between tissue O_2 supply and demand or when oxidative phosphorylation, as well as the tricarboxylic acid cycle, are reduced (DeSalles et al., 1986; Inao et al., 1988; Mizock and Falk, 1992; Magnoni et al., 2003). Lactate is produced and accumulates in the ECF during intense cerebral stimulation under normoxic conditions and is thus an unreliable indicator of tissue hypoxia (Prichard et al., 1991). For the detection of anaerobic metabolism, the simultaneous determination of pyruvate levels is necessary, because pyruvate is reduced to

lactate by lactate-dehydrogenase under anaerobic conditions. The lactate/pyruvate ratio (L/P ratio) specifies the degree of aerobic/anaerobic metabolism and reflects the cytosolic ratio of the reduced/oxidized forms of NAD. For this reason the L/P ratio is a reliable parameter for estimating the energy state of a cell (Magnoni et al., 2003).

Beside the measurement of metabolic end products, a knowledge of substrate levels, such as glucose, is important. The glucose concentration in the ECF reflects the balance between supply from the blood and utilisation by cells (Fellows et al., 1992). Glutamate, an excitatory amino acid released by active neurons into the extracellular space (ECS) and taken up by astrocytes, plays an essential role in normoxic and hypoxic conditions (Hillered et al., 1989, Magistretti et al., 1993). The measurement of glutamate efflux into the ECS after hypoxia and during reperfusion provides information about the compromised status of brain cells and the eventual neuropathological outcome (Phillis et al., 2001). The description of the redox state and the maintenance of the brain tissue from the microdialysis measurements are completed by the recording of DC-potentials and extracellular potassium concentrations.

Current knowledge of extracellular substrate and metabolite concentrations during and after hypoxia/ischemia is insufficient and a correlation with extracellular potassium concentrations and DC-potentials is missing. Although early studies using in vivo microdialysis did not acknowledge tissue diffusion properties, it is now recognized that the diffusion characteristics of the brain must be taken into account to realize a meaningful quantitative interpretation of microdialysis data (Syková and Nicholson, 2008).

1.4. Extracellular diffusion parameters in pathological states

Molecular diffusion in the brain extracellular space is an important determinant of neural function. Changes in the diffusion parameters of the cortical ECS may serve, on the one hand, as an important indicator of pathological processes and, on the other, offer insights into their underlying mechanisms (Sykova and Nicholson, 2008). Consequently, diffusion changes have been studied in several experimental pathological preparations and models using the TMA^+-real-time iontophoretic method together with DW-MRI in some instances. Correlations between the results of the two techniques may be useful for diagnostic purposes.

1.4.1. Hypoxia, ischemia and anoxia

Hypoxia, global and partial ischemia as well as anoxia are accompanied by significant changes in the extracellular diffusion parameters and large ionic shifts in the ECS. The extracellular potassium concentration increases dramatically up to 50-70 mM, while sodium, chloride and calcium levels and pH decrease to 40-59 mM, 70-75 mM, 0.06-0.08 mM and 6.4-6.8, respectively. These ionic changes are accompanied by an extracellular accumulation of excitatory amino acids, particularly glutamate, and a negative DC-potential shift in the ECS (Syková, 1983; Hansen, 1985; Syková, 1997; Somjen, 2004; Syková, 2004). Additionally, substantial changes in the ECS diffusion parameters occur. It has been repeatedly shown *in vivo* (Van Harreveld and Ochs, 1956; Hansen and Olsen, 1980; Lundbaek and Hansen, 1992; Katayama et al., 1992; Syková et al, 1994, Vořišek and Syková, 1997) as well as *in vitro* (Ames and Nesbett, 1983; Pérez-Pinzón et al., 1995) that the ECS of the brain

shrinks during global ischemia, while the tortuosity increases from 1.5 to about 2.1 (Syková et al., 1994; Vořišek and Syková, 1997). This shrinkage is caused by the movement of water from the ECS into the cells, which is accompanied by cellular swelling and changes in cell geometry. The reasons for this water movement are mainly ionic fluxes across the plasma membranes and resultant changes in the osmotic pressure balance of the tissue (Hansen, 1985). The ECS of the brain decreases to as little as 5-6% of the total brain volume during anoxia (Vořišek and Syková, 1997), which is a reduction of 65%-80% from preischemic values. Current knowledge about the behaviour of the extracellular diffusion parameters in the postischemic and posthypoxic period is insufficient and the relationship between the extent of diffusion parameter changes and the severity of hypoxia/ischemia has not been previously described.

1.4.2. Spreading depression

Spreading depression (SD) is a self-propagating wave of cellular depolarisation in the cerebral cortex with a velocity of about 3 mm/min (Bures et al., 1974; Somjen, 2004). SD evokes many similar changes in ECS ionic and diffusion properties as do anoxia and ischemia. The distinction is that spreading depression is a transient event that lasts for about one minute, and the affected regions of the tissue return to apparently normal conditions. During SD extracellular volume fraction α decreases to 0.05-0.09, while tortuosity λ increases to 1.95-2.07 (Anderova et al., 2001; Mazel et al., 2002). After SD α and λ remain elevated compared with controls, and this increase persist for more than one hour. The changes which are found during and after SD are quite similar to those seen during global ischemia.

1.4.3. Seizures

An epileptic seizure is a transient symptom of abnormal, excessive or synchronous neuronal activity in the brain. In the multifactorial development of seizure activity, the size of the ECS is an additional factor (Traynelis and Dingledine, 1989). Reduction of the ECS volume fraction α under hypoosmolaric conditions along with an increase in λ is accompanied by an increase in the frequency of epileptiform discharges, while hyperosmolar conditions reduce neuronal excitability (Kilb et al., 2006). A reduction of the extracellular space and impaired diffusion thus may contribute to the greater local accumulation of neuroactive substances and facilitate the development of epileptic seizures (Syková and Nicholson, 2008). Therefore, the size of the extracellular space influences seizure activitity in the brain by changing the tissue resistance.

1.5. Aims

The aims of the present studies were to study the changes in extracelluar space geometry and metabolite levels in the cortex during and after hypoxic and ischemic events. In detail, the aims could be summarized as follows:

a) Evaluation of the changes in the extracellular diffusion parameters of the ECS during and after transient hypoxia and ischemia of different severity.

b) Determination of energy-related extracellular metabolite and substrate levels (lactate, pyruvate, glucose and glutamate) during and in the recovery from transient ischemia and hypoxia.

c) Measurement of ADC_w using diffusion-weighted magnetic resonance during and after transient ischemia.

d) Recording of extracellular potassium levels and the time courses of cortical DC-potentials during hypoxia and ischemia and in the early recovery period.

e) Comparison of the time courses of changes in the extracellular diffusion parameters with those ofextracellular substrate and metabolite levels during and after hypoxic and ischemic events of different severity.

f) Correlation of extracellular potassium levels and extracellular diffusion parameters during and after different types of ischemia and hypoxia.

g) Comparison of extracellular diffusion parameters with ADC_w maps of the cortex to determine the cytogenic or vasogenic origin of edema formation.

h) Evaluation of the changes in the extracellular diffusion properties due to increased oxygen consumption during seizures and a comparison with the changes seen during ischemia/hypoxia

The results from these studies allowed us to analyse the relationship between the dynamic changes in diffusion properties, energy metabolism and electrical field potentials of the brain cortex. These findings improve our knowledge of the mechanisms that are involved in the development of tolerance to ischemic insults.

2. Methods:

2.1. Animal preparation

Three-month-old male Wistar rats (300-350g) were anaesthetised by an intraperitoneal injection of urethane (1.5 g/kg body weight, Sigma-Aldrich Chemie GmbH, Germany), tracheotomised or intubated, relaxed with suxamethonium chloride (20 mg/kg/h, Lysthenon, NycoMED Pharma, Vienna, Austria) or pancuroniumbromide (0.6 mg/kg body weight, Pavulon, Organon, Netherlands), and ventilated mechanically with oxygen. Before surgery, the depth of anaesthesia was controlled by testing the corneal reflex. If necessary, an additional 100 mg of urethane were injected intraperitoneally. The body temperature was maintained at 37°C by a heating pad. The head of the rat was fixed in a stereotaxic holder, and the somatosensory neocortex was partially exposed by a burr hole 2-3 mm caudal from the bregma and 3-4 mm lateral from the midline. When the dura was removed, the surface of the brain was continuously bathed with a warm solution (36-37°C) containing 1mM TMA, 150mM NaCl and 3mM KCl. All TMA^+-measurements were done in the somatosensory cortex at a depth of 1200-1500 μm from the cortical surface (cortical layers IV and V). Microdialysis measurements were performed in the somatosensory cortex over an insertion depth of 2000 μm. For DW-MRI measurements, the animals were placed in a heated MR-compatible cradle and their heads fitted in a built-in head holder.

The experiments were carried out in accordance with the European Communities Council Directive of 24 November 1986 (86/609/EEC). All efforts were made to minimize both the suffering and the number of animals used.

2.2. Experimental protocol

In our set of experiments we evaluated the changes in extracellular diffusion parameters and metabolite levels during hypoxia, several types of ischemia and seizure. In the first series of experiments a hypoxia of 30 minutes duration was induced by reducing the inspiratory oxygen content to 6% in 94% nitrogen, and the extracellular diffusion parameters, DC-potentials and metabolite levels were measured. Following the hypoxic period, the animals were again ventilated with air (O_2=21%). The control animals were ventilated with air throughout the experiment. In further experiments transient ischemia was induced by unilateral common carotid arterial clamping for 30 minutes or bilateral carotid clamping for 10 or 15 minutes and additionally reducing the inspired oxygen concentration to 6% or 10% in 94% nitrogen. In the experiments with unilateral occlusion, the extracellular diffusion properties and metabolite levels were measured. In the experiments with bilateral occlusion DC-potentials, extracellular potassium concentrations and ADC_w were determined instead of metabolite levels. In the hypoxia and ischemia experiments, measurements were made before, during and up to 90 minutes after the hypoxic/ischemic event. In the last series of experiments we evaluated the changes causes by an increased consumption of oxygen due to seizure. Seizure activity was evoked by the intraperitoneal injection of pilocarpine (300 mg/kg). To potentiate the action of pilocarpine, lithium chloride (127 mg/kg) was given to the animals 14-18 hours before each experiment (Ormandy et al., 1991). Extracellular diffusion properties, metabolite levels and ADC_w were measured over 240 minutes after the injection of pilocarpine in anaesthetized rats.

2.3. The TMA method for measuring the ECS diffusion parameters

The ECS diffusion parameters were studied by the real-time iontophoretic method, described in detail previously (Nicholson and Phillips, 1981; Lehmenkühler et al., 1993; Syková et al., 1994). Briefly, an extracellular marker that is restricted to the extracellular compartment is used, such as tetramethylammonium ions (TMA^+, MW = 74.1 Da), to which cell membranes are relatively impermeable. TMA^+ is administered into the extracellular space by iontophoresis, and the concentration of TMA^+ measured in the ECS using a TMA^+-ion-selective microelectrode (ISM) is inversely proportional to the ECS volume. Double-barreled TMA^+-ISMs were prepared by a procedure described in detail previously (Syková, 1992). The tip of the ion-sensitive barrel was filled with a liquid ion exchanger (Corning 477317); the rest of the barrel was backfilled with 150 mM TMA^+ chloride. The reference barrel contained 150 mM NaCl. The TMA^+-ISMs were calibrated in 0.01, 0.03, 0.1, 0.3, 1.0, 3.0, and 10.0 mM TMA^+ in a background of 3 mM KCl and 150 mM NaCl. Calibration data were fitted to the Nikolsky equation (Nicholson and Phillips, 1981). The shank of the iontophoretic pipette was bent so that it could be aligned parallel to that of the ion-selective microelectrode and was backfilled with 150 mM TMA^+ chloride. An electrode array was made by gluing a TMA^+-ISM to an iontophoretic micropipette with a tip separation of 100–200 μm. The iontophoresis parameters were +20 nA bias current (continuously applied to maintain a constant electrode transport number), with a +180 nA current step of 60 s duration, to generate the diffusion curve. TMA^+ was administered at regular intervals of 5 minutes (Fig. 1A). Before tissue measurements, diffusion curves were first recorded in 0.3% agar (Difco, Detroit, MI) dissolved in a solution containing 150 mM NaCl, 3 mM

KCl, and 1mM TMACl. In agar, α and λ are by definition set to 1 (free-diffusion values). The diffusion curves were analyzed to obtain the electrode transport number (n) and free TMA^+ diffusion coefficient (D) by curve-fitting according to a diffusion equation using the VOLTORO program (Nicholson and Phillips, 1981).

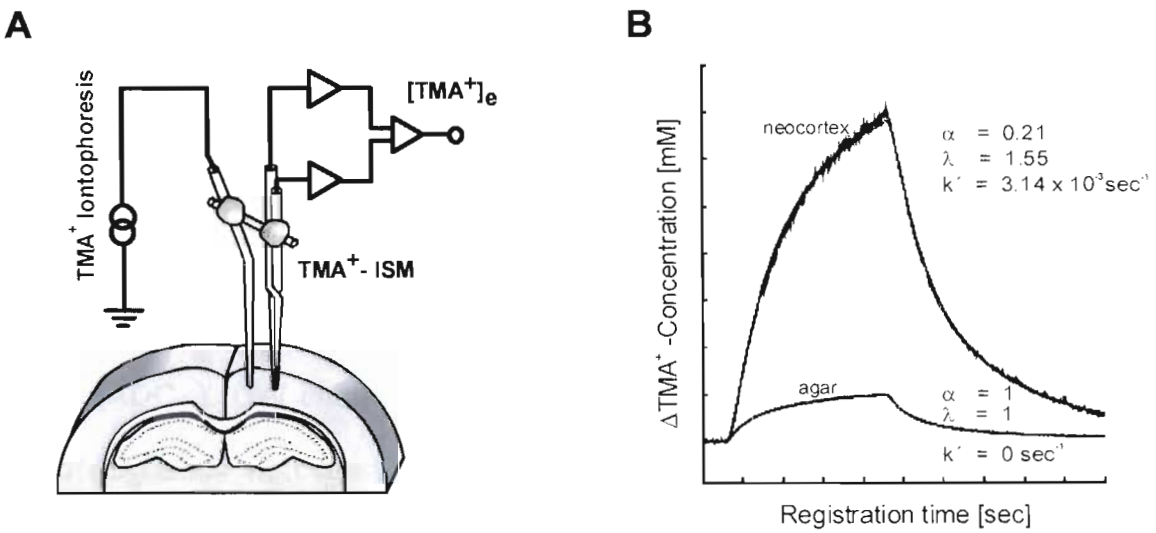

Fig 1: Experimental setup and TMA^+ diffusion curves. Left side (A): Experimental arrangement of a TMA^+-selective double barrelled ion-selective microelectrode (ISM) glued to an iontophoresis microelectrode with a tip distance of 120-200µm. Right side (B): Typical diffusion curves of TMA^+ obtained with this setup in neocortex during normoxia (neocortex) and in a free medium (agar). The concentration scale is linear and the theoretical diffusion curve is superimposed on each data curve. Both recordings were made using the same microelectrode array in the somatosensory neocortex of an adult Wistar rat and in agar (From Zoremba et al., 2007).

Diffusion curves were then recorded in the somatosensory cortex at a depth of 1200-1500 µm. Knowing n and D, the values of α and λ can be obtained from the recorded diffusion curves (Fig. 1B).

2.4. Diffusion-weighted MRI (DW-MRI)

DW-MRI measurements were performed using an experimental MR spectrometer BIOSPEC 4.7 T system (Bruker, Ettlingen, Germany) equipped with a 200 mT/m gradient system (190 μs rise time) and a homemade head surface coil. We acquired a sequence of T_2-weighted sagittal images in order to position coronal slices. For DW measurements, four coronal slices were selected (thickness = 1.0 mm, interslice distance = 1.5 mm, field of view = 3.2x3.2 cm^2, matrix size = 256x128). Diffusion weighting serves to increase the contrast in T_2-weighted images for water diffusion. The b-factor denotes the strength of diffusion weighting. Acquiring at least two DW images with different b-factors allows for the determination of the apparent diffusion coefficient of water (ADC_W). DW images from each slice were acquired using a stimulated echo sequence with the following parameters: b-factors = 75, 499, 1235 and 1731 s/mm^2, Δ = 30 ms, TE = 46 ms, TR = 1200 ms. Diffusion weighting is accomplished by applying a gradient magnetic field; in our measurements the gradient pointed along the rostrocaudal direction, and therefore ADC_W was measured in this direction. Maps of ADC_W were calculated using the linear least squares method and analyzed using ImageJ software (W. Rasband, NIH, USA). The evaluated regions of interest (ROIs) were positioned using a rat brain atlas (Paxinos and Watson, 1998) and T_2-weighted images in both the left and right hemispheres. The minimal area of an individual ROI was 2.5 mm^2. In each animal four coronal slices from the interval between 0.1 mm frontal to bregma and 5.6 mm caudal to bregma were analyzed. The resulting eight values of ADC_W (two ROIs per slice, four slices/rat) were averaged to obtain a single representative value for comparison to other rats. The reproducibility of ADC_W

measurements was verified by means of five diffusion phantoms placed on the top of a rat's head. The phantoms were made from glass tubes (inner diameter = 2.3 mm, glass type: KS80, Rückl Glass, Czech Republic) filled with pure (99%) substances having different diffusion coefficients. The substances were: 1-octanol, n-undecane (Sigma Aldrich, Steinheim, Germany), isopropyl alcohol, n-butanol and tert-butanol (Penta, Prague, Czech Republic). The temperature of the phantoms was maintained at a constant 37°C. The average diffusion coefficient for each compound was determined at the same time as the experimental measurements of each group of rats and compared to the average diffusion coefficient of the same compound measured in conjunction with the measurements of the other groups of rats.

2.5. Microdialysis

The technique of microdialysis is based on sampling fluid via a double-lumen probe with an integrated semipermeable membrane in which the equilibration of substances in the extracellular space and perfusion fluid takes place by diffusion according to the concentration gradient. We used a double-lumen microdialysis probe with a membrane length of 2 mm, an outer diameter of 0.5 mm and a cut-off at 20 000 Dalton (CMA 12, 2mm membrane length, CMA Microdialysis, Sweden). The inserted microdialysis catheter was connected by low-volume Fluorinated Ethylene Propylene (FEP)-tubing (1.2 µl/10cm) to a precision infusion pump (CMA 102, CMA Microdialysis, Sweden) in order to maintain a constant dialysate flow. The microdialysis catheter was continuously perfused with a dialysate (Perfusion fluid CNS, CMA Microdialysis, Sweden) containing 147 mmol/l NaCl, 2.7 mmol/l KCl, 1.2 mmol/l $CaCl_2$ and

0.85 mmol/l $MgCl_2$ at a flow rate of 2 µl/min. Transient increases in metabolite concentrations caused by probe insertion damage were avoided by a stabilisation period of 60 minutes following insertion into the brain. It has been shown that baseline values are stable within 30-60 minutes after probe insertion (Valtysson et al., 1998). After this equilibration time, microdialysate samples were collected over 10 minute intervals and immediately frozen at -40°C until analysed. Thawed and centrifuged dialysate samples were analyzed enzymatically with a CMA 600 Microdialysis Analyser (CMA Microdialysis, Sweden) for lactate, pyruvate, glucose and glutamate concentrations (Fig. 2).

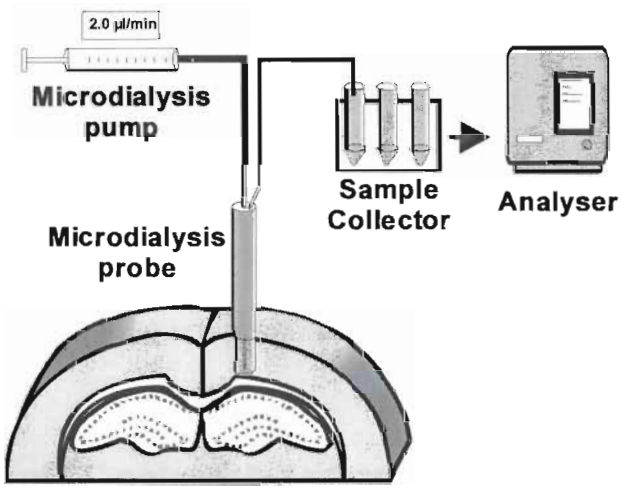

Fig 2: Experimental setup for microdialysis. The microdialysis probe was perfused continuously with a dialysate at defined flow of 2ml/min. The samples were collected over time intervals of 10 minutes and analysed by a microdialysis analyser (From Zoremba et al., 2007).

The exchange of substances across the microdialysis membrane is limited by the total area of the membrane, the perfusion flow rate, the characteristics of the diffusing substance and the diffusion constant in the tissue surrounding the probe (Arner and Bolinder, 1991; Ungerstedt, 1991).

The recovery rate expresses the relation between the concentration of the substance in the microdialysis probe effluent and the concentration in the medium (Muller, 2002). Before and at the end of the experiments, the recovery rates for each probe were determined by continuing the perfusion at the same settings in a calibration solution containing known concentrations of the different analytes. The calibration solution contained 2.50 mmol/l lactate, 250 µmol/l pyruvate, 5.55 mmol/l glucose, 250 mmol/l glycerol and 25 mmol/l glutamate (Calibrator A, CMA microdialysis, Sweden). The concentrations in the calibration solution were compared with the concentrations of the *in vitro* microdialysis samples to determine the relative recovery for each substance. The measured experimental values were weighted by the relative recovery to estimate the *in vivo* extracellular concentration of the substances in the immediate vicinity of the probes. *In vitro* recovery rates were 21.5 ± 0.9 % for lactate, 22.3 ± 0.5 % for pyruvate, 13.4 ± 0.6 % for glutamate and 10.8 ± 0.5 % for glucose (n=15). All results are presented as weighted concentrations.

2.6. Measurement of DC-potentials and extracellular K^+ concentrations

The recording of cortical DC-potentials is a powerful method to monitor the dynamics of sensory and cognitive processing in the brain under normal conditions and in the course of central nervous system disorders. DC-potentials from the cortical surface were recorded by microelectrodes filled with 150 mM NaCl, placed in the cortex and connected to a high impedance buffer amplifier with Ag/AgCl wires. The common reference electrode was positioned on the nasal bone (Lehmenkühler et al., 1999). The signal was amplified and transferred to a PC using a Lab Trax acquisition system (World Precision

Instruments Inc., Sarasota, USA). The extracellular potassium concentration was measured by double-barreled K^+-sensitive microelectrodes as described in detail elsewhere (Syková et al., 1994). Briefly, the tip of the K^+-selective barrel of the microelectrode was filled with the liquid ion-exchanger Corning 477317 and back filled with 0.5 M KCl, while the reference barrel contained 150 mM NaCl. Electrodes were calibrated in a sequence of solutions containing 2, 4, 8, 16, 32 and 64 mM KCl, with a background of either 151, 149, 145, 137, 121, or 89 mM NaCl to keep the ionic strength of the solution constant. The data were fitted to the Nikolsky equation to determine electrode slope and interference. Based on these electrode characteristics, the measured voltage was converted to extracellular concentrations.

2.7. Statistical analysis

The results of the experiments are expressed as the mean ± standard error of the mean (SEM). Statistical analysis of the differences within and between groups was performed using Student´s paired t-test, a two-tailed Mann-Whitney test or ANOVA for repeated measures combined with Dunnett's post hoc test (InStat, GraphPad Software, San Diego, USA). Values of $p<0.05$ were considered significant.

3. Results:

3.1. Hypoxia without a reduction in cerebral blood flow

Using a model of hypoxia, the effects on extracellular diffusion parameter, energy-related metabolites and DC-potentials in the rat cortex before, during and after the reduction of inspiratory oxygen content without a reduction in cerebral blood flow were studied (Zoremba et al., 2006).

3.1.1. Extracellular space diffusion parameters and DC potentials

The mean values of extracellular volume fraction α, tortuosity λ and non-specific uptake k' during normoxia were $\alpha = 0.18 \pm 0.01$, $\lambda = 1.54 \pm 0.01$ and $k' = (3.38 \pm 0.32) \times 10^{-3} s^{-1}$ (n=7), values also observed in previous studies *in vivo* (Cserr et al., 1991; Lehmenkühler et al., 1993; Voříšek and Syková, 1997). During hypoxia, α decreased by about 5% in the first 20 minutes. At 20-30 minutes, α decreased to 0.14 ± 0.01 (n=7), i.e. about 22% (Fig. 4A). Tortuosity λ increased, also in two steps, reaching a value of 1.61 ± 0.02 in the first 20 minutes, then increasing to 1.69 ± 0.03 (n=7) at 20-30 minutes into the hypoxic period (Fig. 4B). During the reoxygenation period, α and λ values normalised within 20 minutes to 0.20 ± 0.01 and 1.55 ± 0.01, respectively, and remained unchanged until the end of the measurement period of 90 minutes after hypoxia. No significant changes in non-specific uptake k' were seen during the entire observation period. The recorded DC-potentials showed an early initial negative shift of up to 3 mV after the onset of hypoxia, which has also been seen in previous studies (Lehmenkuhler et al., 1999). After this early negative shift, the DC-potential returned to baseline levels. A second negative shift of up to 2.5 mV was seen in the last 5-10 minutes of the 30 minute hypoxia. After the

end of hypoxia and the return to ventilation with air, the negative DC-potentials immediately returned to baseline levels (Fig. 4C).

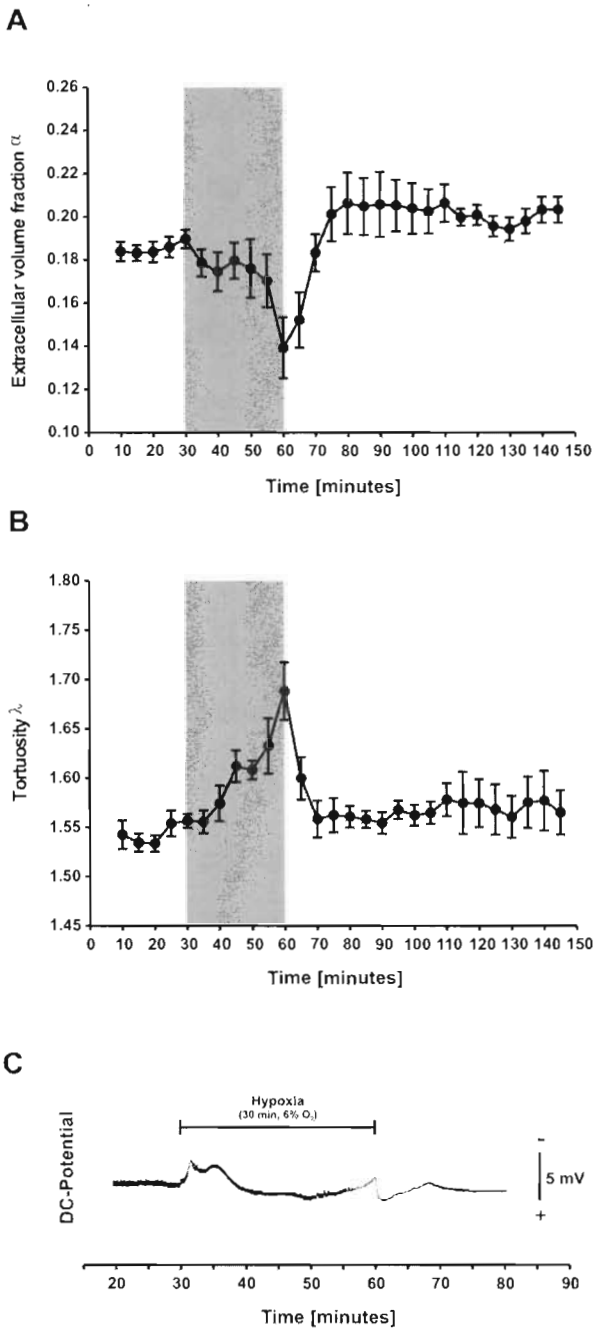

Fig 4: The time course of changes in extracellular space volume fraction α (A) and tortuosity λ (B) during hypoxia and recovery. After establishing a stable baseline, 30 minutes of hypoxia were induced by reducing the inspiratory oxygen content from 21% to 6% (shaded area). After hypoxia the animals were again ventilated with air. Measurements were made at time intervals of 5 minutes. Values are presented as mean ± SEM. The number of experiments was n=7. Part (C) show a typical recording of DC-potentials measured by intracortical microelectrodes filled with 150 mM NaCl against a reference electrode placed on the nasal bone. During early hypoxia, a negative shift of up to 3 mV was observed, returning to baseline within the first 15 minutes of hypoxia. A second negative shift was seen during the last 5-10 minutes of hypoxia of up to 2.5 mV (From Zoremba et al, 2007).

3.1.2. Changes in lactate, the lactate/pyruvate ratio and glucose

Before the induction of hypoxia, stable basal glucose levels of 2.27 ± 0.07 mmol/l (n=15) were found in both hypoxic and control animals. Hypoxia led to a steep decrease in glucose dialysate levels, reaching a plateau of 1.18 ± 0.16 mmol/l within 20 minutes. During the reoxygenation period extracellular glucose concentrations returned to control levels within 20 minutes (Fig. 5A). After a stabilisation period of 60 minutes following probe insertion, basal cortical lactate levels remained stable at 0.75 ± 0.03 mmol/l (n=15). Hypoxia evoked by a reduction of inspiratory oxygen content led to an immediate rise in lactate levels. This rise continued throughout the 30 minute period of hypoxia, reaching a plateau at 25 minutes of 2.65 ± 0.24 mmol/l, when α showed a second decrease (Fig. 5B). The difference between control and hypoxic animals was extremely significant ($p<0.001$). For evaluating the anaerobic pathway, the lactate/pyruvate ratio (L/P ratio) was calculated. In control animals no significant change in the L/P ratio was seen during the entire observation period. In hypoxic animals the L/P ratio increased from 20.88 ± 2.65 to 76.03 ± 13.04 at the end of the hypoxic period (Fig. 5C). In the reoxygenation period, lactate levels as well as the L/P ratio decreased to control levels within 50-60 minutes (Fig. 5B and 5C).

3.1.3. Changes in glutamate

Extracellular glutamate levels prior to hypoxia were 2.37 ± 0.53 µmol/l (n=15). After the beginning of hypoxia, extracellular glutamate levels remained unchanged for about 20 minutes. In the next 20-30 minutes a steep increase was found, reaching concentrations of 35.81 ± 1 2.96 µmol/l. These glutamate

concentrations were correlated with an increase in the extracellular volume fraction α. While α returned to control levels within 20 minutes, the elevated glutamate levels did not return to control levels until 40-50 minutes of the reoxygenation period (Fig. 5D).

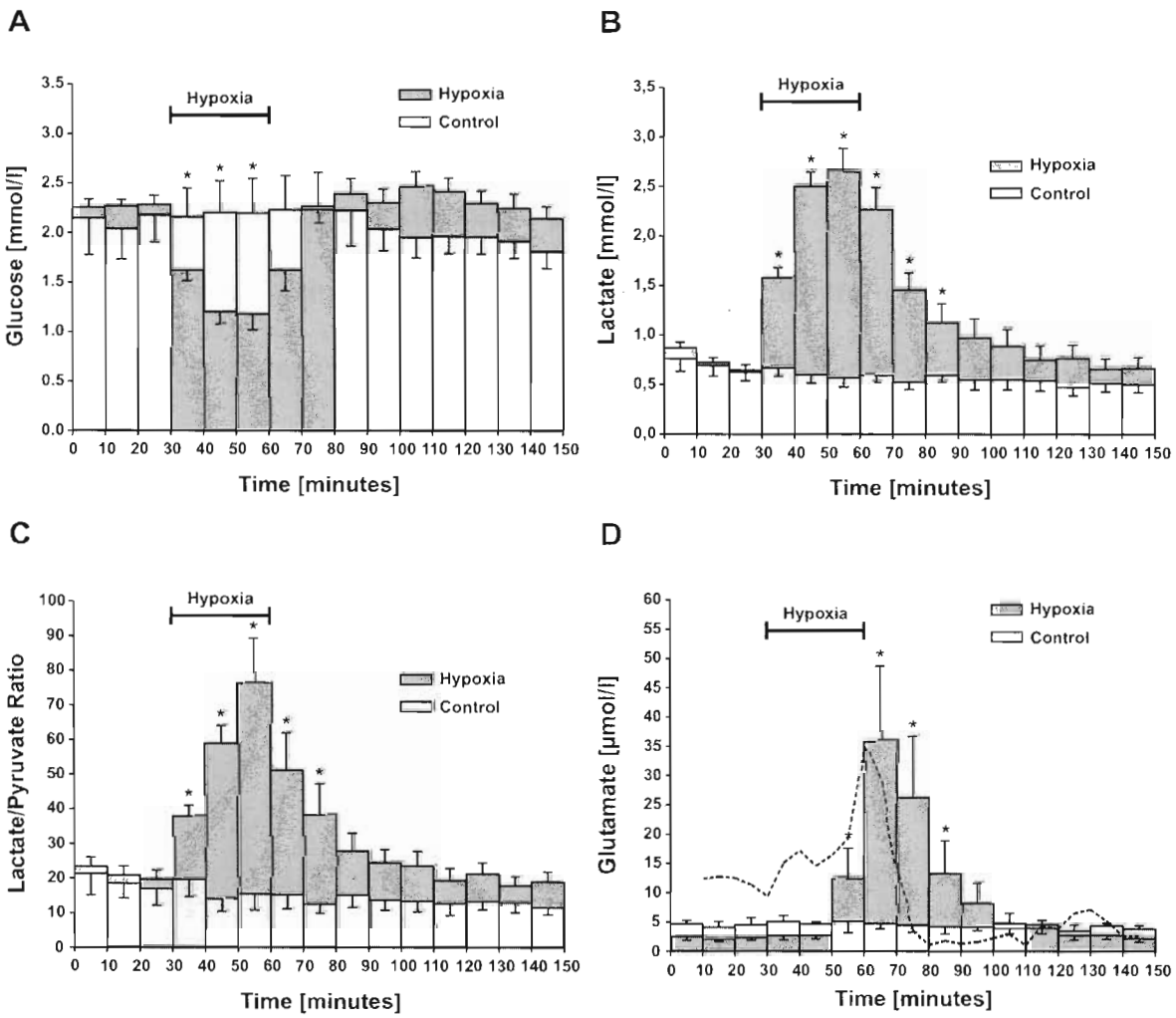

Fig 5: Time course of interstitial glucose levels (A), lactate concentrations (B), the lactate/pyruvate ratio (C) and glutamate concentrations (D) before, during and after hypoxia of 30 minutes duration, compared to controls. After a stabilisation period, 30 minutes of hypoxia were induced by ventilating the animals with 6% oxygen in nitrogen. The hypoxic period is marked by a time line. Microdialysis samples were collected over time intervals of 10 minutes and the measured values were presented as vertical bars. Values are shown as mean ± SEM. The number of experiments was n=10 in the hypoxic and n=5 in the control group. Statistically significant differences ($p<0.05$) between the hypoxic and control animals are marked by asterisks. To show the inverse correlation between ECS volume and glutamate concentration, an inverted time course of the changes in extracellular volume fraction α (taken from Fig. 4A) was superimposed onto Fig 5D (dotted line). For details see Zoremba et al., 2007.

3.2. Hypoxia with a reduction in cerebral blood flow (unilateral occlusion of the carotic artieries)

In the model of ischemia the effects of the reduction of inspiratory oxygen content and the reduction in cerebral blood flow by unilateral clamping of the carotic arteries in the rat cortex were studied. In this experimental setting extracellular diffusion parameters and energy-related metabolites before, during and after ischemia of 30 minutes duration were evaluated.

3.2.1. Extracellular space diffusion parameters

The mean values of extracellular volume fraction α and tortuosity λ during normoxia were α=0.19 ± 0.03 and λ=1.57 ± 0.01, (n=12, mean ± SEM), which are similar to the values observed in rat cortex previously (Lehmenkühler et al., 1993; Voříšek and Syková, 1997).

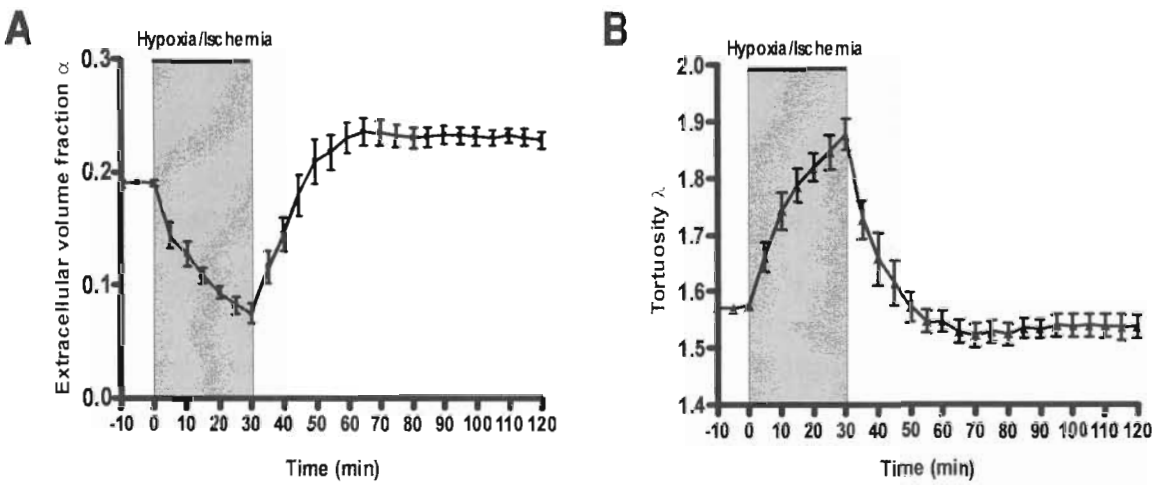

Fig 6: The time course of changes in extracellular space volume fraction α (A) and tortuosity λ (B) during transient hypoxia/ischemia and subsequent reperfusion. Immediately after the onset of hypoxia/ischemia α started to decrease and λ increased, reaching maximum values at the end of the hypoxic/ischemic period. During the reperfusion α and λ recover within 20 minutes. Subsequently, α increased over the preischemic values and stayed at this level until the end of the registration period. The time course of changes in λ was the inverse of the time course of changes in α (From Homola et al, 2006).

Immediately after the onset of hypoxia/ischemia, the extracellular volume fraction α gradually decreased, reaching a minimum of 0.07 ± 0.01 at the end of the hypoxic/ischemic insult of 30 minutes duration (Fig. 6A). Simultaneously with the decrease in α, tortuosity λ increased to maximum values of 1.88 ± 0.03 after 30 minutes of hypoxia/ischemia (Fig 6B). After the release of carotid artery occlusion and the beginning of normoxic ventilation, both α and λ started to return to normal values, reaching them within 20 minutes of the recovery period. During the next 20 minutes, α continued to increase up to 0.23 ± 0.01 while λ decreased to 1.53 ± 0.06, then both parameters remained unchanged at these levels until the end of the 90-minute recovery phase (Fig. 6A and 6B).

3.2.2. Microdialysis

After a stabilisation period of 60 minutes following probe insertion, the basal cortical level of lactate and the lactate/pyruvate ratio remained stable at 0.99 ± 0.06 mmol/l and 23.44 ± 1.85, respectively (n=9). There were no statistical differences compared to the control group (n=5). Combined hypoxia/ischemia led to an immediate rise in lactate dialysate levels, reaching a plateau of 3.01 ± 0.62 mmol/l within 20 minutes (Fig. 7A). The lactate/pyruvate ratio showed a similar time course during hypoxia/ischemia, reaching a plateau of 64.79 ± 11.24 (Fig. 7B). After the release of carotid occlusion and reoxygenation, lactate levels and the lactate/pyruvate ratio decreased, reaching control values within 30-40 minutes. Taking into account the effect of the changes in ECS volume fraction, the calculated extracellular concentrations of lactate during hypoxia/ischemia would be 30-50% lower than those actually measured (Fig. 7A).

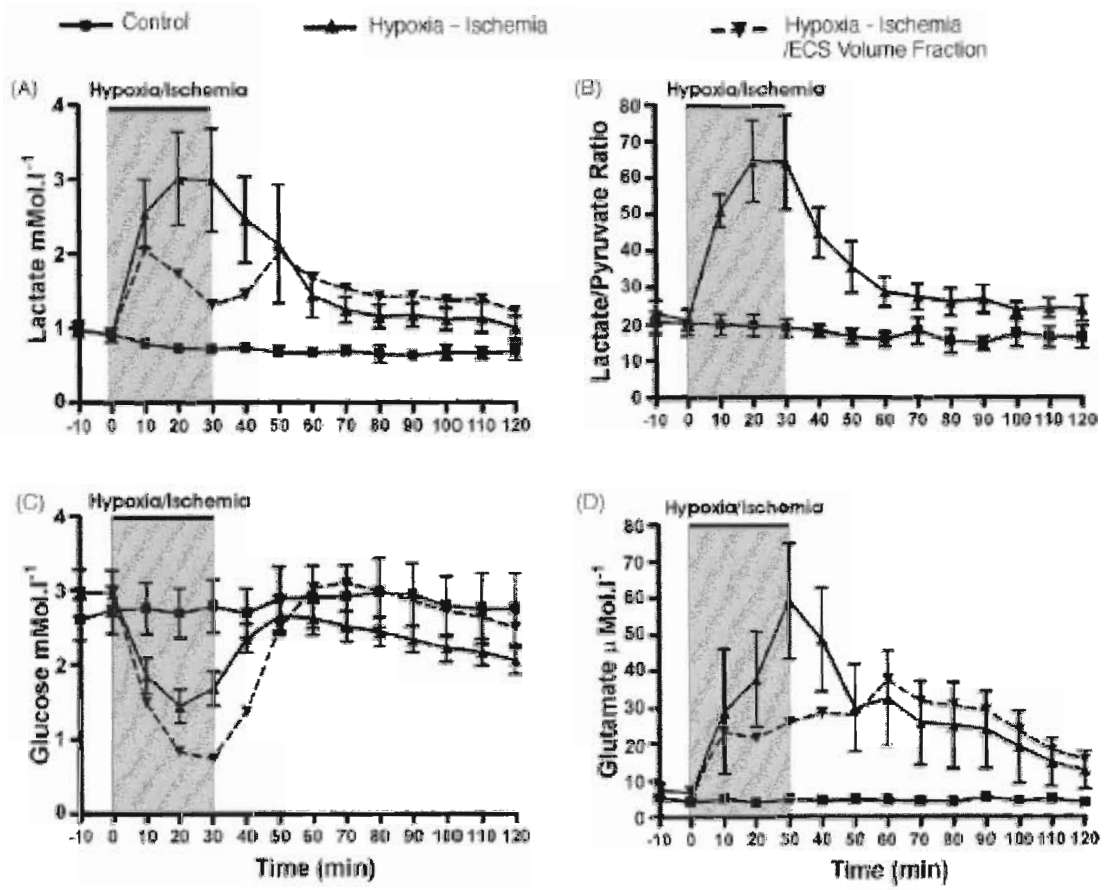

Fig 7: The time course of changes in the concentration of extracellular lactate (A), the lactate/pyruvate ratio (B), and the concentrations of extracellular glucose (C) and glutamate (D) during transient hypoxia/ischemia and subsequent reperfusion, compared to controls. The stated concentrations, representing the actual physiological concentrations, may be underestimated. The time courses of the concentrations of the evaluated metabolites corrected for changes in ECS volume are presented as dashed lines, showing how much of the concentration change is due to the ECS volume change (From Homola et al., 2006).

Before the induction of hypoxia/ischemia, stable basal glucose and glutamate levels of 2.94 ± 0.18 mmol/l and 6.85 ± 0.97 µmol/l respectively (n=9) were found, without any significant differences compared with control animals (n=5). Unilateral carotid occlusion and a reduction in inspiratory oxygen content led to a steep decrease in glucose dialysate concentrations, reaching a minimum of 1.45 ± 0.23 mmol/l after 20 minutes of hypoxia/ischemia.

During the reoxygenation period, extracellular glucose concentrations returned to control levels within 20 minutes and then slowly decreased, reaching a value of 2.05 ± 0.17 mmol/l at the end of the experiment. The glucose concentrations during hypoxia/ischemia would be even lower if we take into account the accompanying changes in ECS volume fraction. During reperfusion, the glucose concentration corrected for the increase in α reached initial values within 20 minutes and remained at this level until the end of the experiment (Fig. 7C). Extracellular glutamate levels increased during hypoxia/ischemia, reaching maximum values of 59.30 ± 15.90 µmol/l at the end of the hypoxic/ischemic insult. During reperfusion the extracellular glutamate levels decreased, reaching control values 90 minutes after reperfusion. The concentration of glutamate corrected for the increase in α would be lower with the greatest increase seen within the first 10 minutes (Fig. 7D).

3.3. Hypoxia with a reduction in cerebral blood flow (bilateral occlusion of the carotic arteries)

In a different model of ischemia the effects of the reduction of inspiratory oxygen content and the reduction in cerebral blood flow by bilateral clamping of the carotic arteries in the rat cortex were studied. In this experimental setting extracellular diffusion parameters, the apparent diffusion coefficient of water, DC-potentials and extracellular potassium concentrations before, during and after ischemia of 10 or 15 minutes duration were evaluated.

3.3.1. Extracellular space diffusion parameters

ECS diffusion parameters were recorded in cortical layers IV or V (at a depth of 1200-1500 μm) of the somatosensory cortex prior to and after 10 or 15 minutes of ischemia. The mean values of extracellular volume fraction α and tortuosity λ during normoxia were similar in both ischemia groups (α=0.19 ± 0.01, λ=1.55 ± 0.01 and α=0.19 ± 0.01, λ=1.55 ± 0.02) and comparable to the values found in previous *in vivo* studies (Nicholson and Phillips, 1981; Lehmenkühler et al., 1993; Voříšek and Syková, 1997; Mazel et al., 2002). During ischemia α decreased to 0.07 ± 0.01 in both groups, while λ increased to 1.80 ± 0.02 and 1.81 ± 0.02 in the 10 minute and 15 minutes ischemia groups, respectively. After releasing the clamps and reoxygenation, recovery to preischemic values of α=0.21 ± 0.01 were found after 15-20 minutes of reperfusion in the rats subjected to 10 minutes of ischemia; the values then remained stable during the entire measurement period of 90 minutes. After ischemia of 15 minutes duration, α recovered within 10-15 minutes of reperfusion, but then increased substantially within a further 30-40 minutes up

to 0.29 ± 0.03 and remained elevated during the postischemic measurement period of 90 minutes. This indicates an ECS enlargement of 40-50% in the somatosensory cortex of rats subjected to longer (15 minutes) ischemia. (see Fig. 8, Table 1).

	Before ischemia	30 min. after ischemia	60 min. after ischemia	90 min. after ischemia
Ischemia 10 minutes n = 5	$\alpha = 0.19 \pm 0.01$ $\lambda = 1.55 \pm 0.01$ $k' = 3.6 \cdot 10^{-3} \pm 0.8 \cdot 10^{-3}$	$\alpha = 0.20 \pm 0.01$ $\lambda = 1.54 \pm 0.02$ $k' = 3.3 \cdot 10^{-3} \pm 0.9 \cdot 10^{-3}$	$\alpha = 0.20 \pm 0.01$ $\lambda = 1.55 \pm 0.02$ $k' = 3.9 \cdot 10^{-3} \pm 1.0 \cdot 10^{-3}$	$\alpha = 0.19 \pm 0.01$ $\lambda = 1.56 \pm 0.03$ $k' = 4.1 \cdot 10^{-3} \pm 1.0 \cdot 10^{-3}$
Ischemia 15 minutes n = 6	$\alpha = 0.19 \pm 0.01$ $\lambda = 1.55 \pm 0.02$ $k' = 3.6 \cdot 10^{-3} \pm 0.6 \cdot 10^{-3}$	$\alpha = 0.26 \pm 0.01^{\#}$ $\lambda = 1.57 \pm 0.01$ $k' = 2.8 \cdot 10^{-3} \pm 0.2 \cdot 10^{-3}$	$\alpha = 0.29 \pm 0.03^{\#}$ $\lambda = 1.60 \pm 0.02$ $k' = 3.6 \cdot 10^{-3} \pm 0.5 \cdot 10^{-3}$	$\alpha = 0.30 \pm 0.03^{\#}$ $\lambda = 1.62 \pm 0.01^{\#}$ $k' = 3.8 \cdot 10^{-3} \pm 0.4 \cdot 10^{-3}$

Tab 1: Values of extracellular volume fraction α and tortuosity λ and non-specific uptake k' before and after transient ischemia of 10 or 15 minutes duration. Values of α, λ and k' are shown as mean values and standard error of the mean (SEM). Significant differences (two-tailed Mann-Whitney test, $p < 0.05$) in postischemic values when compared to values before ischemia are marked with crosshatches. n represents the number of animals (From Zoremba et al., 2008).

The statistical difference between the pre- and postischemic values of α was extremely significant (0.19 ± 0.01 versus 0.29 ± 0.03, $p<0.001$). Typical diffusion curves recorded before and 60 minutes after ischemia of 10 or 15 minutes are shown in Fig. 8. In both groups, preischemic values of λ were observed after 5-10 minutes of reperfusion (10 minutes ischemia: λ=1.57 ± 0.04; 15 minutes ischemia: λ=1.56 ± 0.04). In the group of 10 minutes ischemia, λ remained stable at this level. In the group subjected to 15 minutes ischemia, a marginally significant increase in λ to 1.62 ± 0.01 was found at the end of the

measurement period. The time-course of λ after ischemia in both groups is shown in Fig. 8.

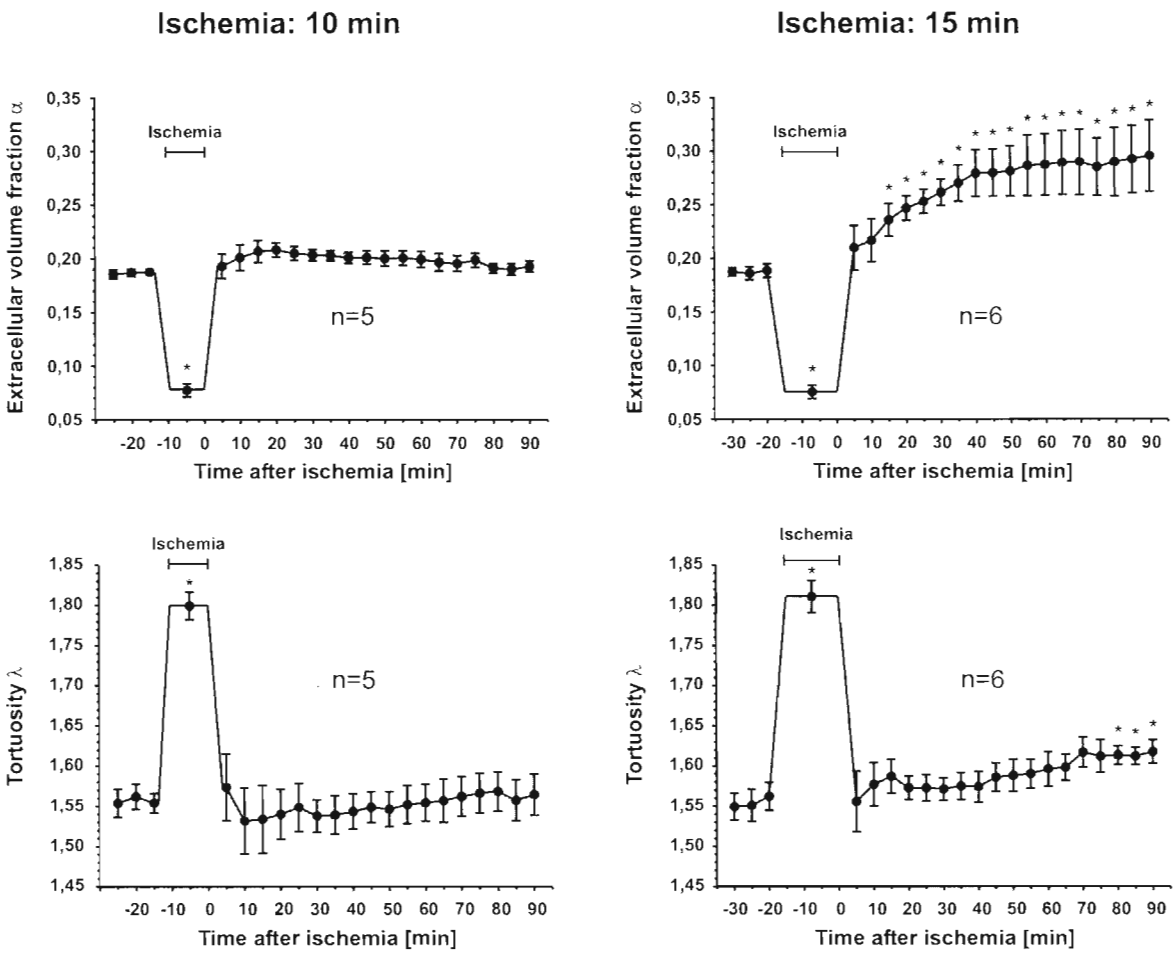

Fig 8: Time course of changes in the values of the extracellular space parameters (α, λ) in the cortex of adult rats before, during and after ischemia of 10 or 15 minutes duration, calculated from TMA^+ diffusion measurements. Data are shown as mean values ± SEM and the number of animals as n. The duration of ischemia is marked by a time line. Upper graphs: Average values of extracellular volume fraction α. After 10 minutes ischemia, a quick recovery of α occurs within 5-10 minutes and the values remain stable at this level. In the group subjected to 15 minutes ischemia, α increases extremely significantly above starting values after 40 minutes of reperfusion ($p<0.001$) and remains at this level until the end of the measurement period. Postischemic values that are significant different from preischemic values ($p<0.05$) are marked by an asterisk. Lower graphs: The time courses of tortuosity λ showed initially no difference between the two groups ($p<0.05$). During ischemia an elevated λ recovered to the starting values within 5 minutes and stayed at this level without any significant difference from preischemic values. In the group of 15 minutes ischemia, λ increased significantly at the end of the registration period (From Zoremba et al., 2008).

3.3.2. MRI measurements

Diffusion-weighted MRI measurements of ADC_w were performed bilaterally in the primary somatosensory cortex and showed similar preischemic values in both groups (597 ± 14 $\mu m^2 s^{-1}$ vs. 594 ± 12 $\mu m^2 s^{-1}$). In the group of 10 minutes ischemia, no significant changes in ADC_w in the postischemic period were found, compared to preischemic values. In the animals exposed to 15 minutes ischemia, a statistically significant increase in ADC_w to 665 ± 15 $\mu m^2 s^{-1}$ was observed 60 minutes after ischemia. This elevated ADC_w level remained until the end of the measurement period, 120 minutes after ischemia (Tab. 2).

	ADC_W ($\mu m^2 s^{-1}$) before ischemia	ADC_W ($\mu m^2 s^{-1}$) 60 min. after ischemia	ADC_W ($\mu m^2 s^{-1}$) 90 min. after ischemia	ADC_W ($\mu m^2 s^{-1}$) 120 min. after ischemia
Ischemia 10 minutes n = 6	597 ± 14	608 ± 8	603 ± 10	605 ± 12
Ischemia 15 minutes n = 6	594 ± 12	665 ± 15 #	651 ± 11 #	647 ± 13 #

Tab 2: The apparent diffusion coefficient of water (ADC_W) before and after 10 or 15 minutes of ischemia was determined by magnetic resonance imaging. Significant differences (two-tailed Mann-Whitney test, $p < 0.05$) between preischemic values and values after ischemia are marked with crosshatches. n represents the number of animals. Data expressed as mean ± SEM (From Zoremba et al., 2008).

Typical MRI images before and after ischemia are shown in Fig. 9. As the carotid occlusion was done outside the magnet, ADC_w values during ischemia were not measured. However, it is known from previous studies that global ischemia induces a rapid drop in ADC_w (Fischer et al., 1995, Van der Toorn et al., 1996).

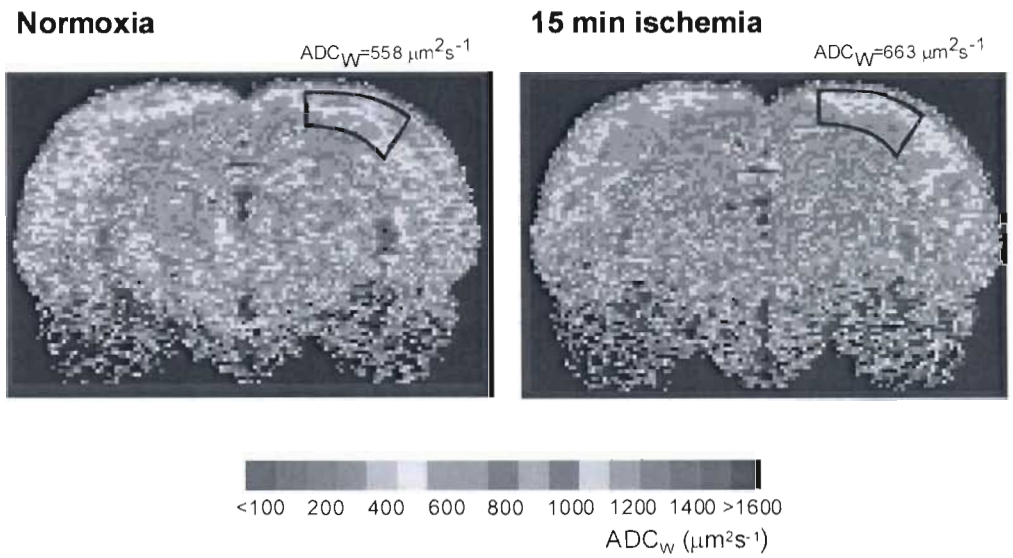

Fig 9: Typical ADC_w maps of a control rat brain and of a rat brain 60 minutes after ischemia of 15 minutes duration. ADC_w was analyzed bilaterally in the primary somatosensory cortex. The analyzed areas are outlined on the right part of the slices, and both images are from the same coronal plane. The scale at the bottom of the figure shows the relation between the intervals of ADC_w values and the colours used for visualization (From Zoremba et al., 2008).

3.3.3. DC-potentials and extracellular potassium concentrations

Before the induction of ischemia, extracellular potassium concentrations of 3 mM were found in both groups. During 1-2 minutes of ischemia, a fast increase up to 70 mM was registered, and the concentration remained stable at this level during the ischemic period in both the 10 minute and the 15 minute ischemia groups. After reoxygenation the extracellular potassium concentrations dropped within 2-3 minutes to preischemic levels of 3 mM and stayed at this level until the entire registration period (Fig. 10).

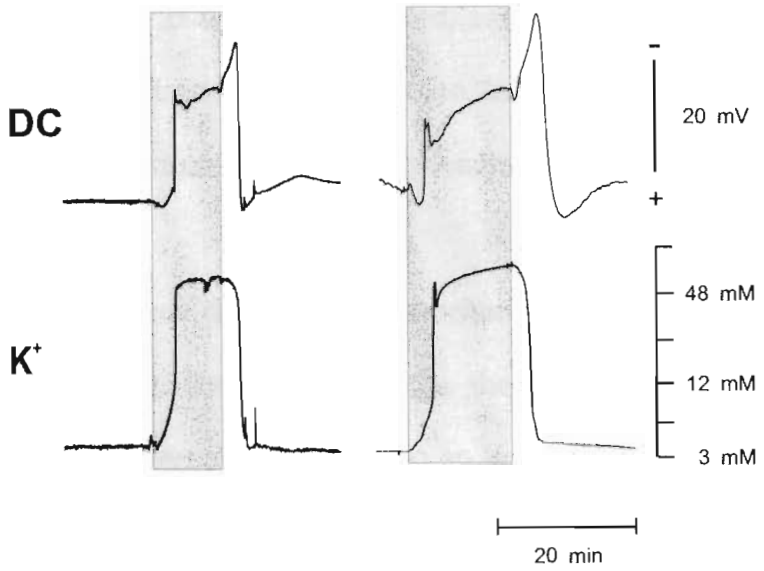

Fig 10: Time course of extracellular potassium concentrations and DC-potentials during an ischemia of 10 minutes (left side) or 15 minutes duration (right side). The duration of ischemia is marked by the shaded fields. The registered depolarisation and recovery of the DC-potential is correlated with an increase in extracellular potassium level during ischemia and normalisation during the recovery (From Zoremba et al., 2008).

The DC-potential changed in a negative direction simultaneously with the increase in extracellular potassium, followed by a small positive change. During the ongoing ischemia, the DC-potential showed a slight increase. Immediately after reopening of the carotid arteries and ventilation with pure oxygen, the DC-potential showed a sharp negative shift, and after the normalisation of extracellular potassium concentrations, DC-potentials recovered to preischemic levels. Typical measurements of extracellular potassium concentrations and DC-potentials during ischemia of 10 and 15 minutes duration are shown in Fig. 10.

3.4. Elevated oxygen consumption due to seizure activity

In the model of pilocarpine-induced seizure activity, the extracellular diffusion properties, extracellular metabolite levels and ADC_w were studied before and up to 240 minutes after the administration of pilocarpine.

3.4.1. Extracellular space diffusion parameters

Before the application of pilocarpine the mean values of extracellular volume fraction α and tortuosity λ were 0.19 ± 0.004 and 1.58 ± 0.01, (n=7), which represent the diffusion parameter values observed in normal brain tissue. Volume fraction α started to decrease several minutes after the application of pilocarpine, reaching a minimum of 0.13 ± 0.01 after 80 - 100 minutes. After reaching these minimum values, α started to increase again and reached values of 0.18 ± 0.01 within 240 minutes after the application of pilocarpine (Fig. 11 A). Following pilocarpine application, there were no significant changes in tortuosity during the entire measurement period (Fig. 11 B).

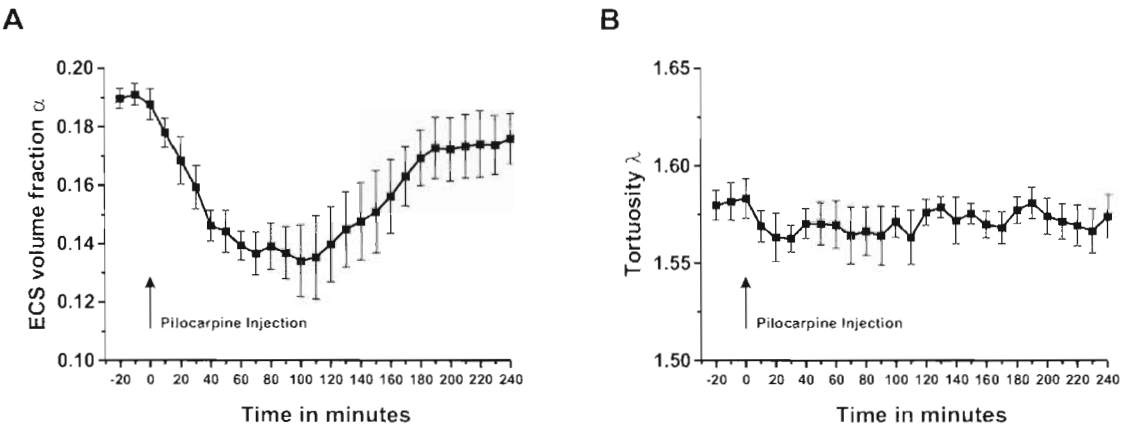

Fig 11: Time course of extracellular space volume fraction α (A) and tortuosity λ (B) over a time period of 240 minutes after the application of pilocarpine. The injection time point is marked by an arrow (From Slais et al., 2008).

3.4.2. Extracellular potassium concentrations

The extracellular potassium concentration in the brain somatosensory cortex was 3.07 ± 0.02 mM (n=7) at the beginning of the experiments. After pilocarpine application, the extracellular potassium levels started to increase after several minutes, reaching a maximal concentration of 13.3 ± 1.04 mM 80 minutes after application. Subsequently, these elevated extracellular potassium levels returned to normal values, reaching values of 4.17 ± 0.21 mM at the end of the experiment (Fig. 12).

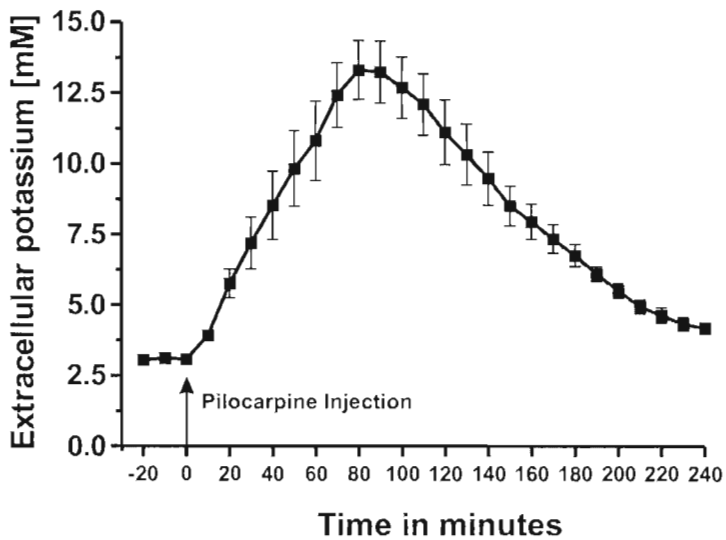

Fig 12: Time course of extracellular potassium concentration over a time period of 240 minutes after the application of pilocarpine. The time point of pilocarpine injection is marked with an arrow (From Slais et al., 2008).

3.4.3. MRI measurements

The mean value of ADC_W before the application of pilocarpine was 603.2 ± 8.6 $\mu m^2 s^{-1}$ (n=6). Following pilocarpine application, ADC_W started to decrease, reaching a minimum of 549.5±10.5 $\mu m^2 s^{-1}$ about 100 minutes later. After reaching these minimum values ADC_w started to increase again and reached values of 612.7±14.7 $\mu m^2 s^{-1}$ within a period of 240 minutes after application of pilocarpine (Fig 13).

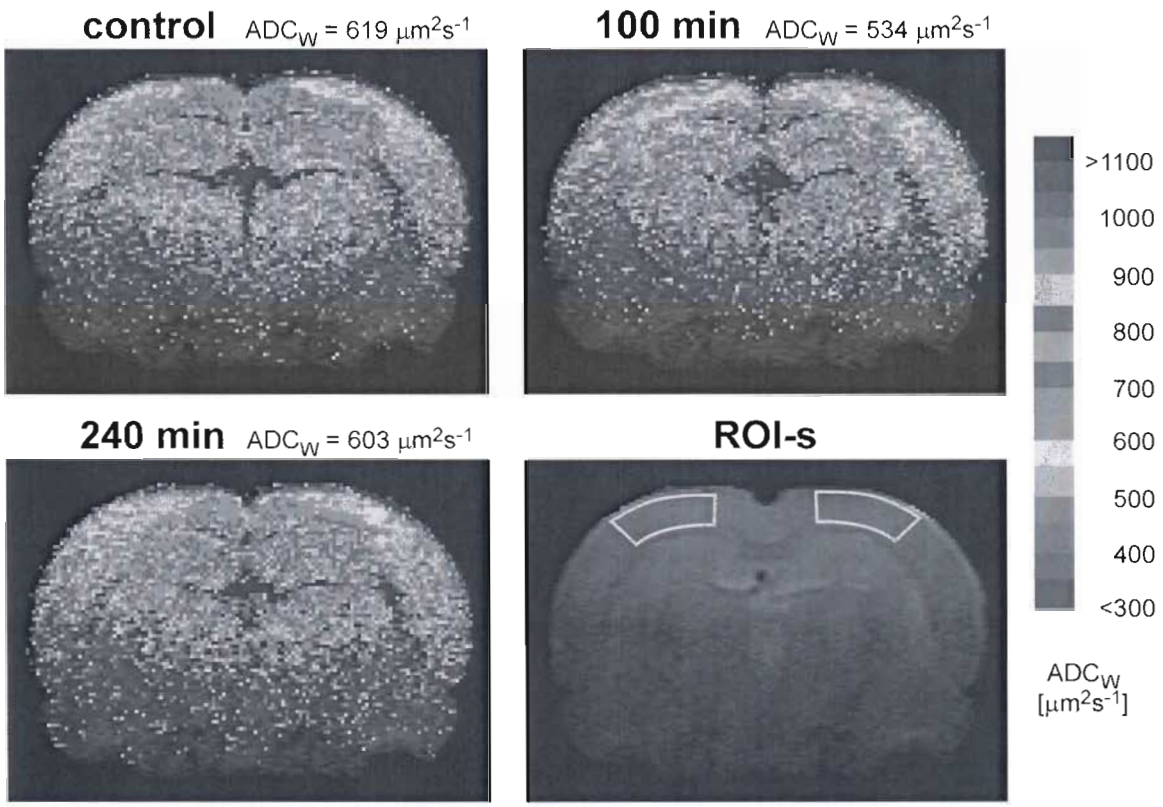

Fig 13: Typical ADC_w maps in a rat before and after pilocarpine injection in the primary somatosensory cortex. The areas are outlined in the T2-weighted image (bottom-right panel). The image shows ADC_w maps taken from the identical coronal plane of the same animal before, 100 and 240 minutes after pilocarpine injection. The scale at the right side of the figure shows the relation between the intervals of ADC_w values and the colors used for visualization. There was a significant decrease in ADC_w in the cerebral cortex 100 minutes after pilocarpine injection. ADC_w returned to control values within four hours (From Slais et al., 2008).

3.4.4. Microdialysis

After a stabilisation period of 60 minutes following probe insertion, the basal cortical level of lactate and the lactate/pyruvate ratio remained stable at 0.61 ± 0.05 mmol/l and 33.16 ± 4.26, respectively (n=8). The application of pilocarpine led to a rise in lactate dialysate levels, reaching a plateau of 2.92 ± 0.60 mmol/l within 100 minutes (Fig. 14 A). The lactate/pyruvate ratio showed a similar time course, reaching a plateau of 84.80 ± 11.72 during the same time interval (Fig. 14 B). Subsequently, lactate levels and the lactate/pyruvate ratio decreased, reaching control values at the end of the experiment. Taking the changes in extracellular volume fraction α into account, the calculated extracellular concentrations of lactate during hypoxia/ischemia would be as much as 30% lower than those actually measured. Basal glucose and glutamate levels were 2.42 ± 0.13 mmol/l and 6.55 ± 1.31 µmol/l, respectively (n=8). Following pilocarpine application, extracellular glucose concentrations increased significantly, reaching a maximum of 3.49 ± 0.24 mmol/l after 40 minutes. In the subsequent recording period, glucose concentrations decreased and dropped below starting values, reaching minimal values of 1.25 ± 0.40 mmol/l at the end of the experiment (Fig 14 C). The calculated glucose concentrations would be even lower if we take the accompanying decrease in ECS volume fraction into account. Extracellular glutamate levels started to increase 40 minutes after the application of pilocarpine and reached maximum values of 22.39 ± 5.85 µmol/l after 100 minutes. Subsequently, the extracellular glutamate levels decreased, reaching control values at the end of the experiment. The calculated concentrations of glutamate, if an increase in α

were taken into account, would be lower than the acquired concentrations (Fig. 14 D).

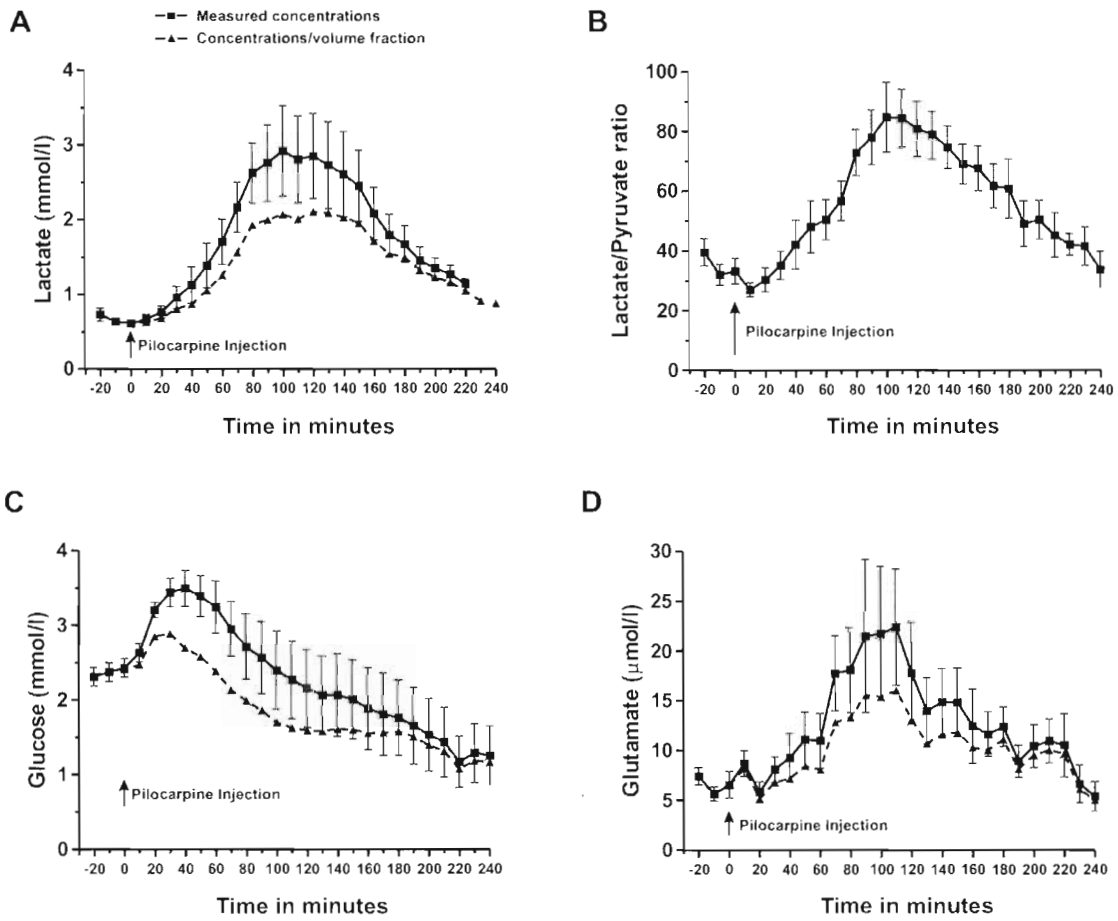

Fig 14: Time course of extracellular lactate concentration (A), the lactate/pyruvate ratio (B), and the extracellular concentrations of glucose (C) and glutamate (D). The time courses of the concentrations of the evaluated metabolites were corrected for changes in ECS volume and are presented as dashed lines. The injection of pilocarpine is marked by an arrow (From Slais et al., 2008).

4. Discussion:

Diffusion in the extracellular space is an important mode of communication between brain cells, and many acute pathological processes in the CNS (i.e. hypoxia, ischemia, seizures, hypoglycaemia), accompanied by cellular swelling, can affect the diffusion of neuroactive substances. Cellular swelling during cerebral hypoxia and ischemia has been described earlier by several authors and is mainly a consequence of massive ionic fluxes across the cell membranes, accompanied by the movement of water, and develops concomitantly with ionic shifts (McKnight and Leaf, 1977; Hansen and Olsen, 1980, Syková et al, 1994). The swelling occurs quickly after the interruption of the energy supply, but never before a rise in K^+ and changes in pH (Sykova et al., 1994).

Before these present investigations, values of the ECS diffusion parameters and values of ADC_w obtained in the rat cortex under hypoxic/ischemic conditions have been reported from experiments using a terminal anoxia model (Van der Toorn et al., 1996; Lundbaek and Hansen, 1992; Sykova et al., 1994). Recently, knowledge of the behaviour of the extracellular diffusion parameters, ADC_w and metabolite levels during and after transient ischemia and hypoxia has been enhanced (Homola et al. 2006; Zoremba et al., 2007; Zoremba et al. 2008). Hypoxia and ischemia of different degree of severity cause substantial changes in the rat cortex. It has been shown that a reduction of inspired oxygen to 8%, although a substantial decrease in oxygen availability, produces no signs of distress in rats, but a further reduction to $\leq$ 7% results in marked restlessness followed by changes in EEG (Jones et al., 2000). Additional reduction in cerebral blood flow can

aggravate the changes and led to substantial changes in extracellular diffusion parameters, metabolite levels, DC-potentials and extracellular potassium levels. Therefore, in all experiments the inspiratory oxygen concentrations was set minimally to 6%, because lower levels result in insufficient circulation due to myocardial hypoxia. Different degrees of cerebral hypoxia and ischemia were achieved by modification in cerebral blood flow.

4.1. Extracellular space diffusion parameters

It is well known that during terminal anoxia, the extracellular space volume decreases to 5-6% of total brain volume (Voříšek and Syková, 1997), which is equivalent to a reduction of 65%-75% from normal values. In the experiments where the animals were exposed to hypoxia without carotid clamping a maximum decrease of the extracellular space of 22% at the end of hypoxia was registered. This hypoxic decrease in ECS volume showed a bi-phasic time course in which the ECS volume decrease during the late-hypoxic period occurred simultaneously with a slow, continuous negative DC-shift without anoxic depolarisation. It is known that negative cortical DC-shifts are associated with changes in oxygen supply (Lehmenkühler et al., 1999). It could be hypothesized that these changes in extracellular space volume were caused by movements of water between the extra- and intracellular compartment or across the blood-brain-barrier into the cortical tissue.

In the experiments in which the severity of hypoxia/ischemia was increased by unilateral carotid occlusion, a continuous decrease of α and an increase of λ during the hypoxic/ischemic insult were found. The final values were not significantly different from those previously found in terminal anoxia

(van der Toorn, 1996; Voříšek and Syková, 1997). Similarly as during terminal anoxia, we observed that the changes in ECS diffusion parameters were accelerated by ischemic depolarization, which usually occurred between 5-10 minutes after the onset of hypoxia/ischemia, suggesting that ionic shifts were also responsible for the initial cellular swelling also in this model. A similar time course for the reduction of ECS size, measured by an electrical impedance technique, was reported by Miyasaka et al. during transient hypoxia/ischemia in the parietal cortex of 4-week-old rats (Qiao et al., 2002). During reperfusion, the tortuosity λ renormalized within 20 minutes, while ECS volume fraction increased and remained elevated about 20% above original normoxic values. This increase in size of ECS corresponds well with findings of increased signals of T1-weighted images and elevated water content in brain cortex of 4-week-old rats after a hypoxic-ischemic insult (Qiao et al. 2004). The authors concluded that changes in T1- but not T2-weighted MRI best serve as indicator of edema associated with an elevation in water content.

In the experimental setting with severe ischemia caused by low inspiratory oxygen content and bilateral carotid occlusion, changes in the extracellular diffusion parameters initially showed the same time course as found in the anoxia experiments. In the group with the shorter ischemic period, the extracellullar diffusion parameter normalized within a short time period. Thus, it could be suggested that this ischemic disturbance is not severe enough to cause any changes. During recovery in the group with longer ischemia, a significant increase in extracellular volume fraction α developed within 40-50 minutes; α remained elevated about 40-50% above the normoxic values, while the tortuosity was initially similar to preischemic values, increasing significantly

at the end of the measurement period. These increase was probably caused by an increase in extracellular water content. Similar time courses of ECS volume fraction and tortuosity were observed in the spinal cord during the recovery from ischemia (Syková et al., 1994).

In the experiments with cerebral seizure activity, we demonstrated that changes in the extracellular volume fraction correlate with changes in ADC_w, similar to the results of a previous study (Syková, et al., 2005). The changes seen in diffusion-weighted images in cases of epilepsy are similar to those observed in early cerebral ischemia (Helpern and Huang, 1995). Our results show that the decrease in ADC_w during SE is caused by a decrease in the volume fraction, without changes in tortuosity, in contrast to findings during ischemia, where a decrease in ADC_w is caused by both a decrease in volume fraction and an increase in tortuosity (van der Toorn, et al., 1996). Possible explanations for this difference are the slower time course of changes in α and the fact that the decrease in α during seizure activity is only moderate (about 30%) in comparison with the 65%-70% reduction in α seen in experimental models of ischemia (Homola, et al., 2006; van der Toorn, et al., 1996; Voříšek and Syková, 1997). It has also been shown that during increase of extracellular potassium concentration up to 20 mM, a decrease of α was registered, while λ stayed unchanged (Sykova et al., 1994). During further increase of extracellular potassium concentration, a further decrease in α was found, accompanied with an increase in λ. Therefore, a strong correlation between the extracellular potassium concentration and the extracellular diffusion properties could be postulated. This is in agreement with the hypothesis that besides excitotoxins (e.g. glutamate), elevated extracellular potassium concentrations are the most

likely mediators of glial cell swelling and, consequently, of changes in ECS diffusion parameters (Sykova, 1992; Sykova et al., 1994; Vargova et al., 2001).

It could be expected that an increase in ECS volume would facilitate extracellular diffusion, but our results show a small increase in tortuosity, indicating a diffusion hindrance and an effect on volume transmission. One reason for this hindered diffusion could be released macromolecules and fixed surface charges, which affect free diffusion by charge-dependent bonding or by van der Waals forces. Increased viscosity impedes molecular movement and is affected by the size and nature of the diffusing molecules and results in their hydrodynamic interactions with macromolecules and fixed charges and the boundaries that define pore structures. Changes in tortuosity λ are influenced by many factors that cannot be presently separated. These factors might include membrane barriers, myelin sheaths, macromolecules, molecules with fixed negative surface charges, extracellular space size and pore geometry. As a result, λ could be changed if certain pathways through the ECS are either blocked off or opened up (Syková et al., 2000). Many studies have shown that λ and α can change independently during the exposure of brain slices to dextran (Hrabetova and Nicholson, 2000), during X-irradiation (Syková et al., 1996) or during osmotic stress (Krizaj et al., 1996; Nicholson and Syková, 1998; Chen and Nicholson, 2000; Kume-Kick, 2002).

The postischemic time course of changes in the extracellular diffusion parameters varied systematically, depending on the severity of the ischemic insult. It has been shown that hypoxia of 30 minutes duration without carotid occlusion lead to a small decrease of α, followed by a quick normalisation during recovery (Zoremba et al., 2007). In contrast to these findings, a hypoxia

of 30 minutes duration with unilateral carotid occlusion caused a decrease in α followed by an increase during recovery to about 20% above original normoxic values (Homola et al., 2006). This postischemic increase in ECS volume fraction was much larger after a more severe ischemia resulting from bicarotid occlusion. Based on these findings, it could be suggested that besides the degree and duration of hypoxia, cerebral blood flow influences the extent of the damage.

4.2. Microdialysis

Microdialysis offers the possibility of obtaining local information on energy metabolism and extracellular metabolite levels *in vivo* in any tissue by introducing a probe directly into the region of interest (Ungerstedt, 1991; Valtysson et al., 1998). In our studies, the microdialysis results were evaluated in relation to the extracellular diffusion parameters to take into account the volume effects on extracellular metabolite concentrations. The onset of hypoxia and seizure activity was accompanied by a significant increase in extracellular lactate concentration. In the experiments with a more severe ischemic insult (unilateral carotid occlusion, 6% O_2), a steeper increase in extracellular lactate concentration was found immediately after the onset of ischemia. The large immediate increase in lactate levels is similar to that reported in previous studies (Harada et al., 1992; Ronne-Engström et al., 1995; Jones et al., 2000). It is well known that the hypoxic elevation of lactate is accompanied by an increase in cerebral blood flow, an increase in glucose uptake and an unchanged rate of oxygen consumption (Hamer et al., 1976; Cohen et al., 1967).

These findings suggest that the increase in lactate concentration is due to an increase in the rate of glycolysis during hypoxia. Extracellular lactate is likely to be derived from glycolysis in both neurones and astrocytes and to reach the extracellular fluid by the action of highly active lactate transporters (Koehler-Stec et al., 1998). After reoxygenation/reperfusion and after reaching maximum seizure activity, elevated lactate levels recovered to pre-ischemic values. This normalisation must represent uptake and utilisation of lactate by neurones and astrocytes, because no significant transport of lactate across the blood-brain barrier has been found in other studies (Kuhr et al., 1988; Harada et al., 1992). In the past decades, lactate has been considered a dead-end waste product of anaerobic glycolysis, contributing to acidosis and tissue damage. Recent studies, however, have shown that lactate can be utilized by neurons as an energy source during aerobic conditions (Bouzier-Sore et al., 2003) and can even support neuronal survival and function during glucose deprivation in organotypic hippocampal slice cultures (Cater et al., 2001). Another study demonstrated a beneficial effect of lactate during the initial phase of reperfusion (Cater et al., 2003). This finding of Cater and colleagues supports studies suggesting that lactate is used as a preferred substrate for the immediate restoration of neuronal ATP after hypoxia (Schurr et al., 1997). In the experiments involving unilateral carotid occlusion, a decrease in extracellular lactate concentration occured, reaching control values within 90 minutes of reoxygenation. This indicates a return to a sufficient oxygen supply and the uptake of lactate, possibly by neurons.

Besides the lactate level as a marker for anaerobic metabolism, the tissue-specific L/P ratio is an excellent indicator of cellular hypoxia, because it is correlated closely with the redox potential (Cabrera et al., 1999; Magnoni et al., 2003). As a marker of anaerobic metabolism, the tissue-specific L/P ratio increased steeply during hypoxia/ischemia, indicating a reversal of the cytosolic redox potential and a switch to anaerobic glycolysis. Another advantage of the L/P ratio is that it is probably not influenced by alterations of the *in vivo* probe recovery (Persson and Hillered, 1992). In these studies a steep increase in the L/P ratio during hypoxia/ischemia as well as during seizure activity was found, which reflects the fact that the cytosolic redox condition switched from aerobic to anaerobic glycolysis. During recovery from hypoxia/ischemia and after passing the maximum degree of seizure activity, a steep decrease in the L/P ratio indicated a return to the aerobic pathway of energy production. These results show that the metabolic enzymes and their related cellular components (e.g. mitochondria) may tolerate longer hypoxic periods without any serious damage. Despite a number of studies showing that lactate and ketone bodies are used for energy supply, particularly for neurons, glucose still plays an essential role in brain metabolism (Pellerin et al., 2004).

The concentration of glucose in the ECF is a balance between supply from the blood and utilization by the cells, and possibly both mechanisms are involved in the decrease seen during hypoxia/ischemia in these experiments. During hypoxia, a fast decrease in glucose levels was found in the experiments, similar to the findings of Silver and Erecinska (1994) using an implanted glucose sensor. A possible explanation for this drop in extracellular glucose could be the increased uptake and utilisation by glycolysis found during hypoxia

(Hamer et al., 1976; Fray et al., 1997). Increased glycolysis results in the consumption of glucose and the production of lactate, which is transported into the extracellular space. This hypothesis is supported by the correlation seen in our results between a decrease in glucose and an increase in lactate levels. In the recovery from hypoxia, a normalisation of extracellular glucose levels occurs within 20 minutes, indicating on the one hand a quick normalisation in the uptake and utilisation by the cells and on the other hand a sufficient supply from the blood. In the recovery from severe ischemia (unilateral carotid occlusion) the glucose concentration returned to initial values within 20 minutes and then slightly decreased again. This small drop is probably caused by a dilution effect of vasogenic edema. The time course of changes in extracellular glucose levels during seizure activity was different and initially showed a small increase. Similar results were found in the rat striatum after maximal electroschocks (Darbin et al., 2005). The ECS volume fraction is possibly a factor contributing to the transient increase in glucose concentration. However, as seizures continue, high cerebral metabolic rates (Fernandes et al., 1999) caused by increased uptake and glycolysis during increased neuronal activity during the seizure (Fray et al., 1997) could be the cause of the subsequent decrease in glucose concentration starting one hour after pilocarpine administration and continuing until the end of our experiments.

In the hypoxia experiments, changes in extracellular glutamate concentration occurred in the late hypoxic and early reoxygenation phases. It has been shown that hypoxia-induced anoxic depolarisation can be delayed at least up to 60 minutes and that during this time a hypoxic transient hypoxic extracellular glutamate increase is seen, derived from the Ca^{2+} dependent

neurotransmitter pool (Kunimatsu et al., 1999; Katayama et al., 1991). The inhibition of the reversed action of Ca^{2+} transporters such as the Na^{+}/Ca^{2+}-exchanger or Ca^{2+}/H^{+}-ATPase might constitute a source of cellular Ca^{2+} accumulation during hypoxia (Blaustein and Lederer, 1999; Kulik et al., 2000). It seems that an increase in cellular Ca^{2+} occurs during hypoxia until critical levels are reached. The consequence is a glutamate release, which is initiated at the end of the hypoxic period and proceed in the early posthypoxic period. Based on the time course of changes in extracellular volume fraction α, it can be hypothesized that a massive glutamate release occur after 30 minutes of hypoxia. This release elevated the concentration of glutamate in the sample which was collected in the last 10 minutes of hypoxia only to a minor degree. The main effect of the glutamate release at the end of hypoxia was found in the first postischemic sample. Thus, it appears that a considerable release of glutamate at the beginning of the first postischemic collection period caused a large increase of glutamate levels in the first postischemic sample, which was collected over a time period of 10 minutes. During reoxygenation, glutamate levels recovered to basal values, indicating a sufficient reuptake by astrocytes. In the ischemia experiments with unilateral carotid occlusion, the concentration of glutamate in the ECF started to increase soon after the onset of hypoxia/ischemia and continued to increase to a level 10-fold above control values at the end of the insult. If the concomitant reduction in ECS volume fraction is taken into account, the actual glutamate concentration would be about 50% lower. The activation of glutamate receptors may result in rapid cellular swelling (Hansson, 1994). However, only very high concentrations (10^{-2} M) have been shown to cause a substantial decrease in the ECS volume in the

isolated spinal cord of rat pups under normoxic conditions (Vargova et al., 2001). Because such concentrations are not achieved even under pathological conditions, it was suggested that glutamate-induced astrocytic swelling *in vivo* could be indirect and mediated by glutamate´s effects on neuronal cells, such as increases in the extracellular potassium concentration promoted by neuronal depolarization (Kimelberg, 2005). Increases in the extracellular concentration of glutamate during brain ischemia and the excessive activation of its receptors is believed to be a major cause of ischemia-related neuronal injury (Benveniste et al., 1984).

4.3. Diffusion weighted MRI

Although a substantial amount of data obtained by DWI-MRI exists on extra- and intracellular diffusion in areas affected by an ischemic/hypoxic insult, the absolute values of the extracellular diffusion parameters measured in the brain cortex during recovery from severe ischemia have not been available. In our severe ischemia experiments, the increase in ECS volume fraction after reperfusion correlated well with changes in the ADC of brain water. The values of ADC_w obtained 60 and 90 min after reperfusion were significantly elevated, suggesting an increased amount of water in the ECS, where ADC_w was reported to be higher, compared to the intracellular compartment (Van Zijl et al., 1991). A correction of orientational dependence was not made, because it was shown in previous studies that there is no significant anisotropy in this part of the rat brain (Voříšek and Syková, 1997). In an earlier study a full recovery of the diffusion constant of brain water was found after 12 minutes of incomplete global ischemia (Davis et al., 1994). The results are comparable with the results

in the 10 minute ischemia group. In contrast to this study, we also performed measurements during and after an ischemia of 15 minutes duration, i.e., a more severe ischemic insult. During recovery from this longer-lasting global ischemia, a significant increase in extracellular volume fraction developed within 60 minutes, probably caused by an increase in extracellular water content. The increase in ECS volume fraction after reperfusion correlates well with changes in the cortical ADC_w. These findings support the hypothesis that in the recovery from severe ischemia, a cerebral vasogenic edema develops.

Using an experimental model of pilocarpine-induced seizure activity, different results were found because during seizure activity a decrease in ADC_w was observed. Similar results have been seen in previous studies (van Eijsden, et al., 2004, Wall, et al., 2000). The changes that have been seen in ADC_w, in combination with a decrease in the extracellular volume fraction, can be explained by a reduction in the size of the ECS due to cellular swelling. The changes seen in diffusion-weighted images in cases of epilepsy are similar to those observed in early cerebral ischemia (Helpern and Huang, 1995).

DW-MRI, a non-invasive method to determine λ and the diffusion coefficient of water, can be used without known complications in humans. These parameters describe diffusion in the brain, but without knowledge of the extracellular diffusion properties measured with the TMA method, the interpretation of the registered changes could be misleading. Therefore, a combination of both of these methods allows a satisfactory description and interpretation of the changes in the diffusion properties in the brain cortex after ischemic/hypoxic events.

4.4. Extracellular potassium concentration and DC-potentials

Hypoxic and ischemic periods can affect the extracellular potassium concentrations and cortical DC-potentials (Lehmenkühler et al., 1999). In the experiments during hypoxia without carotid clamping, a late-hypoxic continuous negative DC-shift was registered. This indicates changes due to a disturbance in oxygen supply, but not severe enough to evoke a cortical anoxic depolarisation. Anoxic depolarisation was found in the ischemia experiments with bilateral carotid clamping. In comparing the DC-potentials, a longer recovery period was necessary in animals subjected to an ischemia of 15 minutes. During ischemia an increase in extracellular potassium levels up to 70 mM was registered, while recovery in both groups was comparable within a few minutes. These findings indicate that the cellular energy state is affected in the same way in both groups, but that the intercellular integrity due to neurotoxicity was more affected in the group that underwent a longer ischemia. It is well known that after ischemia, functional damage of the blood-brain barrier occurs (Qiao et al., 2001) and the hypoxic-ischemic insult initiates a series of events that leads to the disruption of tight junctions and increased permeability mediated by cytokines, VEGF and NO (Ballabh et al., 2004). Due to increased permeability, reperfusion may lead to an early postischemic increase in cerebral water content and to the formation of cortical edema of "vasogenic" origin (Papadopoulos et al., 2005). These changes could also additionally be caused by elevated postischemic tissue osmolarity (Gisselson et al., 1992) or by postischemic shrinkage of nerve cells. It is evident that an ischemia of 10 minutes duration is too short to initiate a cascade of events that lead to a disruption of the blood-brain barrier and the development of vasogenic edema.

This hypothesis is supported by the different time courses of the DC-potential recovery seen in the two groups.

During seizure activity extracellular potassium concentrations increased markedly. It has been shown in previous studies, that experimental convulsions increase extracellular potassium concentrations due to prolonged neuronal depolarization (Macias et al., 2001). Increased metabolism during a seizure causes a depletion of adenosine triphosphate and energy reserves at its later stage. Consequently, this results in impaired ion exchange pump functions and increased membrane ion permeability of the cells, leading to an increase in extracellular potassium concentrations and the accumulation of intracellular Ca^{2+} (Wasterlain, et al., 1993). Accompanied by an increase in extracellular potassium concentrations, cellular swelling occurs. These findings support the MRI results, in which we found a decrease in ADC_w during seizure activity. A dependence of changes in α caused by cellular swelling on changes in the extracellular potassium concentration can also be seen in these results, and a normalization of elevated extracellular potassium concentration leads to a quick normalization of α to control values.

5. Conclusions

Cerebral edema with subsequent brain swelling is the most life threatening consequence of a focal ischemic insult to the brain and can occur in the presence of an intact blood-brain barrier or as a consequence of barrier disruption (Betz et al., 1989). In these studies, a correlation between the severity of the hypoxic or ischemic insult and the development of a brain edema of vasogenic origin could be demonstrated. This increase in extracellular water content caused by a vasogenic edema in turn causes changes in the diffusion properties of the tissue.

In detail, our findings suggest that the extracellular microenvironment of the cerebral cortex may tolerate 30 minutes of hypoxia and that changes occurring during this period can subsequently recover to preischemic values. These results support the clinical observation that young adult patients with hypoxia, caused by acute lung failure or difficult or prolonged airway management during the induction of anaesthesia, can recover without any obvious neurological changes. In more severe hypoxic/ischemic conditions, due to unilateral or bilateral carotic artery occlusion, similar changes in the ECS diffusion parameters occur as found during global anoxia. The observed reduction in ECS volume, reflecting cytotoxic edema, correlates well with the time course of the elevation in extracellular glutamate concentration.

We have also shown the impact of the ECS volume on the concentrations of substances diffusing through the ECS, evidencing to what degree ECS shrinkage contributes to the increased concentrations of toxic metabolites. After ischemia/hypoxia the ECS volume fraction recovers and increases to values 50% above the starting level. The changes in the other

diffusion parameters indicate that an edema of vasogenic origin develops. The postischemic/posthypoxic changes in the extracellular diffusion parameters may affect the diffusion of various substances (ions, neurotransmitters, metabolites and drugs) to the affected region. Our results show that after ischemia of 15 minutes or longer, the observed changes in the ECS diffusion parameters are not reversible within 90 minutes and result in long-lasting and severe edema and perhaps permanent damage. In experiments with pathologically increased neuronal activity induced by pilocarpine, seizure causes cell swelling followed by a reduction in the ECS volume fraction, which can contribute to the accumulation of toxic metabolites and lead to the start of epileptic discharges. These changes, based on an increased consumption of oxygen and other substrates, are similar to those found in hypoxia/ischemia.

Diffusion in the ECS is the underlying mechanism of extrasynaptic volume transmission and intercellular, particularly neuron-glia communication (Syková, 1997). We can thus assume that the observed changes in the diffusion properties of the ECS affect the diffusion of ions, neurotransmitters and metabolic substances, as well as various drugs used in the therapy of nervous system diseases. These changes in diffusion may persist for a long period after an ischemic episode and affect nonsynaptic volume transmission in the CNS. Studies at longer ischemic and postischemic periods are needed to determine the crucial point beyond which the effects are irreversible.

Acknowledgement

These studies were supported by European Community HPMT-CT-2000-00187 and by the grants AVCR AV0Z50390512, MSMT LC554 and GACR 305/061316.

6. Summary:

The extracellular space (ECS) of the brain represents the microenvironment of nerve cells and enables the diffusion of neuroactive substances among neurons, axons and glia. Changes in the ECS diffusion parameters during ischemia are well known, but information about changes in ECS diffusion and energy-related metabolite concentrations in the postischemic and posthypoxic periods is insufficient.

Postischemic and posthypoxic diffusion changes were studied in the rat somatosensory cortex in different experimental models. In one model a transient global hypoxia of 30 minutes duration was induced in adult male Wistar rats by reducing inspired oxygen to 6% O_2 in nitrogen. Intracerebral microdialysis was utilized to monitor changes in the energy-related metabolites lactate, pyruvate, glucose and glutamate in the cortex before, during and after global hypoxia. Changes in metabolite levels were compared with the ECS diffusion parameters volume fraction (α) and tortuosity (λ), determined by the real-time iontophoretic method of diffusion analysis. In other models, transient ischemia was induced in rats by unilateral common carotid artery clamping for 30 minutes or by bilateral clamping for 10 or 15 minutes and concomitant ventilation with 6% O_2 in nitrogen. Volume fraction and tortuosity were measured using the TMA^+ method, and diffusion-weighted magnetic resonance imaging (DW-MRI) was used to determine the apparent diffusion coefficient of water (ADC_w) in the tissue. In a model of elevated oxygen consumption, seizure activity was evoked by an injection of pilocarpine.

In the hypoxia experiments, α decreased by about 5% from 0.18 ± 0.01 during the first 20-25 minutes of hypoxia, followed by a further drop of 22% to

0.14 ± 0.01 after 25 minutes. Within 10 minutes of reoxygenation, α returned to control values, then increased to 0.20 ± 0.01 and remained at this level. Significant increases in lactate concentration and the lactate/pyruvate ratio, as well as decreased glucose levels, were found in the cortex immediately after the induction of hypoxia. Following recovery, extracellular lactate and glucose levels and the lactate/pyruvate ratio returned to control levels within 40, 20 and 30 minutes, respectively. Glutamate levels started to increase 20-30 minutes after the onset of hypoxia and returned to prehypoxic values within 30-40 minutes of reoxygenation. The observed 22% decrease in α markedly influenced the dialysate levels measured during hypoxia.

The results from the ischemia experiments were different. Unilateral carotid artery occlusion led to a decrease in α from 0.19 ± 0.03 to 0.07 ± 0.01 and an increase in λ from 1.57 ± 0.01 to 1.88 ± 0.03. During reperfusion, α returned to control values within 20 minutes and then increased to 0.23 ± 0.01, while λ only returned to control values (1.53 ± 0.06). The concentrations of lactate and glutamate, and the lactate/pyruvate ratio, substantially increased during ischemia, followed by continuous recovery during reperfusion. The glucose concentration decreased rapidly during ischemia with a subsequent return to control values within 20 minutes of reperfusion. Using bilateral carotid artery occlusion, in both the 10 minutes group and the 15 minutes group a negative DC-shift accompanied by increased potassium levels occured after 1-2 minutes of ischemia, then recovered to preischemic values within 3-5 minutes of reperfusion. During ischemia, α decreased to 0.07 ± 0.01 in both groups, while λ increased to 1.80 ± 0.02. In the group of 10 minutes ischemia, normal values of α=0.20 ± 0.01 and λ=1.55 ± 0.01 were registered within 5-10 minutes of

reperfusion. ADC_w recovered within 60 minutes to preischemic values (597 ± 14 $\mu m^2 s^{-1}$ preischemic vs. 608 ± 8 $\mu m^2 s^{-1}$ postischemic) and remained at this level. After 15 minutes of ischemia, α increased within 40-50 minutes of reperfusion to 0.29 ± 0.03 and remained at this level. λ increased to 1.81 ± 0.02 during ischemia, recovered within 5-10 minutes of reperfusion and increased to 1.62 ± 0.01 at the end of the experiment. ADC_w increased within 60 minutes after ischemia to 665 ± 15 $\mu m^2 s^{-1}$ and stayed at this level during the postischemic measurement period of 90 minutes.

During elevated oxygen consumption due to seizure activity, α and ADC_w decreased to minimums of 0.13 ± 0.01 and 549 ± 8 $\mu m^2 s^{-1}$ after 100 minutes, then recovered to 0.18 ± 0.01 and 603 ± 11 $\mu m^2 s^{-1}$ at the end of the recording period, respectively. No significant changes in λ were observed during the time course of the experiment. The basal cortical levels of lactate, the lactate/pyruvate ratio, glucose and glutamate were 0.61 ± 0.05 mmol/l, 33.16 ± 4.26, 2.42 ± 0.13 mmol/l and 6.55 ± 1.31 µmol/l, respectively. Pilocarpine application led to a rise in lactate, the lactate/pyruvate ratio and glutamate levels, reaching 2.92 ± 0.60 mmol/l, 84.80 ± 11.72 and 22.39 ± 5.85 µmol/l within about 100 minutes, then recovered to starting values by the end of the experiment. The time course of changes in glucose levels was different, with maximal levels of 3.49 ± 0.24 mmol/l reached 40 minutes after pilocarpine injection, while a subsequent decrease to 1.25 ± 0.40 mmol/l was observed 200 minutes later. Pathologically increased neuronal activity induced by pilocarpine causes cell swelling followed by a reduction in the ECS volume fraction, which can contribute to the accumulation of toxic metabolites and lead to the start of epileptic discharges.

The data represent *in vivo* changes in the cortical extracellular diffusion parameters during recovery from transient hypoxia/ischemia of different degrees and causes. The observed substantial changes in the extracellular diffusion parameters and ADC_w affect the diffusion of ions, neurotransmitters, metabolic substances and drugs used in the treatment of nervous system diseases. Additionally, extracellular decreases in substrates and increases in metabolite levels during and after ischemic/hypoxic events may affect the function of neuronal structures and the ionic balance of the microenvironment. In conclusion, the observed changes may aggravate functional deficits and lead to damage of the central nervous system.

7. References:

AGNATI L.F., ZOLI M., STROMBERG I., FUXE K. (1995) Intercellular communication in the brain: wiring versus volume transmission. *Neuroscience 69*: 711-726.

AMES III A., NESBETT F.B. (1983) Pathophysiology of ischemic cell death: II. Changes in plasma membrane permeability and cell volume. *Stroke 14: 227-233*

ANDEROVA M., KUBINOVA S., MAZEL T., CHVATAL A., ELIASSON C., PEKNY M., SYKOVA E. (2001) Effect of elevated K^+, hypotonic stress, cortical spreading depression on astrocyte swelling in GFAP-deficient mice. *Glia 35: 189-203*

BALLABH P., BRAUN A., NEDERGAARD M. (2004) The blood-brain barrier: an overview Structure, regulation and clinical implications. *Neurobiology of Disease. 16: 1-13*

BETZ A.L., IANOTTI F., HOFF J.T. (1989) Brain edema: A classification based on blood-brain barrier integrity. *Cerebrovasc. Brain Metab. Rev. 1: 133-154*

BENVENISTE H., DREJER J., SCHOUSBOE A., DIEMER N.H. (1984) Elevation of the extracellular concentrations of glutamate and aspartate in rat hippocampus during transient cerebral ischemia monitored by intracerebral microdialysis. *J Neurochem. 43: 1369-1374.*

BLAUSTEIN M.P., LEDERER W.J. (1999) Sodium/calcium exchange: its physiological implications. *Physiol Rev 79: 763-854*

BOUZIER-SORE A.K., VOISIN P., CANIONI P., MAGISTRETTI P.J., PELLERIN L. (2003) Lactate is a preferential oxidative energy substrate over glucose for neurons in culture. *J Cereb Blood Flow Metab 23: 1298-306*

BURES J., BURESOVA O., KRIVANEK J. (1974) The mechanism and application of Leao´s spreading depression of electroencephalographic activity. *New York, Academic Press*

CABRERA M.E., SAIDEL G.M., KALHAN S.C. (1999) A model analysis of lactate accumulation during muscle ischemia. *J Crit Care 14(4): 151-163*

CATER H.L., BENHAM C.D., SUNDSTROM L.E. (2001) Neuroprotective role of monocarboxylate transport during glucose deprivation in slice cultures of rat hippocampus. *J Physiol 531: 459-66*

CATER H.L., CHANDRATHEVA A., BENHAM C.D., MORRISON B., SUNDSTROM L.E. (2003) Lactate and glucose as energy substrates during, and after, oxygen deprivation in rat hippocampal acute and cultured slices. J *Neurochem. 87: 1381-90*

CHEN K.C., NICHOLSON C. (2000) Changes in brain cell shape create residual extracellular space volume and explain tortuosity behavior during osmotic challenge. *Proc. Natl. Acad. Sci. USA 15: 8306-8311*

CLOUGH R.W., NEESE S.L., SHERILL L.K., TAN A.A., DUKE A., ROOSEVELT R.W., BROWNING R.A., SMITH D.C. (2007) Cortical edema in moderate fluid percussion brain injury is attenuated by vagus nerve stimulation. *Neuroscience 147: 286-293*

COHEN P.J., ALEXANDER S.C., SMITH T.C., REIVICH M., WOLLMAN H. (1967) Effects of hypoxia and normocarbia on cerebral blood flow and metabolism in conscious man. *J Appl Physiol 23: 183-189*

CSERR H.F., DePASQUALE M., NICHOLSON C., PATLAK C.S., PETTIGREW K.D., RICE M.E. (1991) Extracellular volume decreases while cell volume is maintained by ion uptake in rat brain during acute hypernatremia. *J Physiol 442: 277-295*

DARBIN O., RISSO J. J., CARRE E., LONJON M., NARITOKU D. K. (2005) Metabolic changes in rat striatum following convulsive seizures. *Brain Res 1050: 124-129*

DAVIS D., ULATOWSKI J., ELEFF S., IZUTA M., MORI S., SHUNGU D., VAN ZIJL P.C.M. (1994) Rapid monitoring of changes in water diffusion coefficients during reversible ischemia in cat and rat brain. *Magn Res Med 31: 454-460*

DE SALLES A.A., KONTOS H.A., BECKER D.P. (1986) Prognostic significance of ventricular CSF lactic acidosis in severe head injury. *J Neurosurg 65: 615-624*

FELLOWS L.K., BOUTELLE M.G., FILLENZ M. (1992) Extracellular brain glucose levels reflect local neuronal activity: a microdialysis study in awake, freely moving rats. *Neurochem 59: 2141-2147*

FENSTERMACHER J.D., KAYE T. (1988) Drug diffusion within the brain. *Ann NY Acad Sci 531: 29-39*

FERNANDEZ M. J., DUBE C., BOYET S., MARESCAUX C., NEHLIG A. (1999) Correlation between hypermetabolism and neuronal damage during status epilepticus induced by lithium and pilocarpine in immature and adult rats. *J Cereb Blood Flow Metab 19: 195-209*

FICK A. (1995) On liquid diffusion. *J Membr Sci 100: 33-38*

FISHER M., BLOCKHORST K., HOEHN-BERLAGE M., SCHMITZ B., HOSSMANN K.-A. (1995) Imaging of the apparent diffusion coefficient for the evaluation of vertebral metabolic recovery after cardiac arrest. *Mag Res Imag 13: 781-790*

FRAY A.E., BOUTELLE M., FILLENZ M. (1997) Extracellular glucose turnover in the striatum of unanaesthetized rats measured by quantitative microdialysis. *J Physiol 504: 721-726*

FUXE K., AGNATI L.F. (1991) Volume transmission in the brain. Novel mechanisms for neural transmission, New York, Raven Press, 1-602

GISSELSON L., SMITH M.L., SIESJÖ B.K. (1992) Influence of preischemic hyperglycemia on osmolality and early postischemic edema in the rat brain. *J. Cereb. Blood Flow Metab. 12: 809-816*

HAMER J., HOYER S., ALBERTI E., WEINHARDT F. (1976) Cerebral blood flow and oxidative brain metabolism during and after moderate and profound arterial hypoxaemia. *Acta Neurochir. 33: 141-150*

HANSEN A.J., OLSEN C.E. (1980) Brain extracellular space during spreading depression and ischemia. *Acta Physiol. Scand. 108: 355-365*

HANSEN A.J. (1985) Effect of anoxia on ion distribution of the brain. *Physiol Rev. 65: 101-148*

HANSSON E. (1994) Metabotropic glutamate receptor activation induces astroglial swelling. *J Biol Chem. 269: 21955-21961*

HARADA M., OKUDA C., SAWA T., MURAKAMI T. (1992) Cerebral extracellular glucose and lactate concentrations during and after moderate hypoxia in glucose- and saline-infused rats. *Anesthesiology 77: 728-734*

HELPERN J. A., HUANG N. (1995) Diffusion-weighted imaging in epilepsy. *Magn Reson Imaging 13: 1227-1231*

HILLERED L., HALLSTROM A., SEGERSVARD S., PERSSON L., UNGERSTEDT U. (1989) Dynamics of extracellular metabolites in the striatum after middle cerebral artery occlusion in the rat monitored by intracerebral microdialysis. *J Cereb Blood Flow Metab 9: 607-616*

HOMOLA A., ZOREMBA N., SLAIS K., KUHLEN R., SYKOVA E. (2006) Changes in diffusion parameters, energy-related metabolites and glutamate in the rat cortex after transient hypoxia/ischemia. *Neurosci Lett. 404: 137-142*

HORSTMANN E., MEVES H. (1959) Die Feinstruktur des molekulären Rindengrauens und ihre physiologische Bedeutung. *Z Zellforschung 49: 569-604*

HOSSMANN K.A. (1971) Cortical steady potential, impedance and excitability changes during and after total ischemia of cat brain. *Exp Neurol 32: 163-175*

HRABETOVA S., NICHOLSON C. (2000) Dextran decreases extracellular tortuosity in thick-slice ischemia model. *J. Cereb. Blood Flow Metab. 20: 1306-1310*

HRABETOVA S; HRABE J., NICHOLSON C. (2003) Dead-space microdomains hinder extracellular diffusion in rat neocortex during ischemia. J Neurosci 23: 8351-8359

INAO S., MARMAROU A., CLARKE G.D. (1998) Production and clearance of lactate from brain tissue, cerebrospinal fluid, and serum following experimental brain injury. *J Neurosurg 69: 736-744*

JOHNSON E.M., BERK D.A., JAIN R.K., DEEN W.M. (1996) Hindered diffusion in agarose gels : test of effective medium model. *Biophys J 70: 1017-1023*

JONES A.D., ROS J., LANDOLT H., FILLENZ M., BOUTELLE M.G. (2000) Dynamic changes in glucose and lactate in the cortex of the freely moving rat monitored using microdialysis. *J Neurochem 75: 1703-1708*

KATAYAMA Y., KAWAMATA T., TAMURA T., HOVDA D.A., BECKER D.P., TSUBOKAWA T. (1991) Calcium-dependent glutamate release concomitant with massive potassium flux during cerebral ischemia in vivo. *Brain Res 558: 136-140*

KATAYAMA Y., TAMURA T., BECKER D.P., TSUBOKAWA T. (1992) Early cellular swelling during cerebral ischemia in vivo is mediated by excitatory amino acids released from nerve terminals. *Brain Research 577: 121-126*

KILB W., DIERKES P.W., SYKOVA E., VARGOVA L., LUHMANN H.J. (2006) Hypoosmolar conditions reduce extracellular volume fraction and enhance epileptiform activity in the CA3 region of the immature rat hippocampus. *J Neurosci Res 84: 119-129*

KIMELBERG H.K. (2005) Astrocytic swelling in cerebral ischemia as a possible cause of injury and target for therapy. *Glia 50: 389-397*

KOEHLER-STEC E., SIMPSON I., VANUCCI S., LANDSCHULZ K., LANDSCHULZ W. (1998) Monocarboxylate transporter expression in mouse brain. *Am J Physiol 273: 516-524*

KRIZAJ D., RICE M.E., WARDLE R.A., NICHOLSON C. (1996) Water compartmentalization and extracellular tortuosity after osmotic changes in cerebellum of Trachemys scripta. *J. Physiol. 492: 887-896*

KUFFLER S.W., POTTER D.D. (1964) Glia in the leech central nervous sytem: physiological properties and neuron-glia relationship. *J Neurophysiol 27: 290-320*

KUHR W.G., VAN DEN BERG C.J., KORF J. (1988) In vivo identification and quantitative evaluation of carrier mediated transport of lactate at the cellular level in the striatum of conscious, freely moving rats. *J Cereb Blood Flow Metab 8: 848-857*

KULIK A., TRAPP S., BALLANYI K. (2000) Ischemia but not anoxia evokes vesicular and Ca2+-Independent Glutamate release in the dorsal vagal complex in vitro. *J Neurophysiol 83: 2905-2915*

KUME-KICK J., MAZEL T., VORISEK I., HRABETOVA S., TAO L., NICHOLSON C. (2002) Independence of extracellular tortuosity and volume fraction during osmotic challange in rat neocortex. *J. Physiol. 542: 515-527*

KUNIMATSU T., ASAI S., KANEMATSU K., ZHAO H., KOHNO T., MISAKI T., ISHIKAWA K. (1999) Transient in vivo membrane depolarization and glutamate release before anoxic depolarization in rat striatum. *Brain Res 831: 273-282*

LE BIHAN D., BRETON E., LALLEMAND D., GRENIER P., CABANIS E., LAVAL-JEANTET M. (1986) MR imaging of intravoxel incoherent motions: application to diffusion and perfusion in neurologic disorders. *Radiology 161: 401-407*

LE BIHAN D., BASSER P.J. (1995) Diffusion and perfusion magnetic resonance imaging: applications to functional MRI. Raven Press, New York.

LEHMENKÜHLER A., SYKOVA E., SVOBODA J., ZILLES K. (1993) Extracellular space in rat neocortex and subcortical white matter during postnatal development determined by diffusion analysis. *Neuroscience 55: 339-351*

LEHMENKÜHLER A., RICHTER F., POPPELMANN T. (1999) Hypoxia and hypercapnia-induced DC potential shifts in rat at the scalp and the skull are opposite in polarity to those at the cerebral cortex. *Neurosci Lett 270: 67-70*

LEVIN V.A., FENSTERMACHER J.D., PATLAK C.S. (1970) Sucrose and inulin space measurements of cerebral cortex in four mammalian spezies. *Am J Physiol 219: 1528-1533*
LUNDBAEK J.A., HANSEN A.J. (1992) Brain interstitial volume fraction and tortuosity in anoxia. Evaluation of the ion-selective microelectrode method. *Acta Physiol. Scand. 146: 473-484*

MAGISTRETTI P.J., SORG O., YU N., MARTIN J.L., PELLERIN L. (1993) Neurotransmitters regulate energy metabolism in astrocytes: Implications for the metabolic trafficking between neuronal cells. *Dev Neurosci 15: 306-312*

MAGNONI S., GHISONI L., LOCATELLI M. (2003) Lack of improvement in cerebral metabolism after hyperoxia in severe head injury: a microdialysis study. *J Neurosurg 98: 952-958*

MAROUDAS A., WEINBERG P.D., PARKER K.H., WINLOVE C.P. (1988) The distributions and diffusivities of small ions in chondroitin sulphate, hyaluronate and some proteoglycan solutions. *Biophys Chem 32: 257-270*

MACIAS W., CARLSON R., RAJADHYAKSHA A., BARCZAK A., KONRADI C. (2001) Potassium chloride depolarization mediates CREB phosphorylation in striatal neurons in an NMDA receptor-dependent manner. *Brain Res 890: 222-232*

MAZEL T., RICHTER F., VARGOVÁ L., SYKOVÁ E. (2002) Changes in extracellular space volume and geometry induced by cortical spreading depression in immature and aduts rats. Physiol. Res. 51(Suppl1):S85-93

McKNIGHT A.D.C., LEAF A. (1977) Regulation of cellular volume. *Physiol Rev 57: 510-573*

MIZOCK B.A., FALK J.L. (1992) Lactic acidosis in critical illness. *Crit Care Med 20: 80-93*

NOVAK U., KAYE A.H. (2000) Extracellular matrix and the brain: components and function. *J Clin Neurosci 7: 280-290*

NICHOLSON C. (1979) Brain cell microenvironment as a communication channel. In F.O. Schmitt and F.G. Worden, *The Neurosciences: Fourth Study Programm, Cambridge, MA: M.I.T. Press, 457-476*

NICHOLSON C., PHILLIPS J.M. (1981) Ion diffusion modified by tortuosity and volume fraktion in the extracellular microenvironment of the rat cerebellum. *J. Physiol. 321: 225-257*

NICHOLSON C. (1992) Quantitative analysis of extracellular space using the method of TMA^+ iontophoresis and the issue of TMA^+ uptake. *Can. J. Physiol. Pharmacol. 70: 314-322*

NICHOLSON C., TAO L. (1993) Hindered diffusion of high molecular weight compounds in brain extracellular microenvironment measured with integrative optical imaging. *Biophys J 65: 2277-2290*

NICHOLSON C., SYKOVA E. (1998) Extracellular space structure revealed by diffusion analysis. *Trends Neurosci 21: 207-215*

NICHOLSON C. (2001) Diffusion and related transport mechanismus in brain tissue. *Rep. Prog. Phys. 64: 815-884*

ORMANDY G. C., SONG L., JOPE R. S. (1991) Analysis of the convulsant potentiating effects of lithium in rats. *Exp Neurol. 111: 356-361*

PAPADOPOULOS M.C., BINDER D.K., VERKMAN A.S. (2005) Enhanced macromolecular diffusion in brain extracellular space in mouse models of vasogenic edema measured by cortical surface photobleaching. *FASEB J 19: 425-427*

PATLAK C.S., FENSTERMACHER J.D. (1975) Measurements of dog blood-brain barrier transfer constants by ventriculocisternal perfusion. *Am J Physiol 229: 877-884*

PAXINOS G., WATSON C. (1998) The rat brain atlas. *Academic Press*, Fourth edition.

PELLERIN L., MAGISTRETTI P.J. (2004) Neuroenergetics: calling upon astrocytes to satisfy hungry neurons. *Neuroscientist 10: 53-62.*

PÉREZ-PINZÓN M.A., TAO L., NICHOLSON C. (1995) Extracellular potassium, volume fraction and tortuosity in rat hippocampal CA1, CA3 and cortical slices during ischemia. *J. Neurophysiol. 74: 565-573*

PERSSON L., HILLERED L. (1992) Chemical monitoring of neurosurgical intensive care patients using intracerebral microdialysis. *J Neurosurg 76: 72-80*

PHILLIS J.W., REN J., O´REGAN M.H. (2001) Studies on the effects of lactate transport inhibition, pyruvate, glucose and glutamine on amino acid, lactate and glucose release from the ischemic rat cerebral cortex. *J Neurochem 76: 247-257*

PRICHARD J., ROTHMAN D., NOVOTNY E., PETROFF O., KUWABARA T., AVISON M., HOWSEMAN A., HANSTOCK C., SHULMAN R. (1991) Lactate rise detected by 1 H NMR in human visual cortex during physiologic stimulation. *Proc Natl Acad Sci USA 88: 5829-5831*

QIAO M., MALISZA K.L., DelBIGIO M.R., TUOR U.I. (2001) Correlation of cerebral hypoxic-ischemic T2 changes with tissue alterations in water content and protein extravasation. *Stroke 32: 958-963*

QIAO M., MALISZA K.L., Del BIGIO M.R., TUOR U.I. (2002) Transient hypoxia-ischemia in rats: changes in diffusion-sensitive MR imaging findings, extracellular space, and Na^+-K^+ -adenosine triphosphatase and cytochrome oxidase activity. *Radiology 223: 65-75*

QIAO M., LATTA P., MENG S., TOMANEK B., TUOR U.I. (2004) Development of acute edema following cerebral hypoxia-ischemia in neonatal compared with juvenile rats using magnetic resonance imaging. *Pediatr. Res. 55: 101-116*

RANCK J. B. (1963) Analysis of specific impedance of rabbit cerebral cortex. *Exp Neurol 7: 153-174*

RONNE-ENGSTRÖM E., CARLSON H., YANSHENG L., UNGERSTEDT U. (1995) Influence on perfusate glucose concentrations on dialysate lactate, pyruvate, aspartate and glutamate levels under basal and hypoxic conditions: a microdialysis study in rat brain. *J Neurochem 65: 257-262*

RUSAKOV D.A., KULLMANN D.M. (1998) Geometric and viscous components of the tortuosity of the extracellular space in the brain. *Proc Natl Acad Sci 95: 8975-8980*

SCHURR A., PAYNE R.S., MILLER J.J., RIGOR B.M. (1997) Glia are the main source of lactate utilized by neurons for recovery of function posthypoxia. *Brain Res. 774: 221-224*

SILVER I.A., ERECINSKA M. (1994) Extracellular glucose concentration in mammalian brain: continuous monitoring of changes during increased neuronal activity and upon limitation in oxygen supply in normo-, hypo-, and hyperglycaemic animals. *J Neurosci 14: 5068-5076*

SOMJEN G.G. (2004) Ions in the brain. Normal function, seizures, stroke. New York: Oxford Univ. Press

SYKOVA E. (1983) Extracellular K+ accumulation in the central nervous system. *Prog Biophys Mol Biol 42:135-189*

SYKOVA E. (1992) Ionic volume changes in the microenvironment of nerve and receptor cells. Springer-Verlag, Heidelberg.

SYKOVA E., SVOBODA J., POLAK J., CHVATAL A. (1994) Extracellular volume fraction and diffusion characteristics during progressive ischemia and teminal anoxia in the spinal cord of the rat. *J. Cereb. Blood Flow Metab. 14: 301-311*

SYKOVA E., SVOBODA J., SIMONOVA Z., LEHMENKÜHLER A., LASSMANN H. (1996) X-irradiation-induced changes in the diffusion parameters of the developing rat brain. *Neuroscience 70: 597-612*

SYKOVA E. (1997) The extracellular space in the CNS: Its regulation, volume and geometry in normal and pathological neuronal function. *The Neuroscientist 3: 28-41*

SYKOVA E., MAZEL T., VARGOVA L., VORISEK I., PROKOPOVA-KUBINOVA S. (2000) Extracellular space diffusion and pathological states. *In: Progress in Brain Research (Agnati LF, Fuxe C, Nicholson C, Sykova E, eds) 125: 155-178*

SYKOVA E. (2004) Extrasynaptic volume transmission and diffusion parameters of the extracellular space. *Neuroscience 129: 861-867*

SYKOVA E. (2004) Diffusion properties of the brain in health and disease. *Neurochem Int 45: 453-466*

SYKOVA E. (2005) Glia and volume transmission during physiological and pathological states. *J Neural Transm 112: 137-147*

SYKOVA E., NICHOLSON C. (2008) Diffusion in brain extracellular space. *Physiol Rev 88: 1277-1340*

THORNE R.G., NICHOLSON C. (2006) In vivo diffusion analysis with quantum dots and dextrans predicts the width of brain extracellular space. *Proc Natl Acad Sci USA 103: 5567-5572*

TRAYNELIS S.F., DINGLEDINE R. (1989) Role of extracellular space in hyperosmotic suppression of potassium-induced electrographic seizures. *J Neurophysiol 61: 927-938*

UNGERSTEDT U. (1991) Microdialysis – principles and applications for studies in animal and man. *J Intern Med 230(4): 365-373*

VALTYSSON J., PERSSON L., HILLERED L. (1998) Extracellular ischemia markers in repeated global ischemia and secondary hypoxaemia monitored by microdialysis in rat brain. *Acta Neurochir 140: 387-395*

VAN EIJSDEN P., NOTENBOOM R. G., WU O., DE GRAAN P. N., VAN NIEUWENHUIZEN O., NICOLAY K., BRAUN K. P. (2004) In vivo 1H magnetic resonance spectroscopy, T2-weighted and diffusion-weighted MRI during lithium-pilocarpine-induced status epilepticus in the rat. *Brain Res 1030: 11-18*

VAN DER TOORN A., SYKOVA E., DIJKHUIZEN R.M., VORISEK I., VARGOVA L., SKOBISOVA E., VAN LOOKEREN M., REESE T., NICOLAY K. (1996) Dynamic changes in water ADC, energy metabolism, extracellular space volume, and tortuosity in neonatal rat brain during global ischemia. Magn. *Res. Med. 36: 52-60*

VAN HARREVELD A., OCHS S. (1956) Cerebral impedance changes after circulatory arrest. *Am. J. Physiol. 187: 180-192*

VAN HARREVELD A., CROWELL J., MALHOTRA S.K. (1965) A study of extracellular space in central nervous tissue by freeze-substitution. *J Cell Biol 25: 117-137*

VAN ZIJL P.C., MOONEN C.T., FAUSTINO P., PEKAR J., KAPLAN O., COHEN J.S. (1991) Complete separation of intracellular and extracellular information in NMR spectra of perfused cells by diffusion-weighted spectroscopy. *Proc. Natl. Acad. Sci. USA 88: 3228-3232*

VARGOVA L., JENDELOVA P., CHVATAL A., SYKOVA E. (2001) Glutamate, NMDA, and AMPA induced changes in extracellular space volume and tortuosity in the rat spinal cord. *J Cereb Blood Flow Metab 21: 1077-1089*

VARGOVA L., CHVATAL A., ANDEROVA M., KUBINOVA S., ZIAK D., SYKOVA E. (2001) Effect on osmotic stress on potassium accumulation around glial cells and extracellular space volume in rat spinal cord slices. *J Neurosci Res 65: 129-138*

WASTERLAIN C.G., FUJIKAWA D.G., PENIX L., SANKAR R. (1993) Pathophysiological mechanisms of brain damage from status epilepticus. *Epilepsia 34 Suppl 1, S37-53*

VILLEGAS G.M., FERNANDEZ J. (1966) Permeability to thorium dioxide of the intercellular spaces of the frog cerebral hemisphere. *Exp Neurol 15: 18-36*

VORISEK I., SYKOVA E. (1997) Ischemia-induced changes in the extracellular space, diffusion parameters, K^+, and pH in the developing rat cortex and corpus callosum. *J. Cereb. Blood Flow Metab. 17: 191-203*

VORISEK I., SYKOVA E. (1997) Evolution of anisotropic diffusion in the developing rat corpus callosum. *J. Neurophysiol. 78: 912-919*

WALL C.J., KENDALL E.J., OBENAUS A. (2000) Rapid alterations in diffusionweighted images with anatomic correlates in a rodent model of status epilepticus. *AJNR Am J Neuroradiol 21: 1841-1852*

WYKOFF R.W.G., YOUNG J.Z. (1956) The motor-neuron surface. Proc R Soc Lond 144: 440-450

ZOLI M., JANSSON A., SYKOVA E., AGNATI L.F., FUXE K. (1999) Volume transmission in the CNS and its relevance for neuropsychopharmacology. *Trends Pharmacol Sci. 20(4):142-150.*

ZOREMBA N., HOMOLA A., ROSSAINT R., SYKOVA E. (2007) Brain metabolism and extracellular space diffusion parameters during and after transient global hypoxia in the rat cortex. *Exp. Neurol. 203: 34-41*

ZOREMBA N., HOMOLA A., SLAIS K., VORISEK I., ROSSAINT R., LEHMENKÜHLER A., SYKOVA E. (2008) Extracellular diffusion parameters in the rat somatosensory cortex during recovery from transient global ischemia/hypoxia. *J Cereb Blood Flow Metab. 28: 1665-1673*

8. List of publications:

8.1. List of publications included in this dissertation

ZOREMBA N., HOMOLA A., SLAIS K., VORISEK I., ROSSAINT R., LEHMENKÜHLER A., SYKOVA E. (2008) Extracellular diffusion parameters in the rat somatosensory cortex during recovery from transient global ischemia/hypoxia. *J Cereb Blood Flow Metab. 28, 1665-1673;* IF: 5,147

ZOREMBA N., HOMOLA A., ROSSAINT R., SYKOVA E. (2006) Brain metabolism and extracellular space diffusion parameters during and after transient global hypoxia in the rat cortex. *Exp Neurol. 203, 34-41;* IF: 4,156

HOMOLA A., ZOREMBA N., SLAIS K., KUHLEN R., SYKOVA E. (2006) Changes in diffusion parameters, energy-related metabolites and glutamate in the rat cortex after transient hypoxia/ischemia. *Neurosci Lett. 404, 137-142;* IF: 1,898

SLAIS K., VORISEK I., ZOREMBA N., HOMOLA A., DMYTRENKO L., SYKOVA E. (2008) Brain metabolism and diffusion in the rat cerebral cortex during pilocrapine-induced status epilepticus. *Exp Neurol. 209, 145-154;* IF: 3,982

8.2. List of other publications

ZOREMBA N., BICKENBACH J., KRAUSS B., ROSSAINT R., KUHLEN R., SCHÄLTE G. (2007) Comparison of electrical velocimetry and thermodilution techniques for the measurement of cardiac output. *Acta Anaesthesiol Scand. 51, 1314-1319;* IF: 1,863

ZOREMBA N., SCHNOOR J., BERENS M., KUHLEN R., ROSSAINT R. (2007) Brain metabolism during a decrease in cerebral perfussion pressure caused by an elevated intracranial pressure in porcine neocortex. *Anesth Analg. 105, 744-750;* IF: 2,131

SCHNOOR J., ZOREMBA N., ROSSAINT R. (2006) Effects of feeding a standard diet on duodenal impedancometry in pigs. *Acta Vet Hung. 54, 85-93;* IF: 0,530

SCHNOOR J., ZOREMBA N., KORINTH M.C., KOCHS B., SILNY J., ROSSAINT R. (2006) Short-term elevation of intracranial pressure does neither influence duodenal motility nor frequency of bolus transport events: a porcine model. *BMC Emerg Med. 25, 6:1;* IF: 0

8.3. List of abstracts

ZOREMBA N., SCHÄLTE G., BICKENBACH J., KRAUSS B., ROSSAINT R., KUHLEN R. (2007) Comparison of non-invasive and invasive measurements of cardiac output by electrical velocimetry and pulmonary arterial catheter. *Int Care Med. 33, Suppl 2, S164, 635*

ZOREMBA N., SCHNOOR J., BERENS M., KUHLEN R., ROSSAINT R. (2005) Determination of critical cerebral perfusion pressure in cranial hypertension. *Eur J Anaesthesiol. 22, Suppl 34, 89, A335*

ZOREMBA N., HOMOLA A., LEHMENKÜHLER A., SYKOVA E. (2003) Extracellular diffusion parameters in rat neocortex during recovery from mild and severe global ischemia. *In: Proceedings of the Sixth IBRO World Congress of Neuroscience 2003, Prague*

ZOREMBA N., LEHMENKÜHLER A., SYKOVA E. (1993) Diffusion properties of extracellular space in the rat neocortex during recovery from global ischemia. *Pflügers Arch. 422, Suppl. 1: R29*

ZOREMBA N., LEHMENKÜHLER A. (1993) Extracellular space parameters in the brain cortex during recovery from global ischemia. *Europ. J. Cell Biol. 60: Suppl. 37, 27*

BICKENBACH J., ZOREMBA N., FRIES M., DEMBINSKI R., ROSSAINT R., KUHLEN R. (2007) Low tital volume ventilation improves cerebral tissue oxygenation in experimental lung injury. *Crit Care Med 35 (12), A220, 2007*

HOMOLA A., ZOREMBA N., SLAIS K., SYKOVA E. (2006) Changes in diffusion parameters, energy related metabolites and glutamate in the rat cortex after transient global hypoxia and hypoxia/ischemia. *5th Forum of European Neuroscience (FENS), Vienna, 8.-12. July 2006, A132.10*

SCHNOOR J., ZOREMBA N., KORINTH M., SILNY J., ROSSAINT R. (2005) Influence of acute elevation of intracranial pressure on duodenal motility activity and mucosal blood flow. *Eur J Anaesthesiol. 22, Suppl 34, 163, A623*

LEHMENKÜHLER A., SYKOVA E., SVOBODA J., KAUDER C., ZOREMBA N. PEREZ-PINZON M., NICHOLSON C. (1994) Ionic changes and diffusion parameters in CNS during development and anoxia. Proceedings of the First *European Meeting on Glial Cell Function in Health and Disease, Heidelberg, 24.-27. März, 124, 1994*

SYKOVA E., PEREZ-PINZON M., ZOREMBA N., LEHMENKÜHLER A., GIL O., TAO L., NICHOLSON C. (1993) Differentiation of intrinsic and systemic diffusion properties of rat neocortex following *in vivo* and *in vitro* ischemia. *Soc. Neurosci. Abstr. 19: 1660*

9. Appendix

Printout of publications included in this dissertation

Journal of Cerebral Blood Flow & Metabolism (2008) 28, 1665–1673

www.jcbfm.com

Extracellular diffusion parameters in the rat somatosensory cortex during recovery from transient global ischemia/hypoxia

Norbert Zoremba[1], Aleš Homola[2,3], Karel Šlais[3], Ivan Voříšek[2,3], Rolf Rossaint[1], Alfred Lehmenkühler[4] and Eva Syková[2,3]

[1]*Department of Anaesthesiology, University Hospital RWTH Aachen, Aachen, Germany;* [2]*Department of Neuroscience and Center for Cell Therapy and Tissue Repair, 2nd Medical Faculty, Prague, Czech Republic;* [3]*Department of Neuroscience, Institute of Experimental Medicine, Academy of Sciences of Czech Republic, Prague, Czech Republic;* [4]*Center for Pain Therapy, St. Vincent Hospital, Düsseldorf, Germany*

Changes in the extracellular space diffusion parameters during ischemia are well known, but information about changes during the postischemic period is lacking. Extracellular volume fraction (α) and tortuosity (λ) were determined in the rat somatosensory cortex using the real-time iontophoretic method; diffusion-weighted magnetic resonance imaging was used to determine the apparent diffusion coefficient of water. Transient ischemia was induced by bilateral common carotid artery clamping for 10 or 15 mins and concomitant ventilation with 6% O_2 in N_2. In both ischemia groups, a negative DC shift accompanied by increased potassium levels occurred after 1 to 2 mins of ischemia and recovered to preischemic values within 3 to 5 mins of reperfusion. During ischemia of 10 mins duration, α typically decreased to 0.07 ± 0.01, whereas λ increased to 1.80 ± 0.02. In this group, normal values of $\alpha = 0.20 \pm 0.01$ and $\lambda = 1.55 \pm 0.01$ were registered within 5 to 10 mins of reperfusion. After 15 mins of ischemia, α increased within 40 to 50 mins of reperfusion to 0.29 ± 0.03 and remained at this level. Tortuosity (λ) increased to 1.81 ± 0.02 during ischemia, recovered within 5 to 10 mins of reperfusion, and was increased to 1.62 ± 0.01 at the end of the experiment. The observed changes can affect the diffusion of ions, neurotransmitters, metabolic substances, and drugs in the nervous system.
Journal of Cerebral Blood Flow & Metabolism (2008) **28,** 1665–1673; doi:10.1038/jcbfm.2008.58; published online 11 June 2008

Keywords: diffusion; edema; extracellular space; ischemia; MRI; reperfusion

Introduction

The extracellular space (ECS) represents the microenvironment of nerve cells and serves as an important communication channel (Nicholson, 1979; Syková, 1992). The movement of substances in this microenvironment by diffusion is essential for extrasynaptic or 'volume' transmission among neurons, axons, and glia (Fuxe and Agnati, 1991; Zoli *et al*, 1999; Nicholson and Syková, 1998; Syková, 2004). Diffusion in the ECS is also essential for the delivery of oxygen and glucose from the vascular system to brain cells (Nicholson, 2001). Normal brain function depends on a continuous supply of oxygen and glucose to maintain the extracellular/intracellular ionic distribution and to enable synaptic as well as extrasynaptic transmission. Even short periods of ischemia result in a loss of function and changes in the brain microenvironment. It has been repeatedly shown *in vivo* (Van Harreveld and Ochs, 1956; Hansen and Olsen, 1980; Rice and Nicholson, 1991; Lundbaek and Hansen, 1992; Katayama *et al*, 1992; Syková *et al*, 1994; Syková, 1997; Voříšek and Syková, 1997*a*, *b*) as well as *in vitro* (Ames and Nesbett, 1983; Pérez-Pinzón *et al*, 1995) that the ECS of the brain shrinks during global ischemia. This shrinkage is caused by the movement of water from the ECS into the cells, which is accompanied by rapid cellular swelling.

Correspondence: Dr N Zoremba, Department of Anesthesiology, University Hospital RWTH Aachen, Pauwelsstrasse 30, D-52074 Aachen, Germany.
E-mail: nzoremba@ukaachen.de
This study was supported by the European Community project HPMT-CT-2000-00187 and by the Grants AV0Z50390512 of the Academy of Sciences of the Czech Republic, LC554 of the Ministry of Education, Youth and Sports of the Czech Republic, and 305/06/1316 of the Grant Agency of the Czech Republic.
Received 23 February 2008; revised 16 April 2008; accepted 13 May 2008; published online 11 June 2008

The reason for this water movement is an influx of sodium and chloride ions across the cell membranes. The persistent increase of intracellular sodium chloride leads to a reversal of the sodium chloride gradient such that the intracellular sodium chloride concentration may exceed the extracellular levels (Hansen, 1985; Somjen, 2002). Additionally, the swelling of astrocytes under excitotoxic concentrations of glutamate in conjunction with potassium uptake is well known (Somjen, 2002; Kimelberg, 2005). The ECS of the brain decreases to 5% to 6% of the total tissue volume during anoxia (Voříšek and Syková, 1997*a*, *b*), which is equivalent to a reduction of 65% to 80% from preischemic values.

Diffusion of neuroactive substances in the ECS is influenced by the width of the extracellular clefts, presence of membranes, fine neuronal and glial processes, macromolecules of the extracellular matrix, charged molecules, and cellular uptake (Syková *et al*, 2000; Hrabetova and Nicholson, 2000; Syková, 2004). In contrast to a free medium, diffusion in the ECS can only be satisfactorily described by a modified version of Fick's law, if volume fraction, tortuosity, and nonspecific uptake are taken into account (Nicholson and Phillips, 1981; Nicholson, 1992). Volume fraction (α) is the proportion of the tissue volume occupied by the ECS, whereas tortuosity (λ) describes the increased path length of diffusing molecules in a complex medium. The diffusion parameters of the ECS and their dynamic changes can be determined using real-time iontophoretic method. This method uses the iontophoretic application of tetramethylammonium (TMA^+) and TMA^+-selective microelectrodes to record concentration–time profiles of TMA^+ in the ECS (Nicholson and Phillips, 1981). Diffusion-weighted magnetic resonance imaging (DW-MRI) is a noninvasive method to determine the apparent diffusion coefficient of water. It has been used to show a shift of water between the intra- and extracellular compartments after various types of brain injury in animals as well as in humans (Le Bihan and Basser, 1995).

The aim of the present study was to quantify the changes in ECS diffusion parameters during recovery from transient ischemia by TMA^+-diffusion and MRI measurements and to compare their time courses. The data were correlated with DC-potential recordings and measurements of extracellular potassium levels. To the best of our knowledge, this is the first evaluation of the diffusion parameters of the ECS during recovery from transient ischemia in a low cerebral blood flow model of bilateral carotid artery occlusion.

Materials and methods

Animal Preparation

Three-month-old male Wistar rats (300 to 350 g) were anesthetized by an intraperitoneal injection of urethane (1.5 g/kg body weight; Sigma-Aldrich Chemie GmbH, Steinheim, Germany), tracheotomized, relaxed with suxamethonium chloride (20 mg/kg per h; Lysthenon, NycoMED Pharma, Vienna, Austria), and ventilated mechanically with oxygen. Their body temperature was maintained at 37°C by a heating pad. Transient ischemia was induced by bilateral common carotid arterial clamping for 10 mins ($n=5$) or 15 mins ($n=6$), and by reducing the inspired oxygen concentration to 6% in 94% nitrogen. After releasing the clamps, the animals were ventilated with pure oxygen. The head of the rat was fixed in a stereotaxic holder, and the somatosensory neocortex was partially exposed by a burr hole that was 2 to 3 mm caudal from the bregma and 3 to 4 mm lateral from the midline. When the dura was removed, the surface of the brain was continuously bathed in a warm solution (36°C to 37°C) containing 1 mmol/L TMA, 150 mmol/L NaCl, and 3 mmol/L KCl. All measurements were done in the somatosensory cortex at a depth of 1,200 to 1,500 μm from the cortical surface (cortical layer V; Lehmenkühler *et al*, 1993). For DW-MRI measurements ($n=6$ in each group), the animals were placed in a heated MR-compatible cradle and their heads fitted in a built-in head holder.

The experiments were performed in accordance with the European Communities Council Directive of 24 November 1986 (86/609/EEC). All efforts were made to minimize both the suffering and the number of animals used.

Measurement of Extracellular Space Diffusion Parameters

The ECS diffusion parameters were studied by real-time iontophoretic method, described in detail previously (Nicholson and Phillips, 1981; Lehmenkühler *et al*, 1993; Syková *et al*, 1994). Briefly, an extracellular marker that is restricted to the extracellular compartment is used, such as tetramethylammonium ions (TMA^+, MW = 74.1 Da), to which cell membranes are relatively impermeable. TMA^+ is administered into the ECS by iontophoresis, and the concentration of TMA^+ measured in the ECS using a TMA^+-ion-selective microelectrode (ISM) is inversely proportional to the ECS volume. Double-barreled TMA^+-ISMs were prepared by a procedure described in detail previously (Syková, 1992). The tip of the ion-sensitive barrel was filled with a liquid ion exchanger (Corning 477317); the rest of the barrel was backfilled with 150 mmol/L TMA^+ chloride. The reference barrel contained 150 mmol/L NaCl. The TMA^+-ISMs were calibrated in 0.01, 0.03, 0.1, 0.3, 1.0, 3.0, and 10.0 mmol/L TMA^+ in a background of 3 mmol/L KCl and 150 mmol/L NaCl. Calibration data were fitted to the Nikolsky equation (Nicholson and Phillips, 1981). The shank of the iontophoretic pipette was bent so that it could be aligned parallel to that of the ISM and was backfilled with 150 mmol/L TMA^+ chloride. An electrode array was made by gluing a TMA^+-ISM to an iontophoretic micropipette with a tip separation of 100 to 200 μm. The iontophoresis parameters were +20 nA bias current (continuously applied to maintain a constant electrode transport

number), with a +180 nA current step of 60 secs duration, to generate the diffusion curve. TMA^+ was administered at regular intervals of 5 mins. Before tissue measurements, diffusion curves were first recorded in 0.3% agar (Difco, Detroit, MI, USA) dissolved in a solution containing 150 mmol/L NaCl, 3 mmol/L KCl, and 1 mmol/L TMACl. In agar, α and λ are by definition set to 1 and nonspecific uptake k' to 0 (free-diffusion values). The diffusion curves were analyzed to obtain the electrode transport number (n) and free-TMA^+-diffusion coefficient (D) by curve-fitting, according to a diffusion equation using the VOLTORO program (Nicholson and Phillips, 1981). Diffusion curves were then recorded in the somatosensory cortex at depths of 1,200 to 1,500 μm. Knowing n and D, the values of α, λ, and k' can be obtained from the recorded diffusion curves as described by Nicholson and Phillips (1981).

Diffusion-Weighted Magnetic Resonance Imaging

The DW-MRI measurements were performed using an experimental MR spectrometer BIOSPEC 4.7 T system (Bruker, Ettlingen, Germany) equipped with a 200 mT/m gradient system (190 μs rise time) and a homemade head surface coil. We acquired a sequence of T_2-weighted sagittal images to position coronal slices. For DW measurements, four coronal slices were selected (thickness = 1.0 mm, interslice distance = 1.5 mm, field of view = 3.2×3.2 cm^2, matrix size = 256×128). Diffusion weighting serves to increase the contrast in T_2-weighted images for water diffusion. The b-factor denotes the strength of diffusion weighting. Acquiring at least two DW images with different b-factors allows for the determination of the apparent diffusion coefficient of water (ADC_w). The DW images from each slice were acquired using a stimulated echo sequence with the following parameters: b-factors = 75, 499, 1,235, and 1,731 secs/mm^2, Δ = 30 ms, TE = 46 ms, TR = 1,200 ms. Diffusion weighting is accomplished by applying a gradient magnetic field; in our measurements the gradient pointed along the rostrocaudal direction, and, therefore, ADC_w was measured in this direction. Maps of ADC_w were calculated using the linear least-squares method and analyzed using ImageJ software (W. Rasband, NIH, USA). The evaluated regions of interest were positioned using a rat brain atlas (Paxinos and Watson, 1998) and T_2-weighted images in both the left and right hemispheres. The minimal area of an individual region of interest was 2.5 mm^2. In each animal, we analyzed four coronal slices from the interval between 0.1 mm frontal to bregma and 5.6 mm caudal to bregma. The resulting eight values of ADC_w (two regions of interest per slice, four slices/rat) were averaged to obtain a single representative value for comparison to other rats. The reproducibility of the ADC_w measurements was verified by means of five diffusion phantoms placed on the top of a rat's head. The phantoms were made from glass tubes (inner diameter = 2.3 mm, glass type: KS80; Rückl Glass, Nizbor, Czech Republic) filled with pure (99%) substances having different diffusion coefficients. The substances were 1-octanol, n-undecane (Sigma Aldrich, Steinheim, Germany), isopropyl alcohol, n-butanol, and tert-butanol (Penta, Prague, Czech Republic). The temperature of the phantoms was maintained at a constant 37°C. The average diffusion coefficient for each compound was determined at the same time as the experimental measurements of each group of rats and compared with the average diffusion coefficient of the same compound measured in conjunction with the measurements of the other groups of rats.

Measurement of DC Potentials and Extracellular K^+ Concentrations

The registration of cortical DC potentials is a powerful method to monitor the dynamics of sensory and cognitive processing in the brain under normal conditions and in the course of central nervous system disorders. DC potentials from the cortical surface were recorded by microelectrodes filled with 150 mmol/L NaCl, placed in the cortex, and connected to a high impedance buffer amplifier with Ag/AgCl wires. The common reference electrode was positioned on the nasal bone (Lehmenkühler *et al*, 1999). The signal was amplified and transferred to a PC using a Lab Trax acquisition system (World Precision Instruments Inc., Sarasota, FL, USA). The extracellular potassium concentration was measured by double-barreled K^+-sensitive microelectrodes, as described in detail elsewhere (Syková *et al*, 1994). Briefly, the tip of the K^+-selective barrel of the microelectrode was filled with the liquid ion-exchanger Corning 477317 and back-filled with 0.5 mol/L KCl, whereas the reference barrel contained 150 mmol/L NaCl. Electrodes were calibrated in a sequence of solutions containing 2, 4, 8, 16, 32, and 64 mmol/L KCl, with a background of either 151, 149, 145, 137, 121, or 89 mmol/L NaCl to keep the ionic strength of the solution constant. The data were fitted to Nikolsky equation to determine the electrode slope and interference. Based on these electrode characteristics, the measured voltage was converted to extracellular concentrations.

Statistical Analysis

The results of the experiments are expressed as mean ± s.e.m. Statistical analysis of the differences within and between groups was performed using a two-tailed Mann–Whitney test (InStat; GraphPad Software, San Diego, CA, USA). Values of $P < 0.05$ were considered significant.

Results

Extracellular Diffusion Parameters

The ECS diffusion parameters were recorded in cortical layer IV or V (at depths of 1,200 to 1,500 μm) of the somatosensory cortex before and after 10 or 15 mins of ischemia. The mean values of extracellular volume fraction, α, and tortuosity, λ, during normoxia were similar in both ischemia groups

($\alpha = 0.19 \pm 0.01$, $\lambda = 1.55 \pm 0.01$ and $\alpha = 0.19 \pm 0.01$, $\lambda = 1.55 \pm 0.02$) and comparable to the values found in previous *in vivo* studies (Nicholson and Phillips, 1981; Lehmenkühler *et al*, 1993; Vořišek and Syková, 1997*a*, *b*; Mazel *et al*, 2002). During ischemia, α decreased to 0.07 ± 0.01 in both groups, whereas λ increased to 1.80 ± 0.02 and 1.81 ± 0.02 in the 10 and 15 mins ischemia groups, respectively. After releasing the clamps and reoxygenation in the rats subjected to 10 mins of ischemia, recovery to preischemic values of $\alpha = 0.21 \pm 0.01$ were found after 15 to 20 mins of reperfusion; the values then remained stable during the entire measurement period of 90 mins. After ischemia of 15 mins duration, α recovered within 10 to 15 mins of reperfusion, but then increased substantially within a further 30 to 40 mins up to 0.29 ± 0.03 and remained elevated during the postischemic measurement period of 90 mins. This indicates an ECS enlargement of 40% to 50% in the somatosensory cortex of rats subjected to longer (15 mins) ischemia. (see Figure 1, Table 1). The statistical difference between the pre- and postischemic values of α was extremely significant (0.19 ± 0.01 versus 0.29 ± 0.03, $P < 0.001$). Typical diffusion curves recorded before and 60 mins after ischemia of 10 or 15 mins are shown in Figure 2.

In both groups, preischemic values of λ were observed after 5 to 10 mins of reperfusion (10 mins ischemia: $\lambda = 1.57 \pm 0.04$; 15 mins ischemia: $\lambda = 1.56 \pm 0.04$). In the group subjected to 10 mins ischemia, λ remained stable at this level. In the group subjected to 15 mins ischemia, a marginally significant increase in λ to 1.62 ± 0.01 was found at the end of our measurement period. The time course of λ after ischemia in both groups is shown in Figure 1.

Magnetic Resonance Imaging Measurements

Diffusion-weighted MRI measurements of ADC_w were performed bilaterally in the primary somatosensory cortex and showed similar preischemic values in both groups (597 ± 14 versus $594 \pm 12\ \mu m^2/sec$). In the group of 10 mins ischemia, no significant changes in ADC_w in the postischemic period were found, compared with preischemic values. In the animals exposed to 15 mins ischemia, a statistically significant increase in ADC_w to $665 \pm 15\ \mu m^2/sec$ was observed 60 mins after ischemia. This elevated ADC_w level remained until the end of the measurement period, 120 mins after ischemia (Table 2). Typical MRI images before and after ischemia are shown in Figure 3. As the carotid occlusion was performed outside the magnet, we did not measure ADC_w values during ischemia. However, it is known from previous studies that global ischemia induces a rapid decrease in ADC_w (Fisher *et al*, 1995; Van der Toorn *et al*, 1996).

DC Potentials and Extracellular Potassium Concentrations

Before the induction of ischemia, extracellular potassium concentrations of 3 mmol/L were found in both groups. During 1 to 2 mins of ischemia, a rapid increase up to 70 mmol/L was registered, and the concentration remained stable at this level during the ischemic period in both 10 and 15 mins ischemia groups. After reoxygenation, the extracellular potassium concentrations decreased within 2 to 3 mins to preischemic levels of 3 mmol/L. The DC potential changed in a negative direction simultaneously with the increase in extracellular potassium, followed by a small positive change. During the ongoing ischemia the DC potential showed a slight increase. Immediately after reopening of the carotid arteries and ventilation with pure oxygen, the DC potential showed a sharp negative shift, and after the normalization of extracellular potassium concentrations, DC potentials recovered to preischemic levels. Typical measurements of extracellular potassium concentrations and DC potentials during ischemia of 10 and 15 mins duration are shown in Figure 4.

Discussion

Diffusion in the ECS is an important mode of communication between brain cells, and many acute pathologic processes in the CNS (i.e., hypoxia, ischemia, seizures, and hypoglycaemia), accompanied by cellular swelling, can affect the *ADC* of neuroactive substances. We have previously reported that ECS diffusion parameters are altered not only during transient focal hypoxia/ischemia, but also during recovery from this insult (Homola *et al*, 2006). Although a substantial amount of data obtained by DWI-MRI exist on extra- and intracellular diffusion in areas affected by an ischemic/hypoxic insult, the absolute values of the extracellular diffusion parameters measured in the brain cortex during recovery from hypoxia/ischemia have not been available. Up to now, the only values of the ECS diffusion parameters or values of ADC_w obtained in the rat cortex under hypoxic/ischemic conditions have been reported from experiments using a terminal anoxia model (Van der Toorn *et al*, 1996; Lundbaek and Hansen, 1992; Syková *et al*, 1994). In our study, we have evaluated the changes in ECS diffusion parameters after transient global hypoxia/ischemia. These parameters were studied over the course of 90 mins after an ischemic/hypoxic insult and were correlated with changes in ADC_w, DC potential, and extracellular potassium concentration.

Cellular swelling during cerebral ischemia has been described by several authors and is mainly a consequence of massive ionic fluxes across cell membranes, accompanied by the movement of

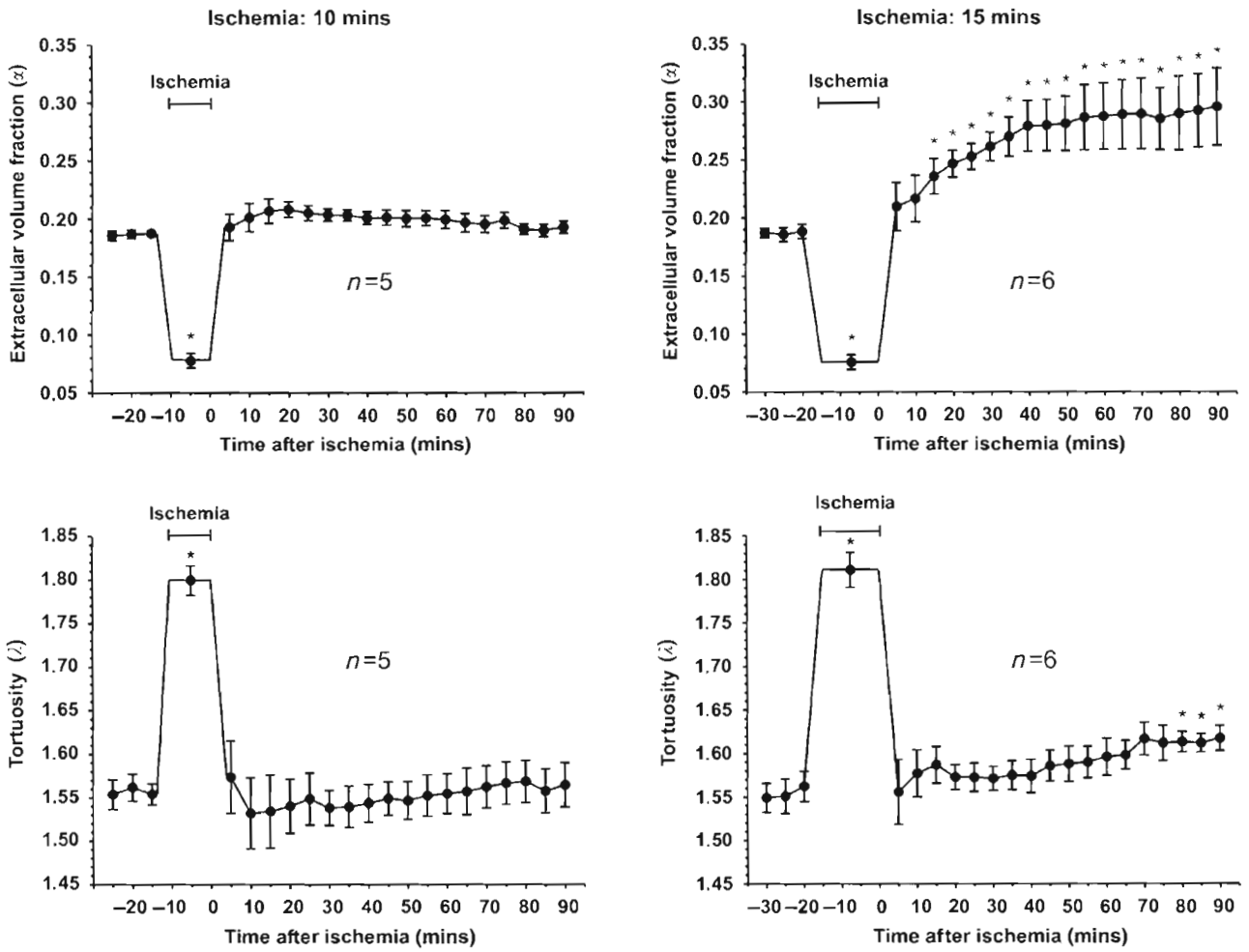

Figure 1 Time course of changes in the values of the extracellular space parameters (α, λ) in the cortex of adult rats before, during, and after ischemia of 10 or 15 mins duration, calculated from TMA^+ diffusion measurements. Data are shown as mean values ± s.e.m. and the number of animals as n. The duration of ischemia is marked by a time line. Upper graphs: average values of extracellular volume fraction (α). After 10 mins ischemia, a quick recovery of α occurs within 5 to 10 mins and the values remain stable at this level. In the group subjected to 15 mins ischemia, α increases extremely significantly above starting values after 40 mins of reperfusion ($P < 0.001$) and remains at this level until the end of the measurement period. *Postischemic values that are significantly different from preischemic values ($P < 0.05$). Lower graphs: the time courses of tortuosity (λ) initially showed no difference between the two groups ($P < 0.05$). During ischemia, an elevated λ recovered to the starting values within 5 mins and stayed at this level without any significant difference from preischemic values. In the group of 15 mins ischemia, λ increased significantly at the end of the registration period.

Table 1 Values of extracellular volume fraction (α) and tortuosity (λ) and nonspecific uptake (k') before and after transient ischemia of 10 or 15 mins duration

	Before ischemia	*30 mins after ischemia*	*60 mins after ischemia*	*90 mins after ischemia*
Ischemia 10 mins $n=5$	$\alpha = 0.19 \pm 0.01$ $\lambda = 1.55 \pm 0.01$ $k' = 3.6 \times 10^{-3} \pm 0.8 \times 10^{-3}$	$\alpha = 0.20 \pm 0.01$ $\lambda = 1.54 \pm 0.02$ $k' = 3.3 \times 10^{-3} \pm 0.9 \times 10^{-3}$	$\alpha = 0.20 \pm 0.01$ $\lambda = 1.55 \pm 0.02$ $k' = 3.9 \times 10^{-3} \pm 1.0 \times 10^{-3}$	$\alpha = 0.19 \pm 0.01$ $\lambda = 1.56 \pm 0.03$ $k' = 4.1 \times 10^{-3} \pm 1.0 \times 10^{-3}$
Ischemia 15 mins $n=6$	$\alpha = 0.19 \pm 0.01$ $\lambda = 1.55 \pm 0.02$ $k' = 3.6 \times 10^{-3} \pm 0.6 \times 10^{-3}$	$\alpha = 0.26 \pm 0.01$* $\lambda = 1.57 \pm 0.01$ $k' = 2.8 \times 10^{-3} \pm 0.2 \times 10^{-3}$	$\alpha = 0.29 \pm 0.03$* $\lambda = 1.60 \pm 0.02$ $k' = 3.6 \times 10^{-3} \pm 0.5 \times 10^{-3}$	$\alpha = 0.30 \pm 0.03$* $\lambda = 1.62 \pm 0.01$* $k' = 3.8 \times 10^{-3} \pm 0.4 \times 10^{-3}$

Values of α, λ, and k' are shown as mean values and s.e.m.; n represents the number of animals.
*Significant differences (two-tailed Mann–Whitney test, $P < 0.05$) in postischemic values when compared with values before ischemia.

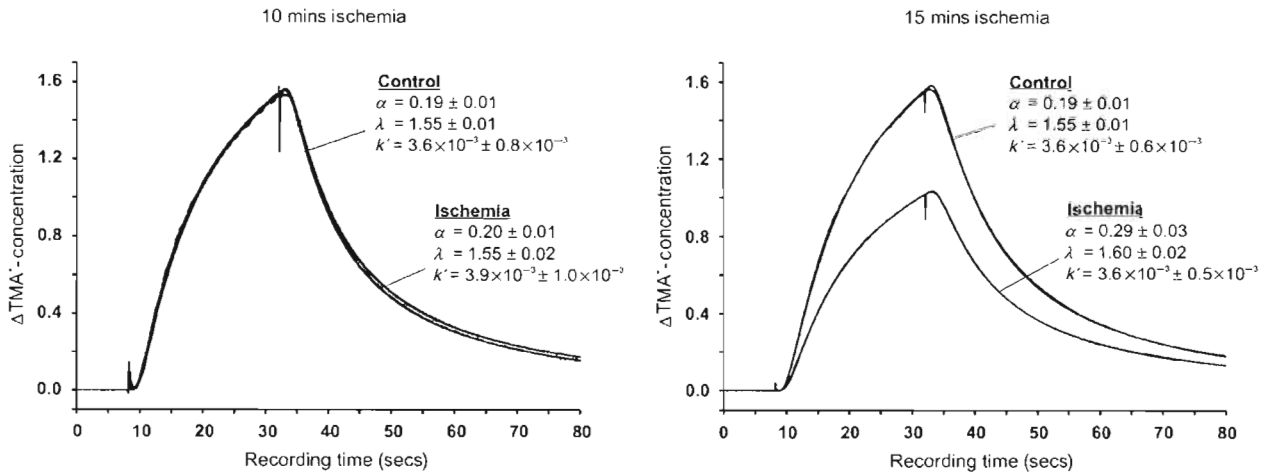

Figure 2 Example of recorded diffusion curves and superimposed theoretical curve fittings as time–concentration plots before (control) and 60 mins after ischemia (ischemia) of 10 or 15 mins duration. Total recording time was 80 secs for each diffusion curve. After 8 secs, the main bias was elevated for 24 secs to 120 nA to apply TMA^+ by iontophoresis. Changes in the diffusion properties after ischemia compared with preischemic conditions were found only in the group subjected to 15 mins ischemia.

Table 2 The apparent diffusion coefficient of water (ADC_w) before and after 10 or 15 mins of ischemia was determined by magnetic resonance imaging

	ADC_w (μm^2/sec) *before ischemia*	ADC_w (μm^2/sec) *60 mins after ischemia*	ADC_w (μm^2/sec) *90 mins after ischemia*	ADC_w (μm^2/sec) *120 mins after ischemia*
Ischemia 10 mins ($n = 6$)	597 ± 14	608 ± 8	603 ± 10	605 ± 12
Ischemia 15 mins $n = 6$	594 ± 12	665 ± 15*	651 ± 11*	647 ± 13*

Data expressed as mean ± s.e.m.; n represents the number of animals.
*Significant differences (two-tailed Mann–Whitney test, $P < 0.05$) between preischemic values and values after ischemia.

water, and develops concomitantly with ionic shifts (McKnight and Leaf, 1977; Hansen and Olsen, 1980; Syková *et al*, 1994). The swelling occurs quickly after the interruption of the energy supply, but never before a rise in K^+ and changes in pH (Syková *et al*, 1994). The dependence of ECS shrinkage because of cellular swelling on ionic changes was also seen in our experiments, and it was observed that a normalization of elevated K^+ leads to a quick normalization of ECS volume and tortuosity. The recovery in extracellular potassium concentration and DC potential indicates a sufficient supply of oxygen and substrates after ischemia. During recovery from longer lasting global ischemia, a significant increase in the extracellular volume fraction α developed within 60 mins, probably caused by an increase in extracellular water content. Similar time courses of ECS volume and tortuosity changes were observed in the spinal cord during recovery from ischemia (Syková *et al*, 1994). The postischemic increase in α, which was observed in this study, was promoted by bilateral carotid occlusion and a reduction in cerebral blood flow. It has been shown that hypoxia of 30 mins duration without carotid occlusion lead to a small decrease in α, followed by rapid normalization during recovery (Zoremba *et al*, 2007). In contrast to these findings, hypoxia of 30 mins duration with unilateral carotid occlusion results in a decrease in α followed by an increase during recovery to about 20% above the original normoxic values (Homola *et al*, 2006). Based on the results from our study, together with the results from earlier studies, it could be suggested that in addition to the degree and duration of hypoxia, cerebral blood flow also influences the extent of damage. The increase in ECS volume fraction after reperfusion correlates well with changes in the *ADC* of brain water. In our study, the values of ADC_w obtained 60 and 90 mins after reperfusion were significantly elevated, suggesting an increased amount of water in the ECS where ADC_w was reported to be higher, compared with the intracellular compartment (Van Zijl *et al*, 1991). A correction of orientational dependence was not necessary because it is known from previous studies that there is no significant anisotropy in the cerebral cortex of the rat brain (Vořišek and Syková, 1997*a*, *b*). In an earlier study, full recovery of the diffusion constant of brain water after 12 mins of incomplete global ischemia was found (Davis *et al*, 1994). The results are comparable

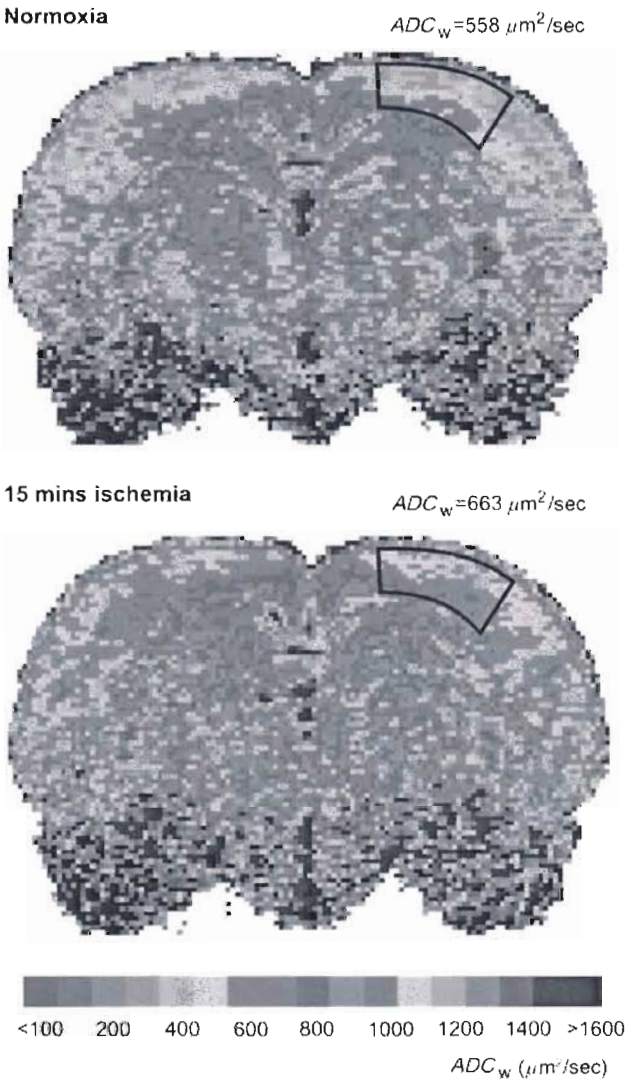

Figure 3 Typical ADC_w maps of a control rat brain and of a rat brain 60 mins after ischemia of 15 mins duration. ADC_w was analyzed bilaterally in the primary somatosensory cortex. The areas are outlined on the left part of the slices, and both images are from the same coronal plane. The scale at the bottom of the figure shows the relation between the intervals of ADC_w values and the colors used for visualization.

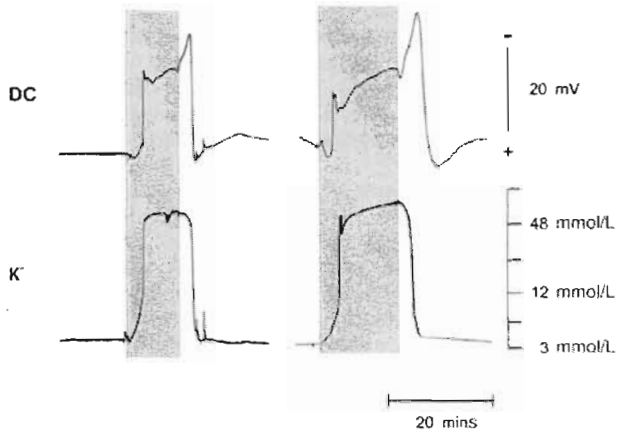

Figure 4 Time course of extracellular potassium concentrations and DC potentials during an ischemia of 10 mins (left side) or 15 mins (right side) duration. The duration of ischemia is marked by the shaded fields.

to the results in our 10 mins ischemia group. In contrast to this earlier study, we also reduced the oxygen content to 6% and therefore a more severe ischemia resulted. These observations support the hypothesis that a certain level of ischemia severity has to be exceeded before cerebral edema develops.

It is well known that after ischemia, functional damage of the blood–brain barrier occurs (Betz *et al*, 1989; Qiao *et al*, 2001) and the hypoxic-ischemic insult initiates a series of events that lead to the disruption of tight junctions and increased permeability mediated by cytokines, vascular endothelial growth factor, and nitric oxide (Ballabh *et al*, 2004). Because of increased permeability, reperfusion may lead to an early postischemic increase in cerebral water content and to the formation of cortical edema of 'vasogenic' origin (Papadopoulos *et al*, 2005). These changes could also be caused by elevated postischemic tissue osmolarity (Gisselson *et al*, 1992) or postischemic shrinkage of nerve cells. It is evident that an ischemia of 10 mins duration is too short to initiate a cascade of events that lead to the disruption of the blood–brain barrier and the development of vasogenic edema. This hypothesis was supported by the different time courses of the DC potential recovery between the two groups. During ischemia, an increase in extracellular potassium levels up to 70 mmol/L was registered, whereas recovery in both groups was comparable within a few minutes. In comparing the DC potentials, a longer recovery period was necessary in animals subjected to an ischemia of 15 mins. These findings indicate that the cellular energy state is affected in the same way in both groups, but that the intercellular integrity because of neurotoxicity was more affected in the group subjected to longer ischemia. Additionally, the longer lasting extracellular potassium increase could have direct effects or modulate the influence of cytokines, vascular endothelial growth factor, and nitric oxide on the blood–brain barrier.

During reperfusion in the group with longer ischemia, the extracellular volume fraction increased within 40 to 50 mins and remained elevated by about 40% to 50% above the normoxic values, whereas the tortuosity was initially similar to preischemic values, increasing significantly at the end of our registration period. It could be expected that the increase in ECS volume would facilitate extracellular diffusion, but our results show a small increase in tortuosity, indicating a diffusion hindrance and an effect on volume transmission. One reason for this hindered diffusion could be released

macromolecules and fixed surface charges, which affect free diffusion by charge-dependent bonding or by van der Waals forces. Increased viscosity impedes molecular movement and is affected by the size and nature of the diffusing molecules and results in their hydrodynamic interactions with macromolecules and fixed charges and the boundaries that define pore structures. The change in tortuosity, λ, is influenced by many factors that cannot be presently separated. These factors might include membrane barriers, myelin sheaths, macromolecules, molecules with fixed negative surface charges, ECS size, and pore geometry. As a result, λ could be changed if certain pathways through the ECS are either blocked off or opened up (Syková *et al*, 2000). Many studies have shown that λ and α can change independently during the exposure of brain slices to dextran (Hrabetova and Nicholson, 2000), during X-irradiation (Syková *et al*, 1996), or during osmotic stress (Krizaj *et al*, 1996; Nicholson and Syková, 1998; Chen and Nicholson, 2000; Kume-Kick *et al*, 2002).

We have shown changes in the extracellular diffusion parameters that may affect the diffusion of various substances (ions, neurotransmitters, metabolites, and drugs) in the affected region. Our results show that after ischemia of 15 mins, and most likely after longer periods, the observed changes in the ECS diffusion parameters are not reversible during 90 mins of reperfusion and result in long-lasting and severe edema and perhaps permanent damage. Studies using longer ischemic and postischemic periods are needed to further clarify the crucial time point between reversible and irreversible effects induced by oxygen deficiency.

References

Ames A, III, Nesbett FB (1983) Pathophysiology of ischemic cell death. II. Changes in plasma membrane permeability and cell volume. *Stroke* 14: 227–33

Ballabh P, Braun A, Nedergaard M (2004) The blood–brain barrier: an overview structure, regulation and clinical implications. *Neurobiol Dis* 16:1–13

Betz AL, Ianotti F, Hoff JT (1989) Brain edema: a classification based on blood–brain barrier integrity. *Cerebrovasc Brain Metab Rev* 1:133–54

Chen KC, Nicholson C (2000) Changes in brain cell shape create residual extracellular space volume and explain tortuosity behavior during osmotic challenge. *Proc Natl Acad Sci USA* 15:8306–11

Davis D, Ulatowski J, Eleff S, Izuta M, Mori S, Shungu D, Van Zijl PCM (1994) Rapid monitoring of changes in water diffusion coefficients during reversible ischemia in cat and rat brain. *Magn Res Med* 31:454–60

Fisher M, Blockhorst K, Hoehn-Berlage M, Schmitz B, Hossmann K-A (1995) Imaging of the apparent diffusion coefficient for the evaluation of cerebral metabolic recovery after cardiac arrest. *Magn Res Imaging* 13: 781–790

Fuxe K, Agnati LF (1991) *Volume transmission in the brain. Novel mechanisms for neural transmission.* New York: Raven Press, pp 1–602

Gisselson L, Smith ML, Siesjö BK (1992) Influence of preischemic hyperglycemia on osmolality and early postischemic edema in the rat brain. *J Cereb Blood Flow Metab* 12:809–16

Hansen AJ (1985) Effect of anoxia on ion distribution of the brain. *Physiol Rev* 65:101–48

Hansen AJ, Olsen CE (1980) Brain extracellular space during spreading depression and ischemia. *Acta Physiol Scand* 108:355–65

Homola A, Zoremba N, Slais K, Kuhlen R, Syková E (2006) Changes in diffusion parameters, energy-related metabolites and glutamate in the rat cortex after transient hypoxia/ischemia. *Neurosci Lett* 404:137–42

Hrabetova S, Nicholson C (2000) Dextran decreases extracellular tortuosity in thick-slice ischemia model. *J Cereb Blood Flow Metab* 20:1306–10

Katayama Y, Tamura T, Becker DP, Tsubokawa T (1992) Early cellular swelling during cerebral ischemia *in vivo* is mediated by excitatory amino acids released from nerve terminals. *Brain Res* 577:121–6

Kimelberg HK (2005) Astrocytic swelling in cerebral ischemia as a possible cause of injury and target for therapy. *Glia* 50:389–97

Krizaj D, Rice ME, Wardle RA, Nicholson C (1996) Water compartmentalization and extracellular tortuosity after osmotic changes in cerebellum of *Trachemys scripta*. *J Physiol* 492:887–96

Kume-Kick J, Mazel T, Vorisek I, Hrabetova S, Tao L, Nicholson C (2002) Independence of extracellular tortuosity and volume fraction during osmotic challenge in rat neocortex. *J Physiol* 542:515–27

Le Bihan D, Basser PJ (1995) *Diffusion and perfusion magnetic resonance imaging: application to functional MRI.* New York: Raven Press

Lehmenkühler A, Richter F, Poppelmann T (1999) Hypoxia and hypercapnia-induced DC potential shifts in rat at the scalp and the skull are opposite in polarity to those at the cerebral cortex. *Neurosci Lett* 270:67–70

Lehmenkühler A, Syková E, Svoboda J, Zilles K (1993) Extracellular space in rat neocortex and subcortical white matter during postnatal development determined by diffusion analysis. *Neuroscience* 55:339–51

Lundbaek JA, Hansen AJ (1992) Brain interstitial volume fraction and tortuosity in anoxia. Evaluation of the ion-selective microelectrode method. *Acta Physiol Scand* 146:473–84

Mazel T, Richter F, Vargová L, Syková E (2002) Changes in extracellular space volume and geometry induced by cortical spreading depression in immature and adult rats. *Physiol Res* 51(Suppl 1):S85–93

McKnight ADC, Leaf A (1977) Regulation of cellular volume. *Physiol Rev* 57:510–73

Nicholson C (1979) Brain cell microenvironment as a communication channel. In: *The neurosciences: fourth study programme,* (Schmitt FO, Worden FG, eds), Cambridge, MA: MIT Press, pp 457–76

Nicholson C (1992) Quantitative analysis of extracellular space using the method of TMA^+ iontophoresis and the issue of TMA^+ uptake. *Can J Physiol Pharmacol* 70:314–22

Nicholson C (2001) Diffusion and related transport mechanisms in brain tissue. *Rep Prog Phys* 64:815–84

Nicholson C, Phillips JM (1981) Ion diffusion modified by tortuosity and volume fraction in the extracellular microenvironment of the rat cerebellum. *J Physiol* 321:225–57

Nicholson C, Syková E (1998) Extracellular space structure revealed by diffusion analysis. *Trends Neurosci* 21:207–15

Papadopoulos MC, Binder DK, Verkman AS (2005) Enhanced macromolecular diffusion in brain extracellular space in mouse models of vasogenic edema measured by cortical surface photobleaching. *FASEB J* 19:425–7

Paxinos G, Watson C (1998) *The rat brain atlas*, 4th edn. Academic Press Inc.

Pérez-Pinzón MA, Tao L, Nicholson C (1995) Extracellular potassium, volume fraction and tortuosity in rat hippocampal CA1, CA3 and cortical slices during ischemia. *J Neurophysiol* 74:565–73

Qiao M, Malisza KL, DelBigio MR, Tuor UI (2001) Correlation of cerebral hypoxic-ischemic T2 changes with tissue alterations in water content and protein extravasation. *Stroke* 32:958–63

Rice M, Nicholson C (1991) Diffusion characteristics and extracellular volume fraction during normoxia and hypoxia in slices of rat neostriatum. *J Neurophysiol* 65: 264–72

Somjen GG (2002) Ion regulation in the brain: implications for pathophysiology. *Neuroscientist* 8:254–67

Syková E (1992) *Ionic volume changes in the microenvironment of nerve and receptor cells*. Heidelberg: Springer-Verlag

Syková E (1997) The extracellular space in the CNS: its regulation, volume and geometry in normal and pathological neuronal function. *Neuroscientist* 3:28–41

Syková E (2004) Extrasynaptic volume transmission and diffusion parameters of the extracellular space. *Neuroscience* 129:861–7

Syková E, Mazel T, Vargova L, Vorisek I, Prokopova-Kubinova S (2000) Extracellular space diffusion and pathological states. In: *Progress in Brain Research*, (Agnati LF, Fuxe C, Nicholson C, Syková E, eds), Elsevier: Amsterdam, Netherlands, vol 125, 155–78

Syková E, Svoboda J, Polak J, Chvatal A (1994) Extracellular volume fraction and diffusion characteristics during progressive ischemia and terminal anoxia in the spinal cord of the rat. *J Cereb Blood Flow Metab* 14: 301–311

Syková E, Svoboda J, Simonova Z, Lehmenkühler A, Lassmann H (1996) X-irradiation-induced changes in the diffusion parameters of the developing rat brain. *Neuroscience* 70:597–612

Van der Toorn A, Syková E, Dijkhuizen RM, Vorisek I, Vargova L, Skobisova E, Van Lookeren M, Reese T, Nicolay K (1996) Dynamic changes in water ADC, energy metabolism, extracellular space volume, and tortuosity in neonatal rat brain during global ischemia. *Magn Res Med* 36:52–60

Van Harreveld A, Ochs S (1956) Cerebral impedance changes after circulatory arrest. *Am J Physiol* 187: 180–192

Van Zijl PC, Moonen CT, Faustino P, Pekar J, Kaplan O, Cohen JS (1991) Complete separation of intracellular and extracellular information in NMR spectra of perfused cells by diffusion-weighted spectroscopy. *Proc Natl Acad Sci USA* 88:3228–32

Vořišek I, Syková E (1997*a*) Ischemia-induced changes in the extracellular space, diffusion parameters, K^+, and pH in the developing rat cortex and corpus callosum. *J Cereb Blood Flow Metab* 17:191–203

Vořišek I, Syková E (1997*b*) Evolution of anisotropic diffusion in the developing rat corpus callosum. *J Neurophysiol* 78:912–9

Zoli M, Jansson A, Syková E, Agnati LF, Fuxe K (1999) Volume transmission in the CNS and its relevance for neuropsychopharmacology. *Trends Pharmacol Sci* 20:142–50

Zoremba N, Homola A, Rossaint R, Syková E (2007) Brain metabolism and extracellular space diffusion parameters during and after transient global hypoxia in the rat cortex. *Exp Neurol* 203:34–41

Available online at www.sciencedirect.com
ScienceDirect
Experimental Neurology 203 (2007) 34–41
Experimental Neurology
www.elsevier.com/locate/yexnr

Brain metabolism and extracellular space diffusion parameters during and after transient global hypoxia in the rat cortex

Norbert Zoremba [a,*], Aleš Homola [b,c], Rolf Rossaint [a], Eva Syková [b,c]

[a] *Department of Anaesthesiology, University Hospital RWTH Aachen, Pauwelsstr. 30, D-52074 Aachen, Germany*
[b] *Department of Neuroscience and Centre for Cell Therapy and Tissue Repair, 2nd Medical Faculty, Prague, Czech Republic*
[c] *Institute of Experimental Medicine, Academy of Sciences of the Czech Republic, Prague, Czech Republic*

Received 24 March 2006; revised 20 July 2006; accepted 21 July 2006
Available online 7 September 2006

Abstract

Hypoxia results in both reversible and irreversible changes in the brain extracellular space (ECS). This study utilized microdialysis to monitor changes in the energy-related metabolites lactate, pyruvate, glucose and glutamate in the rat cortex before, during and after 30-min transient global hypoxia, induced in anesthetized rats by reducing inspired oxygen to 6% O_2 in nitrogen. Changes in metabolite levels were compared with ECS diffusion parameters calculated from diffusion curves of tetramethylammonium applied by iontophoresis.

Significant increases in lactate concentration and the lactate/pyruvate ratio, as well as decreased glucose levels, were found in the cortex immediately after the induction of hypoxia. Following recovery to ventilation with air, extracellular lactate and glucose levels and the lactate/pyruvate ratio returned to control levels within 40, 20 and 30 min, respectively. Glutamate levels started to increase 20–30 min after the onset of hypoxia and returned to prehypoxic values within 30–40 min of reoxygenation. The ECS volume fraction α decreased by about 5% from 0.18±0.01 during the first 20–25 min of hypoxia; after 25 min α dropped a further 22% to 0.14±0.01. Within 10 min of reoxygenation, α returned to control values, then increased to 0.20±0.01 and remained at this level until the end of the experiment. The observed 22% decrease in α markedly influences dialysate levels measured during hypoxia.

In our study, the complete posthypoxic recovery of cortical metabolite levels and ECS diffusion properties suggests that metabolic enzymes and related cellular components (e.g., mitochondria) may tolerate prolonged hypoxic periods and recover to prehypoxic values.

Keywords: Hypoxia; Cortex; Microdialysis; Recovery; Lactate; Glutamate; Extracellular space; DC potential

Introduction

Hypoxia causes profound changes in cellular metabolism, especially in brain tissue, which has a low tolerance to oxygen deficiency. Moderate to severe neuronal damage may occur following hypoxic events. The primary factor is a deficiency of metabolites, which initiates a cascade of cellular events that leads to neurodegeneration through both apoptotic and necrotic mechanisms (Banasiak et al., 2000; Andersson et al., 2004). In clinical practice, hypoxia can be caused by different disorders, e.g., acute and chronic lung failure, arterial stenosis or stress (Aftabuddin et al., 1994; Mortelliti and Manning, 2002).

Intracerebral microdialysis is a highly sensitive technique to monitor cerebral energy metabolism. It allows the determination of brain metabolite levels in the extracellular fluid (ECF) and the measurement of regional metabolic tissue concentrations (Ungerstedt, 1991). In many studies, lactate has been interpreted as one of the markers of anaerobic metabolism, accumulating as the end product of glycolysis, if an imbalance arises between tissue O_2 supply and demand or when oxidative phosphorylation, as well as the tricarboxylic acid cycle, are reduced (De Salles et al., 1986; Inao et al., 1998; Mizock and Falk, 1992; Magnoni et al., 2003). Lactate is produced and accumulates in the ECF during intense cerebral stimulation under normoxic conditions and is thus an unreliable indicator of tissue hypoxia (Prichard et al., 1991). For the detection of anaerobic metabolism, the simultaneous determination of pyruvate levels is necessary, because pyruvate is reduced to lactate by lactate-

* Corresponding author. Fax: +49 241 8082406.
E-mail address: nzoremba@ukaachen.de (N. Zoremba).

0014-4886/$ - see front matter © 2006 Elsevier Inc. All rights reserved.
doi:10.1016/j.expneurol.2006.07.017

dehydrogenase under anaerobic conditions. The lactate/pyruvate ratio (L/P ratio) specifies the degree of aerobic/anaerobic metabolism and reflects the cytosolic ratio of the reduced/oxidized forms of NAD. For this reason the L/P ratio is a reliable parameter for estimating the energy state of a cell (Magnoni et al., 2003). Beside the measurement of metabolic end products, knowledge of substrate levels, such as glucose, is important. The glucose concentration in the ECF reflects the balance between supply from the blood and utilization by cells (Fellows et al., 1992). Glutamate, an excitatory amino acid released by active neurons into the extracellular space (ECS) and taken up by astrocytes, plays an essential role in normoxic and hypoxic conditions (Hillered et al., 1989; Magistretti et al., 1993). The measurement of glutamate efflux into the ECS after hypoxia and during reperfusion provides information about the compromised status of brain cells and the eventual neuropathological outcome (Phillis et al., 2001).

The determination of the extracellular concentrations of these substrates and metabolites can be influenced by the size of the extracellular space. The extracellular volume fraction α, the proportion of the total tissue volume occupied by the ECS, can be determined by the real-time iontophoretic method. In this method, tetramethylammonium (TMA^+) – a substance to which cell membranes are relatively impermeable – is released at a known distance by iontophoresis and its local concentration is measured with a TMA-selective microelectrode located about 100–150 μm from the release site. The time-dependent rise and fall of the extracellular TMA^+ concentration during and after an iontophoretic pulse (TMA^+ diffusion curve) can be fitted to a modified radial diffusion equation to yield the extracellular volume fraction α (Nicholson and Phillips, 1981; Nicholson and Sykova, 1998). Changes in α can substantially affect accumulation of substances in the ECS.

The aim of our study was to measure the changes in the energy-related metabolites lactate, pyruvate, glucose and glutamate before, during and after hypoxia using in vivo microdialysis and compare them with the changes in the ECS diffusion parameters. These findings can improve the knowledge of mechanisms which are involved in the development of tolerance to ischemic insults.

Methods

Animal preparation

Adult male Wistar rats (300–350 g) were anesthetized by an intraperitoneal injection of urethane (1.5 g/kg body weight, Sigma-Aldrich Chemie GmbH, Seelze, Germany). Before surgery, the depth of anesthesia was controlled by testing the corneal reflex. If necessary, an additional 100 mg of urethane was injected intraperitoneally. The animals were intubated and connected to a ventilator (CIV 101, Columbus Instruments, Columbus, Ohio, USA), relaxed with pancuroniumbromide (0.6 mg/kg body weight, Pavulon, Organon, Netherlands), and ventilated with air. The body temperature was maintained at 36–37°C by a heating pad. The head of the rat was fixed in a stereotaxic holder. The somatosensory neocortex of the rat was partially exposed by a burr hole 2–3 mm caudal from the bregma and 2–3 mm lateral from the midline. The dural and arachnoid membranes were removed to avoid damage to the microdialysis probes and microelectrodes during their insertion into the brain. The microdialysis probe was slowly inserted 1.5–2.0 mm deep into the cortex in 5-μm steps, using a nanostepper. To avoid the possible influence of probe insertion tissue trauma on the microdialysis results, measurements were started 1 h after the insertion of the microdialysis probe. It has been shown that baseline values are stable within 30–60 min after probe insertion (Valtysson et al., 1998). The TMA^+ diffusion measurements ($n=7$) were done in the somatosensory cortex at a depth of 1200–1500 μm from the cortical surface (cortical layers IV and V). The microdialysis part of the study was performed on hypoxic ($n=10$) and control animals ($n=5$), which were randomly assigned to the two groups before starting the experiment. A transient hypoxia of 30-min duration was induced by reducing the inspiratory oxygen content to 6% with 94% nitrogen. In our experiments, we used a hypoxia of 30-min duration, because we were interested in evaluating the processes that occur during and after long-lasting hypoxic episodes and hypoxia of this duration does not cause any anoxic depolarization of the brain. Following a hypoxic period of 30 min, the animals were again ventilated with air ($O_2=21\%$). The control animals were ventilated with air throughout the experiment.

All efforts were made to minimize animal suffering and to reduce the number of animals used. The experiments were carried out in accordance with the European Communities Council Directive of 24.November 1986 (86/609/EEC) and approved by the local Institutional Animal Ethics Committee.

Microdialysis

The technique of microdialysis is based on sampling fluid via a double-lumen probe with an integrated semipermeable membrane in which the equilibration of substances in the extracellular space and perfusion fluid takes place by diffusion according to the concentration gradient. We used a double-lumen microdialysis probe with a membrane length of 2 mm, an outer diameter of 0.5 mm and a cut-off at 20,000 Da (CMA 12, 2-mm membrane length, CMA Microdialysis, Sweden). The inserted microdialysis catheter was connected by low-volume Fluorinated Ethylene Propylene (FEP) tubing (1.2 μl/10 cm) to a precision infusion pump (CMA 102, CMA Microdialysis, Sweden) in order to maintain a constant dialysate flow. The microdialysis catheter was continuously perfused with a dialysate containing 147 mmol/l NaCl, 2.7 mmol/l KCl, 1.2 mmol/l $CaCl_2$ and 0.85 mmol/l $MgCl_2$ (Perfusion fluid CNS, CMA Microdialysis, Sweden) at a flow rate of 2 μl/min. Transient increases in metabolite concentrations caused by probe insertion damage were avoided by a stabilization period of 60 min following insertion into the brain. After this equilibration time, microdialysate samples were collected in 10-min intervals and immediately frozen at −40°C until analyzed. Thawed and centrifuged dialysate samples were analyzed enzymatically with a CMA 600 Microdialysis

Analyser (CMA/Microdialysis, Sweden) for lactate, pyruvate, glucose and glutamate concentrations (Fig. 1A).

The exchange of substances across the microdialysis membrane is limited by the total area of the membrane, the perfusion flow rate, the characteristics of the diffusing substance and the diffusion constant in the tissue surrounding the probe (Arner and Bolinder, 1991; Ungerstedt, 1991). The recovery rate expresses the relation between the concentration of the substance in the microdialysis probe effluent and the concentration in the medium (Muller, 2002). Before and at the end of the experiments, the recovery rates for each probe were determined by continuing the perfusion at the same settings in a calibration solution containing known concentrations of the different analytes. The calibration solution contained 2.50 mmol/l lactate, 250 μmol/l pyruvate, 5.55 mmol/l glucose, 250 mmol/l glycerol and 25 mmol/l glutamate (Calibrator A, CMA microdialysis, Sweden). The concentrations in the calibration solution were compared with the concentrations of the in vitro microdialysis samples to determine the relative recovery for each substance. The measured experimental values were weighted by the relative recovery to estimate the in vivo extracellular concentration of the substances in the immediate vicinity of the probes. In vitro recovery rates were 21.5±0.9% for lactate, 22.3±0.5% for pyruvate, 13.4±0.6% for glutamate and 10.8±0.5% for glucose (n=15). All results are presented as weighted concentrations.

Measurement of extracellular space diffusion parameters and DC potentials

The ECS diffusion parameters were studied by the real-time iontophoretic method described in detail previously (Nicholson and Phillips, 1981; Sykova et al., 1994). Briefly, an extracellular marker that is restricted to the extracellular compartment, such as tetramethylammonium ions (TMA^+, MW=74.1 Da) to which cell membranes are relatively impermeable, is released into the extracellular space by iontophoresis and its local concentration measured with a TMA^+-selective microelectrode (TMA^+-ISM) located about 100–200 μm from the release site. The concentration of TMA^+ in the ECS is inversely proportional to the ECS volume. Double-barreled TMA^+-ISMs were prepared by a procedure described in detail previously (Sykova, 1992). The tip of the ion-sensitive barrel was filled with a liquid ion exchanger (Corning 477317); the rest of the barrel was backfilled with 150 mM TMA^+ chloride. The reference barrel contained 150 mM NaCl. The TMA^+-ISMs were calibrated in 0.01, 0.03, 0.1, 0.3, 1.0, 3.0, and 10.0 mM TMA^+ in a background of 3 mM KCl and 150 mM NaCl. Calibration data were fitted to the Nikolsky equation (Nicholson and Phillips, 1981). The shank of the iontophoretic pipette was bent so that it could be aligned parallel to that of the ion-selective microelectrode and was backfilled with 150 mM TMA^+ chloride. An electrode array was made by gluing a TMA^+-ISM to an iontophoretic micropipette with a tip separation of 100–200 μm (Fig. 1B). The iontophoresis parameters were +20 nA bias current (continuously applied current to maintain a constant electrode transport number), and a +180 nA current step of 24-s duration, to generate the diffusion curve. The TMA^+ diffusion curves were generated at regular intervals of 5 min. Before tissue measurements, diffusion curves were first recorded in 0.3% agar (Sigma Aldrich, Steinheim, Germany) dissolved in a solution containing 150 mM NaCl, 3 mM KCl, and 1 mM TMACl. The diffusion curves were analyzed to obtain the electrode transport number (n) and the free TMA^+ diffusion coefficient (D) by curve fitting according to a modified diffusion equation using the VOLTORO program (Nicholson and Phillips, 1981). Diffusion curves were then recorded in the somatosensory cortex at a depth of 1200–1500 μm. Knowing n and D, the values of α, λ and k' can be obtained from the diffusion curves. The volume fraction α is the ratio of the volume of the ECS to total tissue volume in a representative elementary volume of brain tissue (α=ECS/total tissue volume). Tortuosity λ is defined as $\lambda^2 = D/\mathrm{ADC}$ where D is the free diffusion coefficient and ADC is the apparent diffusion coefficient in the brain tissue, describing the increased path

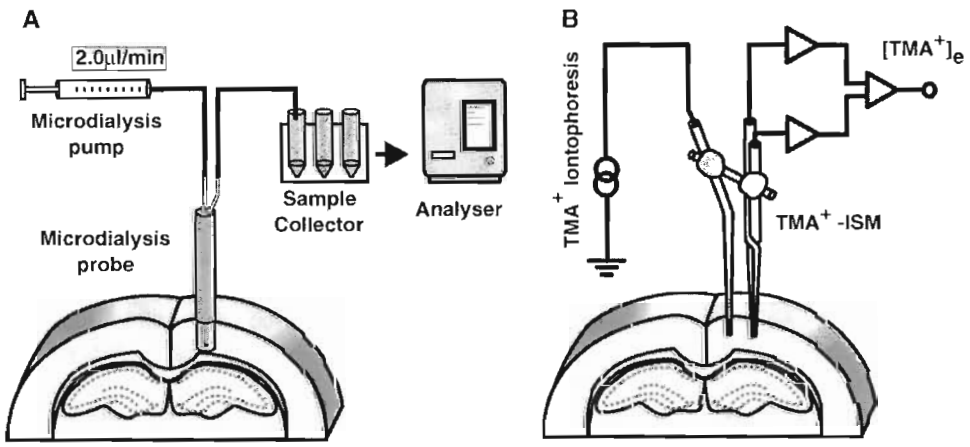

Fig. 1. Experimental setup. Left side (A): experimental setup for microdialysis. The microdialysis probe was perfused continuously with a defined flow. Collected samples were analyzed by a microdialysis analyzer. Right side (B): experimental arrangement of a TMA^+-selective double-barreled ion-selective microelectrode (ISM), which is glued to an iontophoresis microelectrode with an inter-tip distance of 100–200 μm.

length of a diffusing molecule in a complex medium due to cellular membranes, glycoproteins, macromolecules and fixed charges. Finally, non-specific uptake k' describes the loss of substances across cell membranes (Nicholson and Phillips, 1981; Nicholson, 1992). To complete the evaluation of cerebral processes, we recorded and analyzed the cortical DC potentials, a powerful method to monitor the dynamics of sensory and cognitive processing in the brain under normal conditions and in the course of central nervous system disorders. DC potentials from the cortical surface were recorded by microelectrodes filled with 150 mM NaCl, placed in the cortex and connected to a high impedance buffer amplifier with Ag/AgCl wires. The common reference electrode was positioned on the nasal bone (Lehmenkühler et al., 1999).

Statistical analysis

The results of the experiments are expressed as the mean± standard error of the mean (SEM). Differences within and between groups were evaluated using Student's paired t-test (InStat, GraphPad Software, San Diego, USA). Values of $p<0.05$ were considered significant.

Results

Extracellular space diffusion parameters and DC potentials

The mean values of extracellular volume fraction α, tortuosity and non-specific uptake k' during normoxia were $=0.18\pm0.01$, $=1.54\pm0.01$ and $k'=(3.38\pm0.32)\times10^{-3}$ s^{-1} ($n=7$), values also observed in previous studies in vivo (Cserr et al., 1991; Lehmenkühler et al., 1993; Vorisek and Sykova, 1997). During hypoxia, α decreased by about 5% in the first 20 min. At 20–30 min, α decreased to 0.14 ± 0.01 ($n=7$), i.e., about 22% (Fig. 2A). Tortuosity λ also increased in two steps, reaching a value of 1.61 ± 0.02 in the first 20 min, then increasing to 1.69 ± 0.03 ($n=7$) at 20–30 min of the hypoxic period (Fig. 2B). During the reoxygenation period, α and λ values normalized within 20 min to 0.20 ± 0.01 and 1.55 ± 0.01, respectively, and remained unchanged until the end of the measurement period of 90 min after hypoxia. No significant changes in non-specific uptake k' were seen during the entire observation period. The recorded DC potentials showed an early initial negative shift of up to 3 mV after the onset of hypoxia, which has also been seen in previous studies (Lehmenkühler et al., 1999). After this early negative shift, the DC potential returned to baseline levels. A second negative shift of up to 2.5 mV was seen in the last 5–10 min of the 30-min hypoxia. After the end of hypoxia and the return to ventilation with air, the negative DC potentials immediately returned to baseline levels (Fig. 2C).

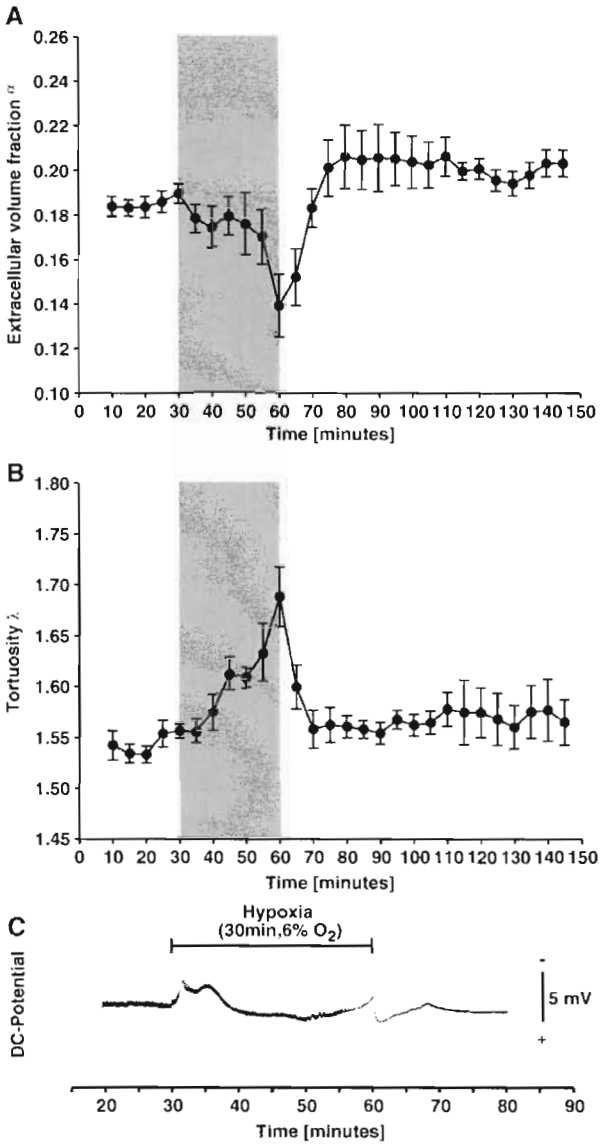

Fig. 2. The time course of changes in extracellular space volume fraction α (A) and tortuosity λ (B) during hypoxia and recovery. After establishing a stable baseline, 30 min of hypoxia was induced by reducing the inspiratory oxygen content from 21% to 6% (shaded area). After hypoxia the animals were again ventilated with air. Measurements were made at time intervals of 5 min. Values are presented as mean±SEM. The number of experiments was $n=7$. Panel (C) shows a typical recording of DC potentials measured by intracortical microelectrodes filled with 150 mM NaCl against a reference electrode placed on the nasal bone. In the early hypoxia a negative shift of up to 3 mV was observed, returning to the baseline in the first 15 min of hypoxia. A second negative shift was seen during the last 5–10 min of hypoxia of up to 2.5 mV.

Changes in lactate, lactate/pyruvate ratio and glucose

Before the induction of hypoxia, stable basal glucose levels of 2.27 ± 0.07 mmol/l ($n=15$) were found in both hypoxic and control animals. Hypoxia led to a steep decrease in glucose dialysate levels, reaching a plateau of 1.18 ± 0.16 mmol/l within 20 min. During the reoxygenation period extracellular glucose concentrations returned to control levels within 20 min (Fig. 3A). After a stabilization period of 60 min following probe insertion, basal cortical lactate levels remained stable at 0.75 ± 0.03 mmol/l ($n=15$). Hypoxia evoked by a reduction of inspiratory oxygen content led to an immediate rise in lactate levels. This rise continued throughout the 30-min period of

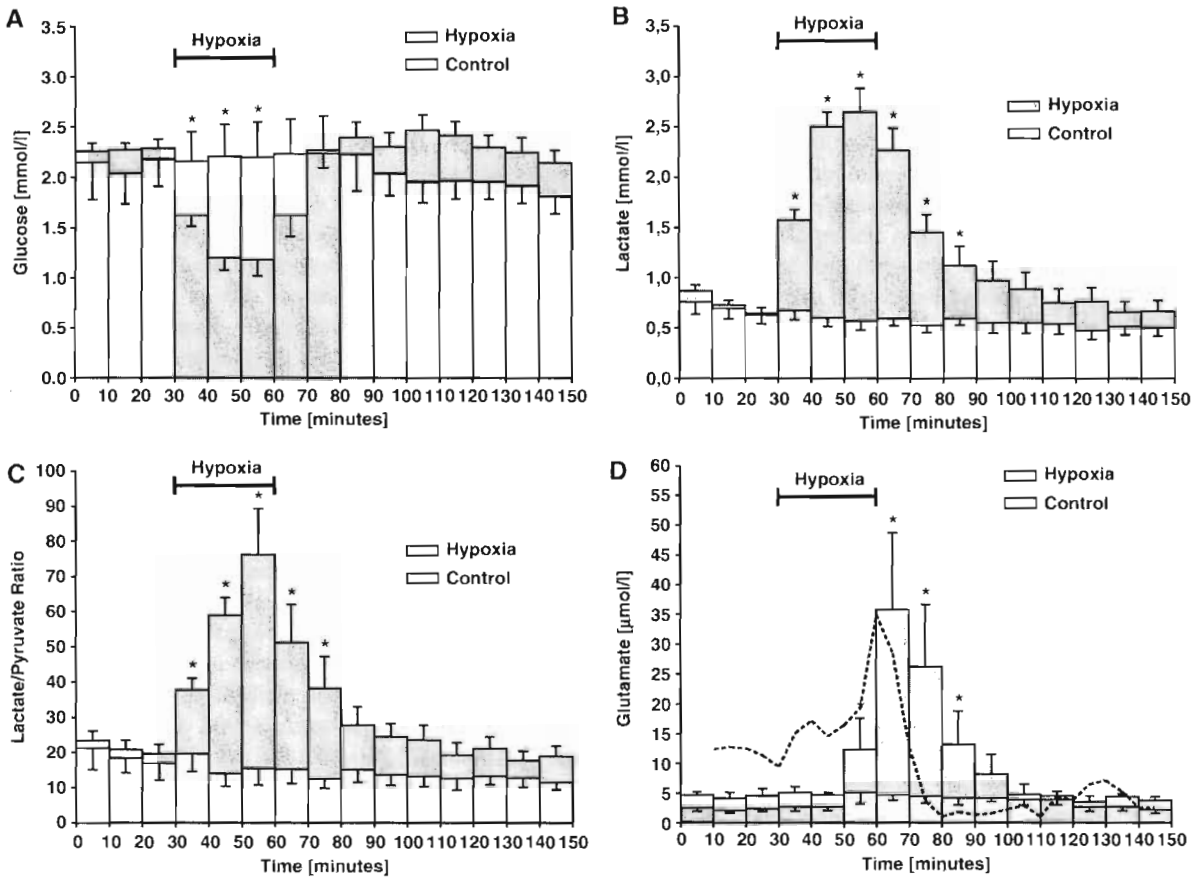

Fig. 3. Time course of interstitial glucose levels (A), lactate concentrations (B), the lactate/pyruvate ratio (C) and glutamate concentrations (D) before, during and after hypoxia of 30-min duration, compared to controls. After a stabilization period, 30 min of hypoxia was induced by ventilating the animals with 6% oxygen in nitrogen. The hypoxic period is marked by a time line. Microdialysis samples were collected over time intervals of 10 min and the measured values were presented as vertical bars. Values are shown as mean±SEM. The number of experiments was $n=10$ in the hypoxic and $n=5$ in the control group. Statistically significant differences ($p<0.05$) between the hypoxic and control animals are marked by asterisks. To show the inverse correlation between ECS volume and glutamate concentration, an inverted time course of the changes in extracellular volume fraction α (taken from Fig. 2A) was superimposed onto panel (D) (dotted line).

hypoxia, reaching a plateau at 25 min of 2.65±0.24 mmol/l, when α showed a second decrease (Fig. 3B). The difference between control and hypoxic animals was extremely significant ($p<0.001$). For evaluating the anaerobic pathway, we calculated the lactate/pyruvate ratio (L/P ratio). In control animals no significant change in the L/P ratio was seen during the entire observation period. In hypoxic animals the L/P ratio increased from 20.88±2.65 to 76.03±13.04 at the end of the hypoxic period (Fig. 3C). In the reoxygenation period, lactate levels as well as the L/P ratio decreased to control levels within 50–60 min (Figs. 3B and C).

Changes in glutamate

Extracellular glutamate levels prior to hypoxia were 2.37± 0.53 µmol/l ($n=15$). After the beginning of hypoxia, extracellular glutamate levels remained unchanged for about 20 min. In the next 20–30 min a steep increase was found, reaching concentrations of 35.81±12.96 µmol/l. These glutamate concentrations were correlated with an increase in the extracellular volume fraction α. While α returned to control levels within 20 min, the elevated glutamate levels did not return to control levels until 40–50 min of the reoxygenation period (Fig. 3D).

Discussion

The aim of this study was to study changes in brain metabolism caused by a defined hypoxic stimulus (6%O_2, 30 min) and their time course during subsequent reoxygenation. It has been shown that a reduction of inspired oxygen to 8%, although a substantial decrease in oxygen availability, produces no signs of distress in rats, but a further reduction to ≤7% results in marked restlessness followed by changes in EEG (Jones et al., 2000). Microdialysis offers the possibility of obtaining local information on energy metabolism in vivo in any tissue by introducing a probe directly into the region of interest (Valtysson et al., 1998). Thus, we reduced the inspired oxygen content to 6% to cause a degree of hypoxia that already influences normal brain function and measured the changes in metabolite concentrations by microdialysis.

In our experiments the onset of hypoxia was accompanied by a significant increase in extracellular lactate concentration. The large immediate increase in lactate levels is similar to that reported in previous studies (Harada et al., 1992; Ronne-Engström et al., 1995; Jones et al., 2000). It is well known that the hypoxic elevation of lactate is accompanied by an increase in cerebral blood flow, an increase in glucose uptake and an unchanged rate of oxygen consumption (Hamer et al., 1976; Cohen et al., 1967). These findings suggest that the increase in lactate concentration is due to an increase in the rate of glycolysis during hypoxia. Extracellular lactate is likely to be derived from glycolysis in both neurones and astrocytes and reaches the extracellular fluid by the action of highly active lactate transporters (Kochler-Stec et al., 1998). After reoxygenation, elevated lactate levels recovered to preischemic values within 40 min in our experiments. This normalization must represent uptake and utilization of lactate by neurones and astrocytes, because no significant transport of lactate across the blood–brain barrier has been found in other studies (Kuhr et al., 1988; Harada et al., 1992). Besides the lactate level as a marker for anaerobic metabolism, the tissue specific L/P ratio is an excellent indicator of cellular hypoxia, because it is correlated closely with the redox potential (Cabrera et al., 1999; Magnoni et al., 2003). Another advantage of the L/P ratio is that it is probably not influenced by alterations of the in vivo probe recovery (Persson and Hillered, 1992). In this study we found a steep increase in the L/P ratio during hypoxia, which reflects the fact that the cytosolic redox condition switched from aerobic to anaerobic glycolysis. During recovery a steep decrease in the L/P ratio indicates a return to aerobic conditions. These results show that the metabolic enzymes and their related cellular components (e.g., mitochondria) may tolerate longer hypoxic periods without any serious damage.

The concentration of glucose in the extracellular space is maintained by a balance between supply from the blood and utilization by cells. During hypoxia a fast decrease in glucose levels was found in our experiments, similar to the findings of Silver and Erecinska (1994) using an implanted glucose sensor. A possible explanation for this drop in extracellular glucose could be the increased uptake and utilization by glycolysis found during hypoxia (Hamer et al., 1976; Fray et al., 1997). Increased glycolysis results in the consumption of glucose and the production of lactate, which is transported into the extracellular space. This hypothesis is supported by the correlation seen in our results between a decrease in glucose and an increase in lactate levels. In the recovery from hypoxia, a normalization of extracellular glucose levels occurs within 20 min, indicating on the one hand a quick normalization in the uptake and utilization by the cells and on the other hand a sufficient supply from the blood. In the present study, changes in extracellular glutamate concentration occurred in the late hypoxic and early reoxygenation phases. It has been shown that hypoxia-induced anoxic depolarization can be delayed at least up to 60 min and that during this time a hypoxic transient extracellular glutamate increase is seen, derived from the Ca^{2+}-dependent neurotransmitter pool (Kunimatsu et al., 1999; Katayama et al., 1991). The inhibition of the reversed action of Ca^{2+} transporters such as the Na^{+}/Ca^{2+}-exchanger or Ca^{2+}/H^{+}-ATPase might constitute a source of cellular Ca^{2+} accumulation during hypoxia (Blaustein and Lederer, 1999; Kulik et al., 2000). It seems that an increase in cellular Ca^{2+} occurs during hypoxia until critical levels are reached. The consequence is a glutamate release, which is initiated at the end of the hypoxic period and proceeds in the early posthypoxic period. Based on the time course of extracellular volume fraction α, it can be supposed that a massive glutamate release occurs after 30 min of hypoxia. This release elevated the concentration of glutamate in the sample which was collected in the last 10 min of hypoxia only in a minor degree. The main effect of the glutamate release at the end of hypoxia was found in the first postischemic sample. So it can be supposed, that a considerable release of glutamate at the early beginning of the first postischemic collection period caused a huge increase of glutamate levels in the first postischemic sample, which was collected over a time period of 10 min. During reoxygenation glutamate levels recover to basal values, indicating a sufficient reuptake by astrocytes. The changes in α had a minimum effect of approximately 5% on dialysate concentrations during the first 20 min of hypoxia. The maximum effect of the 22% decrease in ECS volume fraction on dialysate concentrations can be expected only during the last 5–10 min of hypoxia and in the first 5–10 min of recovery. During other time periods, changes in α were too small to affect dialysate levels.

Microdialysis is a highly sensitive technique for determining regional metabolic tissue concentrations and, in this way, monitor changes in cerebral energy metabolism (Ungerstedt, 1991). However, this method has some methodical limitations that must be addressed. Compared to in vitro calibration, the in vivo recovery of substances strongly depends on the surrounding tissue properties, especially extracellular volume fraction and tortuosity, as well as on various release, uptake and clearance processes (Benveniste and Huttemeier, 1990). Therefore, calculations of metabolite concentrations based on in vitro recovery can result in the underestimation of the actual interstitial concentrations (Benveniste et al., 1989; Benveniste and Huttemeier, 1990; Chen et al., 2002). However, we believe that an evaluation of all the collected data demonstrates that the changes in extracellular microdialysate levels reflect the time course of the dynamic process of hypoxia.

The extracellular space is the microenvironment in which different substances diffuse. Changes in the ECS can affect the concentration of extracellular substances due to the movement of water between the extra- and intracellular compartment. It is well known that during terminal anoxia the extracellular space volume decreases to 5–6% (Vorisek and Sykova, 1997), which is equivalent to a reduction of 65%–75% from normal values. In our experimental setting, hypoxia resulted in a maximum decrease of the extracellular space of 22% at the end of hypoxia. This hypoxic decrease in ECS volume showed a biphasic time course in which the ECS volume decrease during the late-hypoxic period occurred simultaneous with a slow, continuous negative DC shift. It is known that negative cortical DC shifts are associated with changes in oxygen supply (Lehmenkühler et

al., 1999). Based on the findings from DC potential recordings, we can hypothesize that these late hypoxic changes in extracellular diffusion parameters were caused by a worsened oxygenation state or by the beginning of the transformation to anoxia. These changes in extracellular space volume were caused, we believe, by movements of water between the extra- and intracellular compartment or across the blood–brain barrier into the cortical tissue. As a result the mean values of the dialysate levels of lactate, glucose and glutamate harvested in the last 10 min of hypoxia can be obtained by correcting for the influence of the maximal changes in ECS volume from 2.65 mmol/l, 1.18 mmol/l and 12.40 μmol/l to 2.07 mmol/l, 0.92 mmol/l and 9.67 μmol/l, respectively. The microdialysis technique consumes the measured extracellular substances depending on the dialysate flow rate. If the substances were not removed from the tissue by the probe, the measured metabolite levels would be higher than those that we recorded. Therefore, the changes measured in lactate, glucose and glutamate levels can be affected by the size of the extracellular volume fraction α and also by the tortuosity λ, which represent the diffusion characteristics in the tissue, because the measured values reflect the balance between the availability of the substance and their removal rate.

The maximum increase in extracellular glutamate levels was observed over the same time interval as the maximum decrease in ECS volume fraction. Thus, we suggest that a substantial amount of this late hypoxic and early posthypoxic increase in glutamate was caused by a shrinkage of the ECS. Also glutamate dialysate levels can be influenced by the removal rate of the microdialysis probe. If the removal rate was zero, then the measured glutamate increase would be much greater. To reduce the removal rate by the microdialysis probe, we used the slowest dialysate flow rate that still yielded an adequate collection interval. The changes that were seen in the L/P ratio were not affected by the extracellular space volume and tortuosity in any way, since the ratio between two extracellular substances that are subject to the same correction coefficient clearly remains unaffected by the value of that coefficient and the diffusion coefficients of these substances are nearly equal.

In conclusion, our findings suggest that the changes in the extracellular microenvironment of the cerebral cortex may tolerate 30 min of hypoxia and recover to preischemic values. These results support the clinical observation that young adult patients with hypoxia, caused by acute lung failure or difficult or prolonged airway management during the induction of anesthesia, can recover without any obvious neurological changes.

Acknowledgments

This study was supported by the European Commission Marie Curie Training Site Programme HPMT-CT-2000-00187, by grant AV0Z50390512 from the Academy of Sciences of the Czech Republic and by grants 1M0021620803 and LC544 from the Ministry of Sport, Youth and Education of the Czech Republic.

References

Andersson, B., Wu, X., Bjelke, B., Sykova, E., 2004. Temporal profile of ultrastructural changes in cortical neurons after a photochemical lesion. J. Neurosci. Res. 77 (6), 901–912.

Aftabuddin, M., Islam, N., Moriwaki, A., Hori, Y., 1994. Carotid artery occlusion causes reversible brain damage in rat. Indian Heart J. 46 (3), 171–175.

Arner, P., Bolinder, J., 1991. Microdialysis of adipose tissue. J. Int. Med. 230, 381–386.

Banasiak, K.J., Xia, Y., Haddad, G.G., 2000. Mechanisms underlying hypoxia-induced neuronal apoptosis. Ann. Neurobiol. 62, 215–249.

Benveniste, H., Huttemeier, P.C., 1990. Microdialysis—Theory and application. Prog. Neurobiol. 35, 195–215.

Benveniste, H., Hansen, A.J., Ottosen, N.S., 1989. Determination of brain interstitial concentrations by microdialysis. J. Neurochem. 52, 1741–1750.

Blaustein, M.P., Lederer, W.J., 1999. Sodium/calcium exchange: its physiological implications. Physiol. Rev. 79, 763–854.

Cabrera, M.E., Saidel, G.M., Kalhan, S.C., 1999. A model analysis of lactate accumulation during muscle ischemia. J. Crit. Care 14 (4), 151–163.

Chen, K.C., Hoistad, M., Kehr, J., Fuxe, K., Nicholson, C., 2002. Theory relating in vitro and in vivo microdialysis with one or two probes. J. Neurochem. 81, 108–121.

Cohen, P.J., Alexander, S.C., Smith, T.C., Reivich, M., Wollman, H., 1967. Effects of hypoxia and normocarbia on cerebral blood flow and metabolism in conscious man. J. Appl. Physiol. 23, 183–189.

Csemy, H.F., DePasquale, M., Nicholson, C., Patlak, C.S., Pettigrew, K.D., Rice, M.E., 1991. Extracellular volume decreases while cell volume is maintained by ion uptake in rat brain during acute hypernatremia. J. Physiol. 442, 277–295.

De Salles, A.A., Kontos, H.A., Becker, D.P., et al., 1986. Prognostic significance of ventricular CSF lactic acidosis in severe head injury. J. Neurosurg. 65, 615–624.

Fellows, L.K., Boutelle, M.G., Fillenz, M., 1992. Extracellular brain glucose levels reflect local neuronal activity: a microdialysis study in awake, freely moving rats. Neurochem. 59, 2141–2147.

Fray, A.E., Boutelle, M., Fillenz, M., 1997. Extracellular glucose turnover in the striatum of unanaesthetized rats measured by quantitative microdialysis. J. Physiol. 504, 721–726.

Hamer, J., Hoyer, S., Alberti, E., Weinhardt, F., 1976. Cerebral blood flow and oxidative brain metabolism during and after moderate and profound arterial hypoxaemia. Acta Neurochir. (Wien) 33, 141–150.

Harada, M., Okuda, C., Sawa, T., Murakami, T., 1992. Cerebral extracellular glucose and lactate concentrations during and after moderate hypoxia in glucose- and saline-infused rats. Anesthesiology 77, 728–734.

Hillered, L., Hallstrom, A., Segersvard, S., Persson, L., Ungerstedt, U., 1989. Dynamics of extracellular metabolites in the striatum after middle cerebral artery occlusion in the rat monitored by intracerebral microdialysis. J. Cereb. Blood Flow Metab. 9, 607–616.

Inao, S., Marmarou, A., Clarke, G.D., 1998. Production and clearance of lactate from brain tissue, cerebrospinal fluid, and serum following experimental brain injury. J. Neurosurg. 69, 736–744.

Jones, A.D., Ros, J., Landolt, H., Fillenz, M., Boutelle, M.G., 2000. Dynamic changes in glucose and lactate in the cortex of the freely moving rat monitored using microdialysis. J. Neurochem. 75, 1703–1708.

Katayama, Y., Kawamata, T., Tamura, T., Hovda, D.A., Becker, D.P., Tsubokawa, T., 1991. Calcium-dependent glutamate release concomitant with massive potassium flux during cerebral ischemia in vivo. Brain Res. 558, 136–140.

Koehler-Stec, E., Simpson, I., Vanucci, S., Landschulz, K., Landschulz, W., 1998. Monocarboxylate transporter expression in mouse brain. Am. J. Physiol. 273, 516–524.

Kuhr, W.G., Van Den Berg, C.J., Korf, J., 1988. In vivo identification and quantitative evaluation of carrier mediated transport of lactate at the cellular level in the striatum of conscious, freely moving rats. J. Cereb. Blood Flow Metab. 8, 848–857.

Kulik, A., Trapp, S., Ballanyi, K., 2000. Ischemia but not anoxia evokes vesicular and Ca^{2+}-independent glutamate release in the dorsal vagal complex in vitro. J. Neurophysiol. 83 (5), 2905–2915.

Kunimatsu, T., Asai, S., Kanematsu, K., Zhao, H., Kohno, T., Misaki, T., Ishikawa, K., 1999. Transient in vivo membrane depolarization and glutamate release before anoxic depolarization in rat striatum. Brain Res. 831, 273–282.

Lehmenkühler, A., Sykova, E., Svoboda, J., Zilles, K., 1993. Extracellular space in rat neocortex and subcortical white matter during postnatal development determined by diffusion analysis. Neuroscience 55, 339–351.

Lehmenkühler, A., Richter, F., Poppelmann, T., 1999. Hypoxia and hypercapnia-induced DC potential shifts in rat at the scalp and the skull are opposite in polarity to those at the cerebral cortex. Neurosci. Lett. 270, 67–70.

Magistretti, P.J., Sorg, O., Yu, N., Martin, J.L., Pellerin, L., 1993. Neurotransmitters regulate energy metabolism in astrocytes: implications for the metabolic trafficking between neuronal cells. Dev. Neurosci. 15, 306–312.

Magnoni, S., Ghisoni, L., Locatelli, M., et al., 2003. Lack of improvement in cerebral metabolism after hyperoxia in severe head injury: a microdialysis study. J. Neurosurg. 98, 952–958.

Mizock, B.A., Falk, J.L., 1992. Lactic acidosis in critical illness. Crit. Care Med. 20, 80–93.

Mortelliti, M.P., Manning, H.L., 2002. Acute respiratory distress syndrome. Am. Fam. Physician 65 (9), 1823–1830.

Muller, M., 2002. Science, medicine, and the future: microdialysis. Br. Med. J. 324 (7337), 588–591.

Nicholson, C., 1992. Quantitative analysis of extracellular space using the method of TMA^+ iontophoresis and the issue of TMA^+ uptake. Can. J. Physiol. Pharmacol. 70, 314–322.

Nicholson, C., Phillips, J.M., 1981. Ion diffusion modified by tortuosity and volume fraction in the extracellular microenvironment of the rat cerebellum. J. Physiol. 321, 225–257.

Nicholson, C., Sykova, E., 1998. Extracellular space structure revealed by diffusion analysis. Trends Neurosci. 21, 207–215.

Persson, L., Hillered, L., 1992. Chemical monitoring of neurosurgical intensive care patients using intracerebral microdialysis. J. Neurosurg. 76, 72–80.

Phillis, J.W., Ren, J., O'Regan, M.H., 2001. Studies on the effects of lactate transport inhibition, pyruvate, glucose and glutamine on amino acid, lactate and glucose release from the ischemic rat cerebral cortex. J. Neurochem. 76, 247–257.

Prichard, J., Rothman, D., Novotny, E., Petroff, O., Kuwabara, T., Avison, M., Howseman, A., Hanstock, C., Shulman, R., 1991. Lactate rise detected by 1 H NMR in human visual cortex during physiologic stimulation. Proc. Natl. Acad. Sci. U. S. A. 88, 5829–5831.

Ronne-Engström, E., Carlson, H., Yansheng, L., Ungerstedt, U., 1995. Influence on perfusate glucose concentrations on dialysate lactate, pyruvate, aspartate and glutamate levels under basal and hypoxic conditions: a microdialysis study in rat brain. J. Neurochem. 65, 257–262.

Silver, I.A., Erecinska, M., 1994. Extracellular glucose concentration in mammalian brain: continuous monitoring of changes during increased neuronal activity and upon limitation in oxygen supply in normo-, hypo-, and hyperglycaemic animals. J. Neurosci. 14, 5068–5076.

Sykova, E., 1992. Ionic volume changes in the microenvironment of nerve and receptor cells. Springer-Verlag, Heidelberg.

Sykova, E., Svoboda, J., Polak, J., Chvatal, A., 1994. Extracellular volume fraction and diffusion characteristics during progressive ischemia and terminal anoxia in the spinal cord of the rat. J. Cereb. Blood Flow Metab. 14, 301–311.

Ungerstedt, U., 1991. Microdialysis—Principles and applications for studies in animal and man. J. Intern. Med. 230 (4), 365–373.

Valtysson, J., Persson, L., Hillered, L., 1998. Extracellular ischemia markers in repeated global ischemia and secondary hypoxaemia monitored by microdialysis in rat brain. Acta Neurochir. (Wien) 140, 387–395.

Vorisek, I., Sykova, E., 1997. Ischemia-induced changes in the extracellular space, diffusion parameters, K^+, and pH in the developing rat cortex and corpus callosum. J. Cereb. Blood Flow Metab. 17, 191–203.

Available online at www.sciencedirect.com
SCIENCE DIRECT
Neuroscience Letters 404 (2006) 137–142
Neuroscience Letters
www.elsevier.com/locate/neulet

Changes in diffusion parameters, energy-related metabolites and glutamate in the rat cortex after transient hypoxia/ischemia

Aleš Homola [a,b], Norbert Zoremba [c], Karel Šlais [b,d], Ralf Kuhlen [c], Eva Syková [a,b,*]

[a] Department of Neuroscience and Centre for Cell Therapy and Tissue Repair, 2nd Medical Faculty, Prague, Czech Republic
[b] Institute of Experimental Medicine, Academy of Sciences of the Czech Republic, Vídeňská 1083, 142 20 Prague 4, Czech Republic
[c] Department of Intensive Care Medicine, University Hospital RWTH Aachen, Aachen, Germany
[d] Department of Pharmacology, Faculty of Medicine, Masaryk University, Brno, Czech Republic

Received 21 March 2006; received in revised form 12 May 2006; accepted 14 May 2006

Abstract

It has been shown that global anoxia leads to dramatic changes in the diffusion properties of the extracellular space (ECS). In this study, we investigated how changes in ECS volume and geometry in the rat somatosensory cortex during and after transient hypoxia/ischemia correlate with extracellular concentrations of energy-related metabolites and glutamate. Adult male Wistar rats ($n = 12$) were anesthetized and subjected to hypoxia/ischemia for 30 min (ventilation with 10% oxygen and unilateral carotid artery occlusion). The ECS diffusion parameters, volume fraction and tortuosity, were determined from concentration–time profiles of tetramethylammonium applied by iontophoresis. Concentrations of lactate, glucose, pyruvate and glutamate in the extracellular fluid (ECF) were monitored by microdialysis ($n = 9$). During hypoxia/ischemia, the ECS volume fraction decreased from initial values of 0.19 ± 0.03 (mean ± S.E.M.) to 0.07 ± 0.01 and tortuosity increased from 1.57 ± 0.01 to 1.88 ± 0.03. During reperfusion the volume fraction returned to control values within 20 min and then increased to 0.23 ± 0.01, while tortuosity only returned to original values (1.53 ± 0.06). The concentrations of lactate and glutamate, and the lactate/pyruvate ratio, substantially increased during hypoxia/ischemia, followed by continuous recovery during reperfusion. The glucose concentration decreased rapidly during hypoxia/ischemia with a subsequent return to control values within 20 min of reperfusion. We conclude that transient hypoxia/ischemia causes similar changes in ECS diffusion parameters as does global anoxia and that the time course of the reduction in ECS volume fraction correlates with the increase of extracellular concentration of glutamate. The decrease in the ECS volume fraction can therefore contribute to an increased accumulation of toxic metabolites, which may aggravate functional deficits and lead to damage of the central nervous system (CNS).

Keywords: Hypoxia; Extracellular space; Microdialysis; Ischemia; Diffusion

The diffusion of neuroactive substances through the extracellular space of the CNS is the underlying mechanism of extrasynaptic (volume) transmission, which is an important mode of communication between nerve cells [1]. Diffusion in the ECS obeys Fick's law but is constrained by two factors: extracellular volume fraction α, which is the ratio of the ECS volume to total tissue volume and tortuosity λ, a parameter describing the impact of tissue geometry on diffusion compared to a free diffusion medium. Tortuosity is defined as $\lambda = (D/\mathrm{ADC})^{1/2}$, where ADC is the apparent diffusion coefficient in the brain and D is the free diffusion coefficient. The absolute values of the ECS difusion parameters can be determined by the real-time iontophoretic method using tetramethylammonium (TMA^+)-selective microelectrodes [15,16].

It has been shown that many pathological states result in changes in extracellular space volume and geometry, significantly affecting signal transmission [22,23]. Among those of major clinical relevance and experimental interest are conditions leading to brain hypoxia or ischemia. Acute hypoxia or ischemia, and also some other acute neurological disorders that involve cell membrane depolarization (cortical spreading depression, status epilepticus and hypoglycaemia), cause excessive transmembrane ionic shifts that are accompanied by the movement of water from the extracellular to the intracellular compartment (cytotoxic edema). Rapid cellular swelling inevitably results in a shrinkage of the ECS, the impaired diffusion of substances

* Corresponding author at: Institute of Experimental Medicine, Academy of Sciences of the Czech Republic, Vídeňská 1083, 142 20 Prague 4, Czech Republic. Tel.: +420 2 41062230; fax: +420 2 41062783.
E-mail address: sykova@biomed.cas.cz (E. Syková).

0304-3940/$ – see front matter © 2006 Elsevier Ireland Ltd. All rights reserved.
doi:10.1016/j.neulet.2006.05.028

through the ECS and the greater accumulation of toxic metabolites. In turn, these consequences can contribute to functional deficits and CNS damage. Experimentally, ischemia-evoked changes in the ECS diffusion parameters in the brain cortex in vivo have, so far, been studied only in a model of global anoxia induced by cardiac arrest. These studies have revealed a dramatic decrease in ECS volume fraction and an increase in tortuosity, occurring only a few minutes after the interruption of the blood supply to the brain [25,27]. In the present study, we have examined the ECS diffusion parameters in the somatosensory cortex of adult rats during transient hypoxia combined with unilateral common carotid artery occlusion and also during subsequent reperfusion. The obtained data were correlated with changes in the energy-related metabolites lactate and glucose, the lactate/pyruvate-ratio and glutamate, monitored by intracerebral microdialysis.

Adult male Wistar rats (300–350 g) were anesthetized by an intraperitoneal injection of urethane (1.5 g/kg, Sigma-Aldrich Chemie GmbH, Seelze, Germany). The animals were intubated and connected to a ventilator (CIV 101, Columbus Instruments, Columbus, OH, USA), relaxed with pancuroniumbromide (0.6 mg/kg, Pavulon, Organon, Netherlands), and ventilated with air. The body temperature was maintained at 36–37 °C by a heating pad. The somatosensory cortex of the rat was partially exposed by a burr hole 2–3 mm caudal from the bregma and 2–3 mm lateral from the midline. A transient hypoxia/ischemia of 30 min duration was induced by reducing the inspiratory oxygen content to 10% (in nitrogen) and unilateral clamping of the common carotid artery. Following the hypoxic period, the animals were again ventilated with air ($pO_2 = 21\%$). The control animals were sham-operated and ventilated with air throughout the experiment. In order to measure in the ipsilateral somatosensory cortex, diffusion and microdialysis measurements were not performed simultaneously.

All efforts were made to minimize animal suffering and to reduce the number of animals used. The experiments were carried out in accordance with the European Communities Council Directive of 24.November 1986 (86/609/EEC) and approved by the local Institutional Animal Ethics Committee.

The ECS diffusion parameters were studied by the real-time iontophoretic method described in detail previously [13]. Briefly, an extracellular marker that is restricted to the extracellular compartment, such as tetramethylammonium ions (TMA^+, MW = 74.1 Da) to which cell membranes are relatively impermeable, is released into the extracellular space by iontophoresis and its local concentration measured with a TMA^+-selective microelectrode (TMA^+-ISM) located about 100–200 μm from the release site. The concentration of TMA^+ in the ECS is inversely proportional to the ECS volume. Double-barrelled TMA^+-ISMs were prepared by a procedure described in detail previously [21]. The tip of the ion-sensitive barrel was filled with a liquid ion exchanger (Corning 477317); the rest of the barrel was backfilled with 150 mM TMA^+ chloride. The reference barrel contained 150 mM NaCl. The shank of the iontophoretic pipette was bent so that it could be aligned parallel to that of the ion-selective microelectrode and was backfilled with 150 mM TMA^+ chloride. An electrode array was made by gluing a TMA^+-ISM to an iontophoretic micropipette with a tip separation of 100–200 μm. The iontophoresis parameters were +20 nA bias current (continuously applied current to maintain a constant electrode transport number), and a +180 nA current step of 24 s duration, to generate the diffusion curve. The TMA^+ diffusion curves were generated at regular intervals of 5 min. Before tissue measurements, diffusion curves were first recorded in 0.3% agar (Sigma-Aldrich, Steinheim, Germany) dissolved in a solution containing 150 mM NaCl, 3 mM KCl, and 1 mM TMACl. The diffusion curves were analysed to obtain the electrode transport number (n) and the free TMA^+ diffusion coefficient (D) by curve-fitting according to a modified diffusion equation using the VOLTORO program [15]. Diffusion curves were then recorded in the somatosensory cortex at a depth of 1200–1500 μm. Knowing n and D, the values of extracellular volume fraction α and tortuosity λ could be obtained from the diffusion curves.

The technique of microdialysis is based on sampling fluid via a double-lumen probe with an integrated semipermeable membrane in which the equilibration of substances in the extracellular space and perfusion fluid takes place by diffusion according to the concentration gradient. We used a double-lumen microdialysis probe with a membrane length of 2 mm, an outer diameter of 0.5 mm and a cut-off at 20,000 Da (CMA 12, 2 mm membrane length, CMA Microdialysis, Sweden). The inserted microdialysis catheter was connected by low-volume fluorinated ethylene propylene (FEP)-tubing (1.2 μl/10 cm) to a precision infusion pump (CMA 102, CMA Microdialysis, Sweden) in order to maintain a constant dialysate flow. The microdialysis catheter was continuously perfused with a dialysate containing 147 mmol/l NaCl, 2.7 mmol/l KCl, 1.2 mmol/l $CaCl_2$ and 0.85 mmol/l $MgCl_2$ (Perfusion fluid CNS, CMA Microdialysis, Sweden) at a flow rate of 2 μl/min. After a stabilisation period of 60 min following insertion into the brain, microdialysate samples were collected in 10 min intervals and immediately frozen at −40 °C until analysed. Thawed and centrifuged dialysate samples were analysed enzymatically with a CMA 600 Microdialysis Analyser (CMA/Microdialysis, Sweden) for lactate, pyruvate, glucose and glutamate concentrations.

The exchange of substances across the microdialysis membrane is limited by the total area of the membrane, the perfusion flow rate, the characteristics of the diffusing substance and the diffusion constant in the tissue surrounding the probe [24]. The recovery rate expresses the relation between the concentration of the substance in the microdialysis probe effluent and the concentration in the medium [14]. Before and at the end of the experiments, the recovery rates for each probe were determined by continuing the perfusion at the same settings in a calibration solution containing known concentrations of the different analytes. The calibration solution contained 2.50 mmol/l lactate, 250 μmol/l pyruvate, 5.55 mmol/l glucose, 250 mmol/l glycerol and 25 μmol/l glutamate (Calibrator, CMA Microdialysis, Sweden). The concentrations in the calibration solution were compared with the concentrations of the in vitro microdialysis samples to determine the relative recovery for each substance. The measured experimental values were weighted by the relative recovery to estimate the in vivo extracellular concentration of the substances in the immediate vicinity of the probes. In

vitro recovery rates were 24.3 ± 1.6% for lactate, 23.1 ± 0.6% for pyruvate, 13.7 ± 0.8% for glutamate and 14.1 ± 0.8% for glucose ($n = 14$). All results are presented as weighted concentrations.

The concentration of a metabolite in the extracellular fluid is clearly affected by changes in the extracellular space volume fraction. A decrease in α would, in the absence of any changes in metabolite supply or utilization, result in an increase in the measured metabolite concentration. Similarly, an increase in α would cause the measured metabolite concentration to decrease. To take into account the effects of changes in α, we have expressed our results as both the actual measured metabolite concentrations and also as the concentrations corrected for changes in α relative to its pre-hypoxic/ischemic baseline values. However, the physiological concentrations are those without a correction factor.

The results of the experiments are expressed as the mean ± standard error of the mean (S.E.M.). Differences within and between groups were evaluated using Student's paired t-test. Values of $p < 0.05$ were considered significant.

The mean values of extracellular volume fraction α and tortuosity λ during normoxia were $\alpha = 0.19 \pm 0.03$ and $\lambda = 1.57 \pm 0.01$ ($n = 12$, mean ± S.E.M.), which are similar to the values observed in rat cortex previously [13,27]. During 30 min of hypoxia-ischemia, α gradually decreased, reaching a minimum of 0.07 ± 0.01 at the end of the hypoxic/ischemic insult (Fig. 1A). The tortuosity simultaneously increased to 1.88 ± 0.03 (Fig. 1B). After the release of carotid artery occlusion and the beginning of normoxic ventilation, both α and λ started to return to normal values, reaching them within 20 min of the recovery period. During the next 20 min, α continued to increase to 0.23 ± 0.01 while λ decreased to 1.53 ± 0.06, then both parameters remained unchanged at these levels until the end of the 90-min recovery phase (Fig. 1A and B).

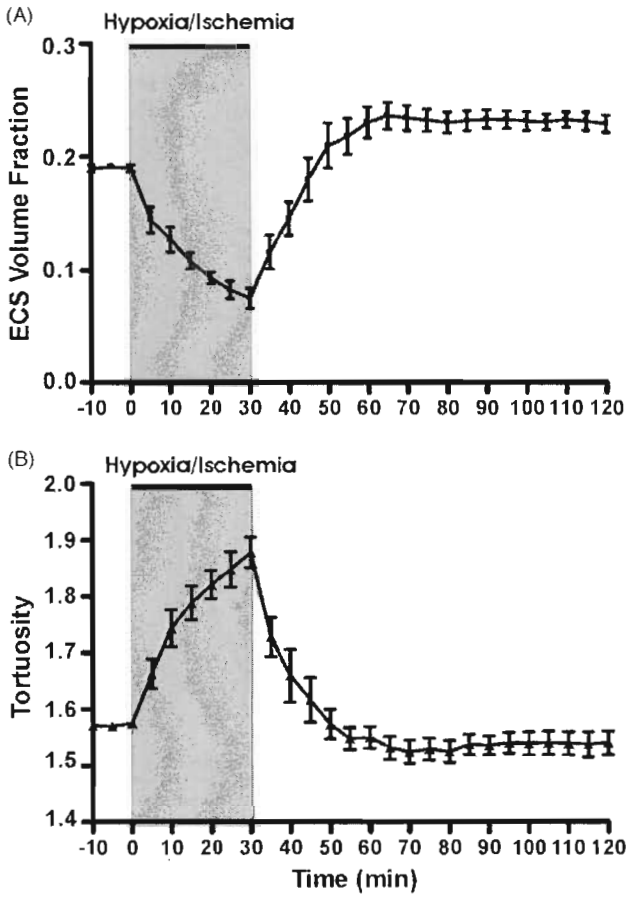

Fig. 1. The time course of changes in extracellular space volume fraction α (A) and tortuosity λ (B) during transient hypoxia/ischemia and subsequent reperfusion.

After a stabilisation period of 60 min following probe insertion, the basal cortical level of lactate and the lactate/pyruvate ratio remained stable at 0.99 ± 0.06 mmol/l and 23.44 ± 1.85, respectively ($n = 9$). There were no statistical differences compared to the control group ($n = 5$). Combined hypoxia/ischemia led to an immediate rise in lactate dialysate levels, reaching a plateau of 3.01 ± 0.62 mmol/l within 20 min (Fig. 2A). The lactate/pyruvate ratio showed a similar time course during hypoxia/ischemia, reaching a plateau of 64.79 ± 11.24 (Fig. 2B). After the release of carotid occlusion and reoxygenation, lactate levels and the lactate/pyruvate ratio decreased, reaching control values within 30–40 min. Taking into account the effect of the changes in ECS volume fraction, the calculated extracellular concentrations of lactate during hypoxia/ischemia would be 30–50% lower than those actually measured (Fig. 2A).

Before the induction of hypoxia/ischemia, we found stable basal glucose and glutamate levels of 2.94 ± 0.18 mmol/l and 6.85 ± 0.97 μmol/l, respectively ($n = 9$), without any significant differences compared with control animals ($n = 5$). Unilateral carotid occlusion and a reduction in inspiratory oxygen content led to a steep decrease in glucose dialysate concentrations, reaching a minimum of 1.45 ± 0.23 mmol/l after 20 min of hypoxia/ischemia. During the reoxygenation period extracellular glucose concentrations returned to control levels within 20 min and then slowly decreased, reaching a value of 2.05 ± 0.17 mmol/l at the end of the experiment. The glucose concentrations during hypoxia/ischemia would be even lower if we take into account the accompanying changes in ECS volume fraction. During reperfusion, the glucose concentration corrected for the increase in α reached initial values within 20 min and remained at this level until the end of the experiment (Fig. 2C). Extracellular glutamate levels increased during hypoxia/ischemia, reaching maximum values of 59.30 ± 15.90 μmol/l at the end of the hypoxic/ischemic insult. During reperfusion the extracellular glutamate levels decreased, reaching control values 90 min after reperfusion. The concentration of glutamate corrected for the increase in α would be lower with the greatest increase seen within the first 10 min (Fig. 2D).

The aim of this study was to investigate changes in the diffusion parameters of the ECS and the extracellular concentrations of energy-related metabolites and glutamate in the rat somatosensory cortex during transient hypoxia/ischemia and reperfusion. This allowed us to analyse the relationship between the dynamic changes in the diffusion properties of the brain cortex and energy metabolism.

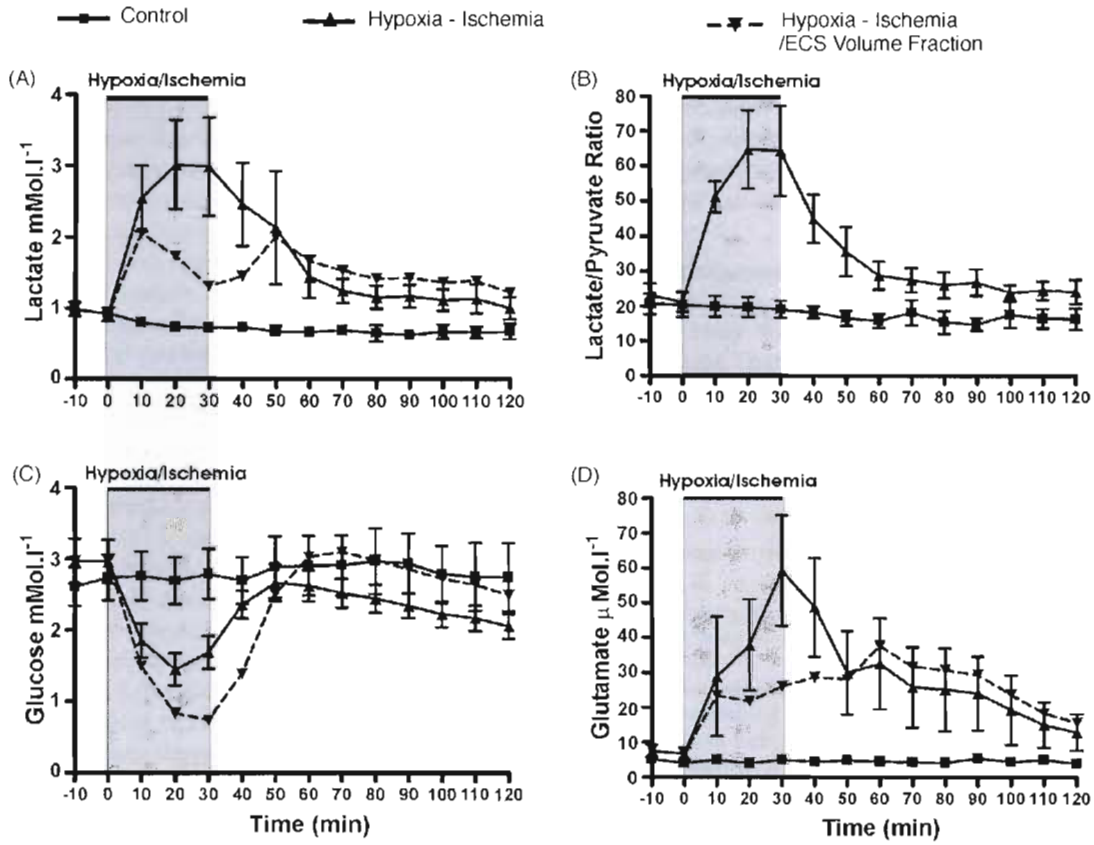

Fig. 2. The time course of changes in the concentration of extracellular lactate (A), the lactate/pyruvate ratio (B), and the concentrations of extracellular glucose (C) and glutamate (D) during transient hypoxia/ischemia and subsequent reperfusion, compared to controls. The stated concentrations, representing the actual physiological concentrations, may be underestimated. The time courses of the concentrations of the evaluated metabolites corrected for changes in ECS volume are presented as dashed lines, and they show how much of the concentration change is due to the ECS volume change.

Previous studies using a model of terminal anoxia in the rat cortex have shown a fast decrease in ECS volume and an increase in tortuosity within a few minutes following cardiac arrest [25,27]. The ultimate changes in ECS diffusion parameters were associated with an abrupt elevation of $[K^+]_e$ and an acid shift in pH_e [27] and correlated well with a reduction in the apparent diffusion coefficient of water (ADC_w) as measured by diffusion-weighted MRI [25]. Also, another study demonstrated a temporary reduction in ADC_w during transient hypoxia/ischemia with subsequent renormalization during reperfusion [10]. The present study found a continuous decrease in α and increase in λ during a hypoxic/ischemic insult, with final values similar to those previously found in terminal anoxia [25,27]. Similarly as during terminal anoxia, we observed that the changes in ECS diffusion parameters were accelerated by ischemic depolarization, which usually occurred between 5 and 10 min after the onset of hypoxia/ischemia, suggesting that ionic shifts were also responsible for the initial cellular swelling in this model. A similar time course in the reduction of the ECS size, measured by the electrical impedance technique, was reported during transient hypoxia/ischemia in the parietal cortex of 4-week-old rats [17].

During reperfusion the tortuosity renormalized within 20 min, while the ECS volume fraction increased and remained elevated about 20% above original normoxic values. This increase in the size of the ECS corresponds well with the findings of an increased signal in T1 weighted images and an elevated water content in the brain cortex of 4-week-old rats after a hypoxic-ischemic insult [17,18]. The authors concluded that changes in T1, but not T2, weighted MRI best serve as an indicator of edema associated with an elevation in water content. Also, a temporary increase in ADC_w without significant changes in the signal of T2 weighted MRI has been found in the parietal cortex of adult rats during reperfusion after hypoxia-ischemia [10].

To monitor changes in cerebral energy metabolism we used microdialysis, which is considered a highly sensitive technique for determining regional metabolic tissue concentrations [24], but it has some methodical limitations. Changes in the extracellular space volume during hypoxic conditions may have effects on microdialysate concentrations and probe efficiency. Relative recovery can change in the same probe during different physiological and pathological conditions [9]. Compared to in vitro calibration the in vivo recovery of substances strongly depends on the surrounding tissue properties especially extracellular volume fraction and tortuosity as well as various release, uptake and clearance processes [4]. Based on these findings the calculation of the interstitial concentrations based entirely on the in vitro recovery can be underestimated and possibly

could not predict tissue interstitial concentration accurately [3,4,9]. However, we suggest that the changes in extracellular microdialysate levels reflect the time course of this dynamic process.

In our experiments we found a steep increase in extracellular lactate concentration immediately after the onset of hypoxia/ischemia, which has also been seen previously [19]. In the past decades, lactate has been considered a dead-end waste product of anaerobic glycolysis, contributing to acidosis and tissue damage. Recent studies, however, have shown that lactate can be utilized by neurons as an energy source during aerobic conditions [5] and can even support neuronal survival and function during glucose deprivation in organotypic hippocampal slice cultures [7]. Another study demonstrated a beneficial effect of lactate during the initial phase of reperfusion [8]. This finding supports studies suggesting that lactate is used as a preferred substrate for the immediate restoration of neuronal ATP after hypoxia [20]. In our experiments, during reperfusion, we have seen a decrease in extracellular lactate concentration, reaching control values within 90 min of reoxygenation. This indicates a return to a sufficient oxygen supply and the uptake of lactate, possibly by neurons. A second marker for anaerobic metabolism is the tissue-specific L/P ratio, because it is closely correlated with the redox potential of cells [6]. Our results show a steep increase in the L/P ratio during hypoxia/ischemia, indicating a reversal of the cytosolic redox potential and a switch to anaerobic glycolysis. During reperfusion the L/P ratio normalized, which again corresponds with a return to the aerobic pathway of energy production.

The concentration of glucose in the ECF is a balance between supply and utilization, and possibly both mechanisms are involved in the decrease seen during hypoxia/ischemia in our experiments. During recovery the glucose concentration returned to initial values within 20 min and then slightly decreased again. This small drop is probably caused by a dilution effect of vasogenic edema.

It has been shown that the extracellular concentration of glutamate increases during brain ischemia, and the excessive activation of its receptors is believed to be a major cause of ischemia-related neuronal injury [2]. In our experiments, the concentration of glutamate in the ECF started to increase soon after the onset of hypoxia/ischemia and continued to increase to a level 10-fold above control values at the end of the insult. We have also shown how the ECS volume decrease contributes to the increase in the extracellular glutamate concentration. The activation of glutamate receptors may result in rapid cellular swelling [11]. However, only very high concentrations (10^{-2} M) were shown to cause a substantial decrease in the ECS volume in the isolated spinal cord of rat pups under normoxic conditions [26]. Because such concentrations are not achieved even under pathological conditions, it was suggested that glutamate-induced astrocytic swelling in vivo could be indirect and mediated by glutamate's effects on neuronal cells, such as increases in the extracellular potassium concentration promoted by neuronal depolarization [12].

In conclusion, we have demonstrated that transient hypoxia/ischemia causes similar changes in ECS diffusion parameters as does global anoxia. The observed reduction in ECS volume, reflecting cytotoxic edema, correlates well with the time course of the elevation in extracellular glutamate concentration. We have also shown the impact of the ECS volume on the concentrations of substances diffusing through the ECS, evidencing to what degree ECS shrinkage contributes to the increased concentrations of toxic metabolites.

Acknowledgements

This study was supported by the European Commission Marie Curie Training Site Programme HPMT-CT-2000-00187, by a grant from the Academy of Sciences of the Czech Republic AV0Z50390512, and by grants from the Ministry of Education, Youth and Sports of the Czech Republic 1M0021620803 and MSM0021622404.

References

[1] L.F. Agnati, M. Zoli, I. Stromberg, K. Fuxe, Intercellular communication in the brain: wiring versus volume transmission, Neuroscience 69 (1995) 711–726.
[2] H. Benveniste, J. Drejer, A. Schousboe, N.H. Diemer, Elevation of the extracellular concentrations of glutamate and aspartate in rat hippocampus during transient cerebral ischemia monitored by intracerebral microdialysis, J. Neurochem. 43 (1984) 1369–1374.
[3] H. Benveniste, A.J. Hansen, N.S. Ottosen, Determination of brain interstitial concentrations by microdialysis, J. Neurochem. 52 (1989) 1741–1750.
[4] H. Benveniste, P.C. Huttemeier, Microdialysis—theory and application, Prog. Neurobiol. 35 (1990) 195–215.
[5] A.K. Bouzier-Sore, P. Voisin, P. Canioni, P.J. Magistretti, L. Pellerin, Lactate is a preferential oxidative energy substrate over glucose for neurons in culture, J. Cereb. Blood Flow Metab. 23 (2003) 1298–1306.
[6] M.E. Cabrera, G.M. Saidel, S.C. Kalhan, A model analysis of lactate accumulation during muscle ischemia, J. Crit. Care 14 (1999) 151–163.
[7] H.L. Cater, C.D. Benham, L.E. Sundstrom, Neuroprotective role of monocarboxylate transport during glucose deprivation in slice cultures of rat hippocampus, J. Physiol. 531 (2001) 459–466.
[8] H.L. Cater, A. Chandratheva, C.D. Benham, B. Morrison, L.E. Sundstrom, Lactate and glucose as energy substrates during, and after, oxygen deprivation in rat hippocampal acute and cultured slices, J. Neurochem. 87 (2003) 1381–1390.
[9] K.C. Chen, M. Hoistad, J. Kehr, K. Fuxe, C. Nicholson, Theory relating in vitro and in vivo microdialysis with one or two probes, J. Neurochem. 81 (2002) 108–121.
[10] R.M. Dijkhuizen, S. Knollema, H.B. van der Worp, G.J. Ter Horst, D.J. De Wildt, J.W. Berkelbach van der Sprenkel, K.A. Tulleken, K. Nicolay, Dynamics of cerebral tissue injury and perfusion after temporary hypoxia-ischemia in the rat: evidence for region-specific sensitivity and delayed damage, Stroke 29 (1998) 695–704.
[11] E. Hansson, Metabotropic glutamate receptor activation induces astroglial swelling, J. Biol. Chem. 269 (1994) 21955–21961.
[12] H.K. Kimelberg, Astrocytic swelling in cerebral ischemia as a possible cause of injury and target for therapy, Glia 50 (2005) 389–397.
[13] A. Lehmenkuhler, E. Sykova, J. Svoboda, K. Zilles, C. Nicholson, Extracellular space parameters in the rat neocortex and subcortical white matter during postnatal development determined by diffusion analysis, Neuroscience 55 (1993) 339–351.
[14] M. Muller, Science, medicine, and the future: microdialysis, BMJ 324 (2002) 588–591.
[15] C. Nicholson, J.M. Phillips, Ion diffusion modified by tortuosity and volume fraction in the extracellular microenvironment of the rat cerebellum, J. Physiol. 321 (1981) 225–257.

[16] C. Nicholson, E. Sykova, Extracellular space structure revealed by diffusion analysis, Trends Neurosci. 21 (1998) 207–215.
[17] M. Qiao, P. Latta, S. Meng, B. Tomanek, U.I. Tuor, Development of acute edema following cerebral hypoxia-ischemia in neonatal compared with juvenile rats using magnetic resonance imaging, Pediatr. Res. 55 (2004) 101–106.
[18] M. Qiao, K.L. Malisza, M.R. Del Bigio, U.I. Tuor, Transient hypoxia-ischemia in rats: changes in diffusion-sensitive MR imaging findings, extracellular space, and Na+-K+-adenosine triphosphatase and cytochrome oxidase activity, Radiology 223 (2002) 65–75.
[19] E. Ronne-Engstrom, H. Carlson, Y. Liu, U. Ungerstedt, L. Hillered, Influence of perfusate glucose concentration on dialysate lactate, pyruvate, aspartate, and glutamate levels under basal and hypoxic conditions: a microdialysis study in rat brain, J. Neurochem. 65 (1995) 257–262.
[20] A. Schurr, R.S. Payne, J.J. Miller, B.M. Rigor, Glia are the main source of lactate utilized by neurons for recovery of function posthypoxia, Brain Res. 774 (1997) 221–224.
[21] E. Sykova, Ionic and Volume Changes in the Microenvironment of Nerve and Receptor Cells, Springer-Verlag, 1992, pp. 1–167.
[22] E. Sykova, Glia and volume transmission during physiological and pathological states, J. Neural. Transm. 112 (2005) 137–147.
[23] E. Sykova, A. Chvatal, Glial cells and volume transmission in the CNS, Neurochem. Int. 36 (2000) 397–409.
[24] U. Ungerstedt, Microdialysis—principles and applications for studies in animals and man, J. Intern. Med. 230 (1991) 365–373.
[25] A. van der Toorn, E. Sykova, R.M. Dijkhuizen, I. Vorisek, L. Vargova, E. Skobisova, M. van Lookeren Campagne, T. Reese, K. Nicolay, Dynamic changes in water ADC, energy metabolism, extracellular space volume, and tortuosity in neonatal rat brain during global ischemia, Magn. Reson. Med. 36 (1996) 52–60.
[26] L. Vargova, P. Jendelova, A. Chvatal, E. Sykova, Glutamate, NMDA, and AMPA induced changes in extracellular space volume and tortuosity in the rat spinal cord, J. Cereb. Blood Flow Metab. 21 (2001) 1077–1089.
[27] I. Vorisek, E. Sykova, Ischemia-induced changes in the extracellular space diffusion parameters, K+, and pH in the developing rat cortex and corpus callosum, J. Cereb. Blood Flow Metab. 17 (1997) 191–203.

Available online at www.sciencedirect.com
ScienceDirect
Experimental Neurology 209 (2008) 145–154
Experimental Neurology
www.elsevier.com/locate/yexnr

Brain metabolism and diffusion in the rat cerebral cortex during pilocarpine-induced status epilepticus

Karel Slais [a,b,*], Ivan Vorisek [a,c,d], Norbert Zoremba [e], Ales Homola [a,c], Lesia Dmytrenko [a], Eva Sykova [a,c]

[a] Institute of Experimental Medicine, Academy of Sciences of the Czech Republic, Prague, Czech Republic
[b] Department of Pharmacology, Faculty of Medicine, Masaryk University, Brno, Czech Republic
[c] Department of Neuroscience and Centre for Cell Therapy and Tissue Repair, 2nd Medical Faculty, Prague, Czech Republic
[d] Department of Radiology, Institute for Clinical and Experimental Medicine, Prague, Czech Republic
[e] Department of Intensive Care Medicine, University Hospital RWTH Aachen, Aachen, Germany

Received 14 March 2007; revised 13 August 2007; accepted 11 September 2007
Available online 20 September 2007

Abstract

The real-time iontophoretic method using tetramethylammonium-selective microelectrodes and diffusion-weighted magnetic resonance imaging were used to measure the extracellular space volume fraction α, tortuosity λ and apparent diffusion coefficient of water (ADC_W) 240 min after the administration of pilocarpine in urethane-anaesthetized rats. The obtained data were correlated with extracellular lactate, glucose, and glutamate concentrations and the lactate/pyruvate-ratio, determined by intracerebral microdialysis. The control values of α and λ were 0.19 ± 0.004 and 1.58 ± 0.01, respectively. Following pilocarpine application, α decreased to 0.134 ± 0.012 100 min later. Thereafter α increased, reaching 0.176 ± 0.009 140 min later. No significant changes in λ were observed during the entire time course of the experiment. ADC_W was significantly decreased 100 min after pilocarpine application ($549 \pm 8\ \mu m^2\ s^{-1}$) compared to controls ($603 \pm 11\ \mu m^2\ s^{-1}$); by the end of the experiments, ADC_W had returned to control values. The basal cortical levels of lactate, the lactate/pyruvate ratio, glucose and glutamate were 0.61 ± 0.05 mmol/l, 33.16 ± 4.26, 2.42 ± 0.13 mmol/l and 6.55 ± 1.31 μmol/l. Pilocarpine application led to a rise in lactate, the lactate/pyruvate ratio and glutamate levels, reaching 2.92 ± 0.60 mmol/l, 84.80 ± 11.72 and 22.39 ± 5.85 μmol/l within about 100 min, with a subsequent decrease to control values 140 min later. The time course of changes in glucose levels was different, with maximal levels of 3.49 ± 0.24 mmol/l reached 40 min after pilocarpine injection and a subsequent decrease to 1.25 ± 0.40 mmol/l observed 200 min later. Pathologically increased neuronal activity induced by pilocarpine causes cell swelling followed by a reduction in the ECS volume fraction, which can contribute to the accumulation of toxic metabolites and lead to the start of epileptic discharges.

Keywords: Diffusion; ADC_W; Microdialysis; Pilocarpine; Epilepsy; Glucose; Glutamate; Pyruvate; Lactate; Potassium

Introduction

The acute administration of a high dose of the muscarinic cholinergic agonist pilocarpine in rodents is an experimental model widely used to study the pathophysiology of seizures. This seizure model demonstrates the potent proconvulsant effect of pilocarpine and produces behavioural and electroencephalographic alterations that are similar to those of human temporal lobe epilepsy (Turski et al., 1983).

The extracellular space (ECS) forms the microenvironment of nerve cells, and many neuroactive substances diffuse through this space to reach their target receptors. The diffusion of neuroactive substances through the ECS of the central nervous system (CNS) is the underlying mechanism of extrasynaptic (volume) transmission, an important mode of communication between nerve cells (Agnati et al., 1995; Nicholson and Sykova, 1998; Sykova, 1997, 2004; Zoli et al., 1999). Diffusion in the ECS obeys Fick's laws but is constrained by two factors: the extracellular volume fraction α, which is the ratio of the ECS volume to total tissue volume, and tortuosity λ, a parameter describing the impact of tissue geometry on diffusion compared to a free diffusion medium. Tortuosity is defined as $\lambda = (D/ADC)^{1/2}$, where ADC is

* Corresponding author. Institute of Experimental Medicine, ASCR, Videnska 1083, 142 20 Prague 4, Czech Republic. Fax: +420 241062783.
E-mail address: kslais@med.muni.cz (K. Slais).

0014-4886/$ - see front matter © 2007 Elsevier Inc. All rights reserved.
doi:10.1016/j.expneurol.2007.09.008

the apparent diffusion coefficient in the brain and D is the free diffusion coefficient (Nicholson and Phillips, 1981; Nicholson and Sykova, 1998). Extracellular diffusion parameters are significantly altered in many pathological states (Sykova, 2005; Sykova et al., 2000), among them pathological conditions characterized by increased neuronal activity (Kilb et al., 2006; Svoboda and Sykova, 1991; Sykova et al., 2003).

Diffusion-weighted magnetic resonance imaging (DW MRI) is a noninvasive technique that allows the in situ measurement of water diffusion predominantly within the interstitial space (Le Bihan et al., 1986). Measurements of the apparent diffusion coefficient of water (ADC_W) in experimental models of status epilepticus (SE) show a decrease of ADC_W in the brain parenchyma several hours after the induction of seizures (Fabene et al., 2006; Righini et al., 1994; van Eijsden et al., 2004; Wall et al., 2000; Wang et al., 1996; Zhong et al., 1993). However, all of these studies observed changes over long intervals (several hours between measurements) and no study has investigated diffusion changes in the first hours following the onset of SE. It is also not known to what extent changes in volume fraction and/or tortuosity contribute to the observed decrease in ADC_W during SE.

The objective of the present work was to determine the diffusion parameters in the brain cortex of adult rats before and after pilocarpine-induced seizures. The real-time iontophoretic method using tetramethylammonium (TMA^+)-selective microelectrodes (Nicholson and Phillips, 1981; Nicholson and Sykova, 1998) and DW MRI were used to measure the ECS volume fraction, tortuosity and ADC_W 4 h after the administration of pilocarpine. The obtained data were correlated with changes in the energy-related metabolites lactate and glucose, the lactate/pyruvate-ratio and glutamate, monitored by intracerebral microdialysis. This allowed us to analyse the relationship between the dynamic changes in the diffusion properties of the brain cortex and energy metabolism. The extracellular concentration of potassium and extracellular field potentials (EFP) were also recorded.

Materials and methods

Animals

Adult male Wistar rats (300–350 g) were used for experiments. Animals were housed in cages with free access to food and water and maintained at a temperature of 22 °C on a 12:12 h light–dark cycle (lights on at 08:00). The experiments were carried out in accordance with the European Communities Council Directive of 24 November 1986 (86/609/EEC) and approved by the local Institutional Animal Ethics Committee. All efforts were made to minimize animal suffering and to reduce the number of animals used.

Experimental procedure

Animals were anesthetized by an intraperitoneal injection of urethane (1.2 g/kg; Sigma-Aldrich Chemie Gmbh, Steinheim, Germany), intubated and connected to a ventilator (CIV 101, Columbus Instruments, Columbus, Ohio, USA) and ventilated with air. The body temperature was maintained at 36–37 °C by a heating pad. The head of the rat was fixed in a stereotaxic holder. For TMA^+, $[K^+]_e$ and microdialysis measurements, the somatosensory cortex of the rat was partially exposed by a burr hole 2–3 mm caudal from the bregma and 2–3 mm lateral from the midline and the dura mater was removed. The exposed cortex was washed with artificial cerebrospinal fluid at 37 °C. All measurements were recorded in the somatosensory cortex at a depth of 1000–1100 μm. For technical reasons, TMA^+ diffusion, $[K^+]_e$, microdialysis and DW MRI measurements were performed separately using four groups of animals. To potentiate the subsequent action of pilocarpine (Ormandy et al., 1991), lithium chloride (127 mg/kg, i.p.; Sigma-Aldrich) was given to the animals 14–18 h before each pilocarpine experiment. Methylscopolamine bromide (Sigma-Aldrich), an anticholinergic agent that does not cross the blood–brain barrier, was dissolved in normal saline at 1 mg/ml, and 1 mg/kg was given subcutaneously 20 min before the pilocarpine injection to block its peripheral activity. Pilocarpine hydrochloride (Sigma-Aldrich) was dissolved in normal saline at 100 mg/ml, and one dose of 300 mg/kg was administered i.p. — a dose sufficient to produce, in combination with lithium chloride pre-treatment, SE in urethane anaesthetized animals (Stringer and Sowell, 1994).

Local field potential recording

Local field potentials (FP) were recorded in all animals used for TMA^+ diffusion, extracellular K^+ and microdialysis measurements. For technical reasons, it was not possible to record neuronal activity in animals used for DW MRI measurements. Local FP were recorded on the reference barrel of a TMA^+- or K^+-sensitive microelectrode or a glass microelectrode filled with NaCl in the case of microdialysis experiments. The signal was amplified 10-fold and simultaneously displayed on a digital oscilloscope and transferred into PC using a Lab-Trax acquisition system (World Precision Instruments, Inc., Sarasota, USA).

In vivo measurement of extracellular space diffusion parameters

The ECS diffusion parameters were studied by the real-time iontophoretic method described in detail previously (Nicholson and Phillips, 1981; Sykova et al., 1994). Briefly, an extracellular marker that is restricted to the extracellular compartment, such as tetramethylammonium ions (TMA^+, MW = 74.1 Da) to which cell membranes are relatively impermeable, is released into the extracellular space by iontophoresis and its local concentration measured with a TMA^+-selective microelectrode (TMA^+-ISM) located about 100–200 μm from the release site. The concentration of TMA^+ in the ECS is inversely proportional to the ECS volume. Double-barreled TMA^+-ISMs were prepared by a procedure described in detail previously (Vorisek and Sykova, 1997). The tip of the ion-sensitive barrel was filled with a liquid ion exchanger (Corning 477317); the rest of the barrel was backfilled with 150 mM TMA^+ chloride. The reference barrel contained 150 mM NaCl. The shank of the iontophoretic pipette was bent so that it could be aligned parallel to that of the

ion-selective microelectrode and was backfilled with 150 mM TMA^+ chloride. An electrode array was made by gluing a TMA^+-ISM to an iontophoretic micropipette with a tip separation of 100–200 μm. The iontophoresis parameters were +20 nA bias current (continuously applied current to maintain a constant electrode transport number) and a +180 nA current step of 24 s duration to generate the diffusion curve. The TMA^+ diffusion curves were generated at regular intervals of 10 min. Before tissue measurements, diffusion curves were first recorded in 0.3% agar (Sigma-Aldrich) dissolved in a solution containing 150 mM NaCl, 3 mM KCl, and 1 mM TMACl. The diffusion curves were analysed to obtain the electrode transport number (n) and the free TMA^+ diffusion coefficient (D) by curve-fitting according to a modified diffusion equation using the VOLTORO program (Nicholson and Phillips, 1981). Knowing n and D, the values of α, λ and k' can be obtained from the diffusion curves. The volume fraction α is the ratio of the volume of the ECS to total tissue volume in a representative elementary volume of brain tissue (α=ECS/total tissue volume). Tortuosity λ is defined as $\lambda^2 = D/ADC$, where D is the free diffusion coefficient and ADC is the apparent diffusion coefficient in the brain tissue, reflecting the increased path length of a diffusing molecule in a complex medium due to cellular membranes, glycoproteins, macromolecules and fixed charges. Finally, non-specific uptake k' describes the loss of substances across cell membranes (Nicholson, 1992; Nicholson and Phillips, 1981).

In vivo measurements of extracellular K^+ concentration

The extracellular K^+ concentration was measured by means of double-barreled K^+-sensitive microelectrodes (K^+-ISMs) as described elsewhere (Sykova et al., 1994). The liquid ion-exchanger sensitive to K^+ was Corning 477317. The K^+-sensitive barrel of the microelectrode was back filled with 0.5 M KCl, while the reference barrel contained 150 mM NaCl. Electrodes were calibrated using the fixed-interference method (Nicholson and Tao, 1993) in a sequence of solutions containing 2, 4, 8, 16, 32 and 64 mM KCl, with a background of either 151, 149, 145, 137, 121 or 89 mM NaCl to keep the ionic strength of the solutions constant. Calibration data were fitted to the Nikolsky equation to determine electrode slope and interference.

Diffusion-weighted magnetic resonance imaging

Diffusion-weighted imaging measurements were performed using an experimental MR spectrometer BIOSPEC 4.7 T system (Bruker, Ettlingen, Germany) equipped with a 200 mT/m gradient system (190 μs rise time) and a homemade head surface coil. We acquired nine T_2-weighted sagittal images in order to position coronal slices. Two DW images per slice were acquired using the following parameters: Δ=30 ms, b-factors=75 and 1732 s/mm^2, TE=46 ms, TR=1200 ms, field of view 3.2×3.2 cm^2, matrix size=256×128, four 1.0 mm thick coronal slices, interslice distance=1.5 mm. DW images were measured using the stimulated echo sequence. In DW measurements, the diffusion gradient direction pointed along the rostrocaudal direction. The b-factor denotes the strength of diffusion weighting. The higher the b-factor, the stronger the diffusion weighting and the darker the images are in areas with fast water diffusion. Four pairs of diffusion-weighted measurements (a series of slices acquired with both low and high diffusion weighting) were performed before the pilocarpine injection. Thereafter, one pair of measurements was done at 11-min intervals for the next 4 h.

Maps of the apparent diffusion coefficients were calculated from 2 DW images, which corresponded to 2 different b-factors, by fitting the decay signal intensities to Eq. (1) (Le Bihan and Basser, 1995). The signal intensity S decays with increasing diffusion weighting (b-factor).

$$S(b) = S_0 \cdot \exp(-b \cdot ADC_W) \quad (1)$$

ADC_W was assumed to be zero in pixels where the acquired data did not fit well to theoretical dependence (correlation coefficient was less than 0.2). These zero-values were ignored for statistical evaluation if they occurred in the region of interest. ADC_W maps (see Fig. 3) were calculated using custom-made software (V. Herynek, IKEM, Prague, Czech Rep.) by a linear least squares algorithm. The results were analyzed using ImageJ software (W. Rasband, NIH, Bethesda, USA). The evaluated regions of interest were positioned using a rat brain atlas (Paxinos and Watson, 1998) and T_2-weighted images in both the left and right hemispheres. The minimal area of an individual region was 1.5 mm^2. We evaluated coronal slices positioned −3.2 mm caudal to bregma in each animal. The resulting ADC_W maps were evaluated in the primary somatosensory cortical region, the area corresponding to the site of the TMA measurements.

The reproducibility of ADC_W measurements was verified by means of six diffusion phantoms placed on the top of the rats' heads. The phantoms were made from glass tubes (inner diameter=2.3 mm, glass type: KS80, Rückl Glass, Otvovice, Czech Republic) filled with pure (99%) substances having different diffusion coefficients. The substances were: 1-octanol, n-tridecane (Sigma-Aldrich), isoamyl alcohol, isopropyl alcohol, n-butanol and *tert*-butanol (Penta, Prague, Czech Republic). The temperature of the phantoms was maintained at a constant 37 °C.

Microdialysis

The technique of microdialysis is based on sampling fluid via a double-lumen probe with an integrated semipermeable membrane in which the equilibration of substances in the extracellular space and perfusion fluid takes place by diffusion according to the concentration gradient. We used a double-lumen microdialysis probe with a membrane length of 2 mm, an outer diameter of 0.5 mm and a cut-off at 20 kDa (CMA 12, 2 mm membrane length, CMA Microdialysis, Sweden). The inserted microdialysis catheter was connected by low-volume Fluorinated Ethylene Propylene (FEP)-tubing (1.2 μl/10 cm) to a precision infusion pump (CMA 102, CMA Microdialysis, Sweden) in order to maintain a constant dialysate flow. The microdialysis catheter was continuously perfused with a dialysate containing

147 mmol/l NaCl, 2.7 mmol/l KCl, 1.2 mmol/l $CaCl_2$ and 0.85 mmol/l $MgCl_2$ (Perfusion fluid CNS, CMA Microdialysis, Sweden) at a flow rate of 2 µl/min. After a stabilization period of 60 min following insertion into the brain, microdialysate samples were collected over 10-min intervals and immediately frozen at −40 °C until analysed. Thawed and centrifuged dialysate samples were analysed enzymatically with a CMA 600 Microdialysis Analyser (CMA/Microdialysis, Sweden) for lactate, pyruvate, glucose and glutamate concentrations.

The exchange of substances across the microdialysis membrane is limited by the total area of the membrane, the perfusion flow rate, the characteristics of the diffusing substance and the diffusion constant in the tissue surrounding the probe (Ungerstedt, 1991). The recovery rate expresses the

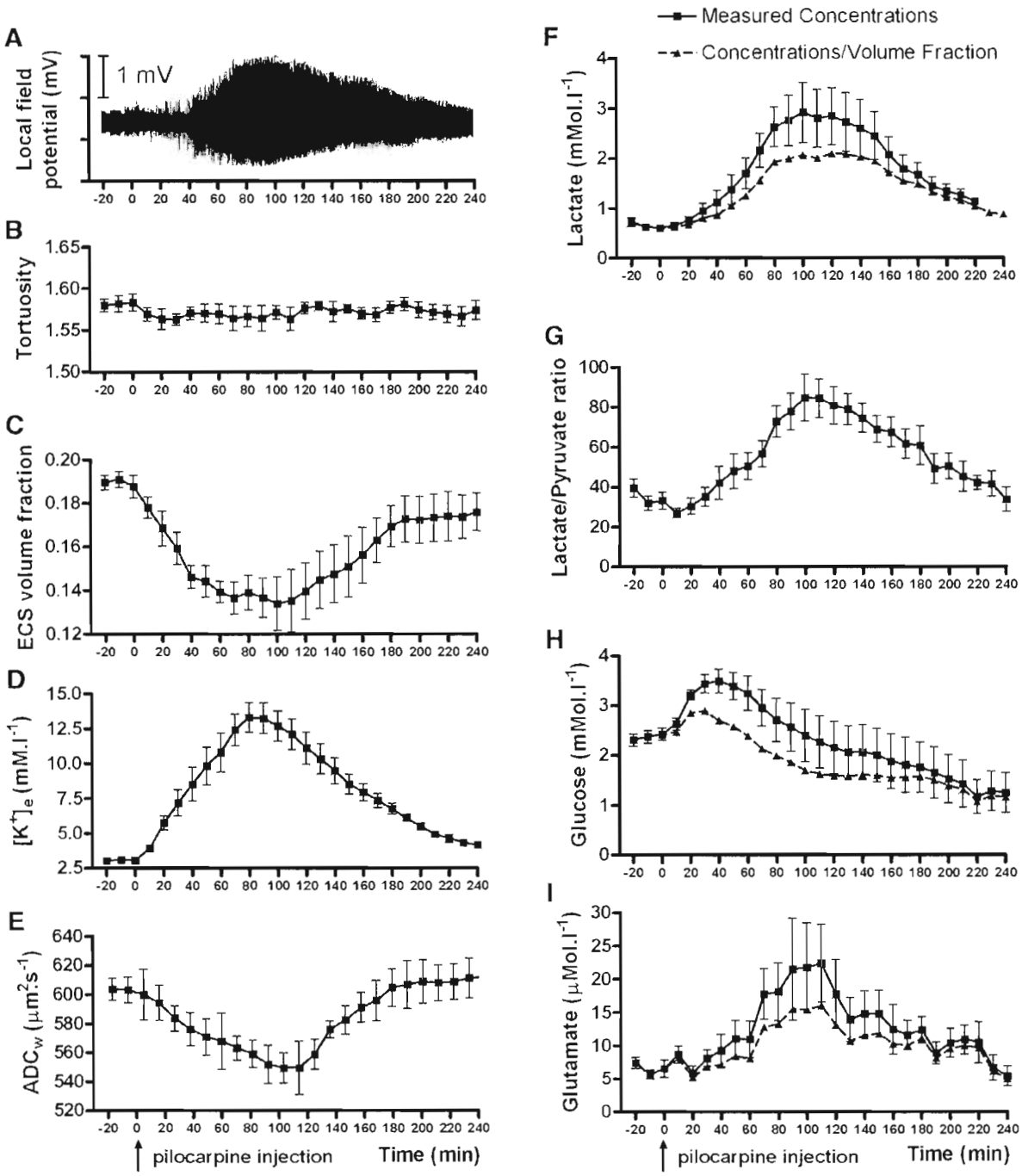

Fig. 1. The time course of local field potentials (A), tortuosity λ (B), extracellular space volume fraction α (C), extracellular potassium concentration $[K^+]_e$ (D), apparent diffusion coefficient of water (E), extracellular lactate concentration (F), lactate/pyruvate ratio (G) and the concentrations of extracellular glucose (H) and glutamate (I). The time courses of the concentrations of the evaluated metabolites corrected for changes in ECS volume are presented as dashed lines, and they show how much of the concentration change is due to the ECS volume change.

relation between the concentration of the substance in the microdialysis probe effluent and the concentration in the medium (Muller, 2002). Before and at the end of the experiments, the recovery rates for each probe were determined by continuing the perfusion at the same settings in a calibration solution containing known concentrations of the different analytes. The calibration solution contained 2.50 mmol/l lactate, 250 μmol/l pyruvate, 5.55 mmol/l glucose, 250 mmol/l glycerol and 25 μmol/l glutamate (Calibrator, CMA Microdialysis, Sweden). The concentrations in the calibration solution were compared with the concentrations of the in vitro microdialysis samples to determine the relative recovery for each substance. The measured experimental values were weighted by the relative recovery to estimate the in vivo extracellular concentration of the substances in the immediate vicinity of the probes. In vitro recovery rates were 19.2±0.69% for lactate, 20.4±0.48% for pyruvate, 9.5±0.30% for glutamate and 10.1±0.31% for glucose (mean±S.E.M., $n=8$). All results are presented as weighted concentrations.

The concentration of a metabolite in the extracellular fluid is clearly affected by changes in the extracellular space volume fraction. A decrease in α would, in the absence of any changes in metabolite supply or utilization, result in an increase in the measured metabolite concentration. Similarly, an increase in α would cause the measured metabolite concentration to decrease. To take into account the effects of changes in α, we have expressed our results as both the actual measured metabolite concentrations and also as the concentrations corrected for changes in α relative to its baseline values.

Statistical analysis

Data obtained from recordings during the period prior to pilocarpine injection were used as control data. After the injection of pilocarpine, data were recorded over 10-min intervals for 4 h. The results of the experiments are expressed as the mean± standard error of the mean (S.E.M.). Differences between different time intervals were evaluated using ANOVA for repeated measures test and Dunnett's post hoc test. Values of $p<0.05$ were considered significant.

Results

Extracellular field potentials

The amplitude of extracellular field potentials was 0.3–0.4 mV. Several minutes after the injection of pilocarpine, the amplitude decreased to 0.2–0.25 mV. The ictal activity in the neocortex began 25–40 min following the pilocarpine injection (average latency 30 min). The amplitude of the ictal discharges increased and reached a maximum of 2.0–2.5 mV about 80–100 min after the application of pilocarpine. The amplitude then started to diminish, but epileptiformic manifestations lasted up to the end of the experimental period. A typical record of one experiment is shown in Fig. 1A. Fig. 2 shows an example of local field potential records before and 60, 120, 180 and 240 min after the injection of pilocarpine. Pilocarpine injection led to bursts of spike-wave activity (Fig. 2B), as well as episodes of high-frequency activity (Fig. 2C). No behavioural manifestations of seizures were observed during anaesthesia.

Extracellular space diffusion parameters

The mean values of extracellular volume fraction α and tortuosity λ before the application of pilocarpine were 0.19± 0.004 and 1.58±0.01 ($n=7$, mean±S.E.M.). Following pilocarpine application, there were no significant changes in tortuosity (Fig. 1B). The volume fraction started to decrease several minutes after the application of pilocarpine, reaching a minimum (0.13±0.01) 80–100 min later. At 120 min, α started to increase and reached 0.18±0.01 240 min after the application of pilocarpine (Fig. 1C).

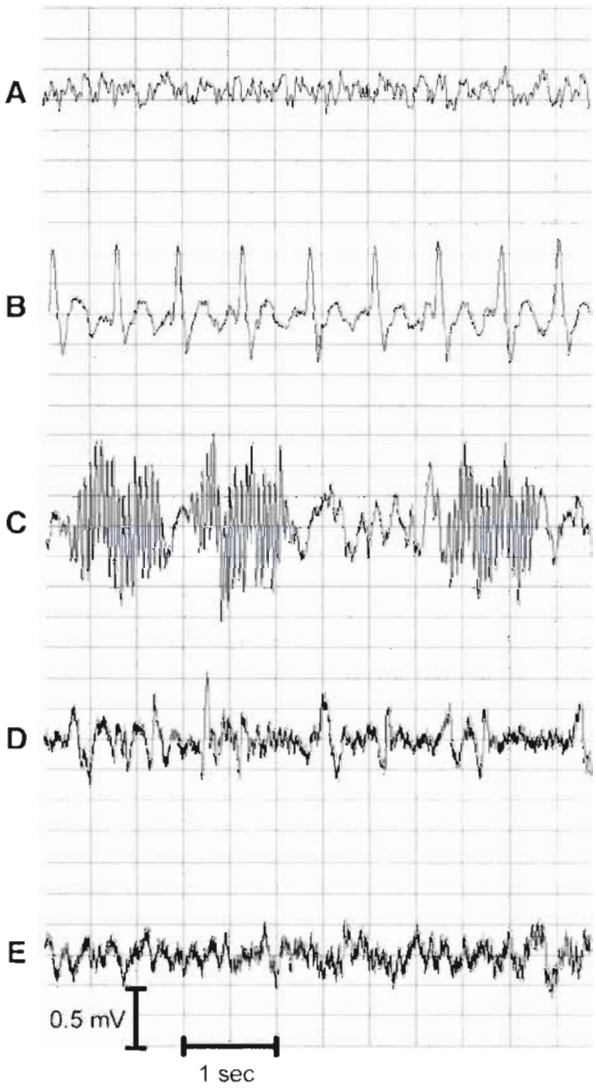

Fig. 2. Local field potential recordings of a urethane anesthetized pilocarpine-injected rat. (A) Irregular baseline local field potential before pilocarpine injection. (B) Spike-wave complexes 60 min after pilocarpine injection. (C) Intervals of high-frequency activity 120 min after pilocarpine injection. (D, E) Local field potential records 180 and 240 min after pilocarpine injection.

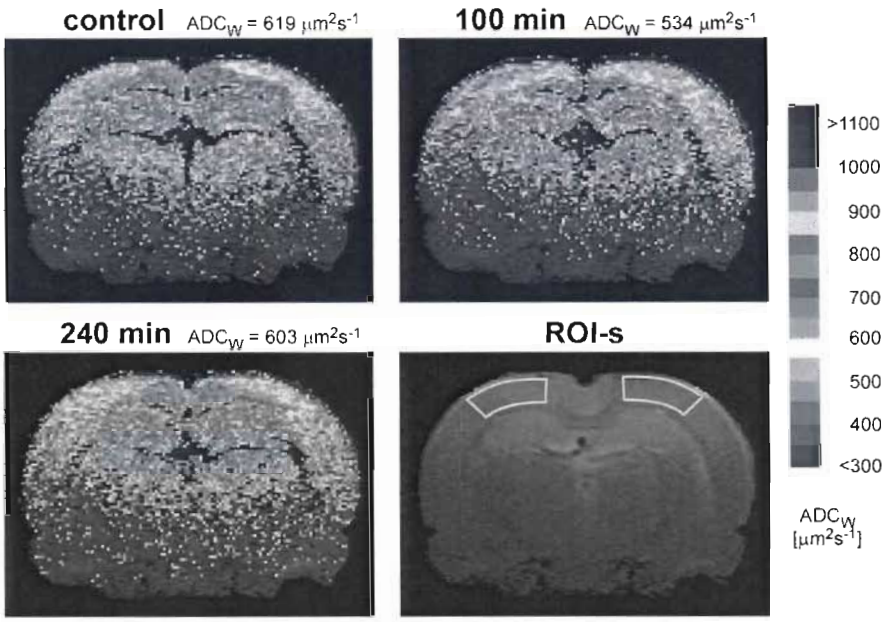

Fig. 3. Typical ADC_W maps in rat before and after pilocarpine injection in primary somatosensory cortex. The areas are outlined in T_2-weighted image (bottom-right panel). The image shows ADC_W maps taken from the identical coronal plane of the same animal. The scale at the right side of the figure shows the relation between the intervals of ADC_W values and the colors used for visualization. Note the significantly decreased ADC_W in the cerebral cortex 100 min after pilocarpine injection. ADC_W returned to the control values after 4 h.

Measurements of extracellular K^+ concentration

Extracellular potassium concentration $[K^+]_e$ in the brain somatosensory cortex at the beginning of the experiments was 3.07±0.02 mM (n=7, mean±S.E.M.). Following pilocarpine application, $[K^+]_e$ started to increase after several minutes, reaching a maximal concentration of 13.3±1.04 mM 80 min later. Subsequently, $[K^+]_e$ returned to normal values, and at the end of the experiment $[K^+]_e$ was 4.17±0.21 mM (Fig. 1D).

Measurements of apparent diffusion coefficient of water

The mean value of ADC_W before the application of pilocarpine was 603.2±8.6 μm^2 s^{-1} (n=6, mean±S.E.M.). Following pilocarpine application, ADC_W started to decrease, reaching a minimum 549.5±10.5 μm^2 s^{-1} 100 min later. At 120 min, ADC_W started to increase and reached 612.7± 14.7 μm^2 s^{-1} 240 min after the application of pilocarpine (Figs. 1E and 3).

Microdialysis

After a stabilization period of 60 min following probe insertion, the basal cortical level of lactate and the lactate/pyruvate ratio remained stable at 0.61±0.05 mmol/l and 33.16± 4.26, respectively (n=8). The application of pilocarpine led to a rise in lactate dialysate levels, reaching a plateau of 2.92± 0.60 mmol/l within 100 min (Fig. 1F). The lactate/pyruvate ratio showed a similar time course, reaching a plateau of 84.80±11.72 (Fig. 1G). Subsequently, lactate levels and the lactate/pyruvate ratio decreased, reaching control values at the end of experiment. Taking into account the effect of the decrease in ECS volume fraction, the calculated extracellular concentrations of lactate during hypoxia/ischemia would be as much as 30% lower than those actually measured (Fig. 1F).

Basal glucose and glutamate levels were 2.42±0.13 mmol/ l and 6.55±1.31 μmol/l, respectively (n=8). Following pilocarpine application, glucose dialysate concentrations increased, reaching a maximum of 3.49±0.24 mmol/l 40 min later. Thereafter, glucose concentrations decreased, reaching a value of 1.25±0.40 mmol/l at the end of the experiment. The glucose concentrations during hypoxia/ischemia would be even lower if we take into account the accompanying decrease in ECS volume fraction (Fig. 1H). Extracellular glutamate levels started to increase 40 min after the application of pilocarpine and reached maximum values of 22.39±5.85 μmol/l. Subsequently, the extracellular glutamate levels decreased, reaching control values at the end of the experiment. The concentrations of glutamate corrected for the increase in α would be therefore lower than the acquired concentrations (Fig. 1I).

Discussion

The initiation and early expression of the seizures induced by pilocarpine are a cholinergic phenomenon; anticholinergics readily terminate seizures at this stage and no neuropathology is evident. Following the toxicity induced by an initial cholinergic phase, a distinct noncholinergic phase occurs, in which excessive glutamate release induces SE in this epilepsy model (McDonough and Shih, 1997).

To induce SE in urethane anesthetized animals, we used a high dose of pilocarpine in combination with lithium chloride

pre-treatment (Stringer and Sowell, 1994). Although it is difficult to induce status epilepticus under anaesthesia, records of local field potentials showed epileptiform neuronal activity, and the levels of K^+ reached were (Stringer and Lothman, 1996) comparable to values measured during status epilepticus. We believe that our model, with some limitation due to the use of anaesthesia, is comparable with SE in awake animals.

The first report of the use of DW MRI in epilepsy is from Zhong et al. (1993), who documented early ADC_W decrease in a model of bicuculline-induced SE in rats. By using the experimental model of kainic acid-induced SE in rats, it has been shown that postictal ADC_W was decreased in the piriform cortex, hippocampus, and amygdala within 24 h with subsequent normalization (Righini et al., 1994; Wang et al., 1996). Using pilocarpine-induced seizures, van Eijsden et al. (2004) and Wall et al. (2000) observed an ADC_W decrease in the amygdala and the piriform cortex within the first hours after pilocarpine application in rats. Also, a recent study by Fabene et al. (2006) showed a decrease of ADC_W throughout the brain 2 h after a 4-aminopyridine injection in rats. Our DW MRI results are in agreement with previous works and show, as we know, for the first time in detail the entire time course of the start, maximal decrease and renormalization of ADC_W in somatosensory cortex during SE.

Acute experimental convulsions increase $[K^+]_e$ and the extracellular concentrations of various transmitter substances due to prolonged neuronal depolarization (Macias et al., 2001). With SE, the metabolism is markedly increased, resulting in the depletion of adenosine triphosphate and energy reserves at its later stage. Consequently, this results in impaired ion exchange pump functions and increased membrane ion permeability of the cells, resulting in an increase in $[K^+]_e$ and the accumulation of intracellular Ca^{2+} (Wasterlain et al., 1993). The increase in $[K^+]_e$ is followed by cell swelling. The swelling, which never occurs before a rise in K^+ and changes in pH, then results in a shrinkage of the ECS (Sykova et al., 1994, 1999). The dependence of changes in α caused by cellular swelling on changes in $[K^+]_e$ is also demonstrated in our results, and a normalization of elevated $[K^+]_e$ leads to a quick normalization of α to control values. The increase of $[K^+]_e$ and the decrease of α start in the first minutes after the pilocarpine injection as a consequence of increased neuronal activity after cholinergic activation (McDonough and Shih, 1997). The onset of the first ictal discharges comes later, about 30 min after pilocarpine injection. A more pronounced increase in the discharge amplitude follows 40–50 min after pilocarpine application, when the ECS volume is about 30% smaller than its initial value, showing the possible contribution of ECS volume reduction to the initiation of SE (Kilb et al., 2006).

The results of our extracellular diffusion parameter measurements represent, according to our best knowledge, the first time the absolute values of the cortical diffusion parameters have been determined in vivo during SE. In our previous studies we demonstrated (Sykova et al., 2005) that changes in extracellular volume fraction correlate with changes in ADC_W, as we confirmed also in this study. The changes seen in diffusion-weighted images in cases of epilepsy are similar to those observed in early cerebral ischemia (Helpern and Huang, 1995). Our results show that the decrease in ADC_w during SE is caused by a decrease in the volume fraction, without changes in tortuosity, in contrast to findings during ischemia, where a decrease in ADC_w is caused by both a decrease in volume fraction and an increase in tortuosity (van der Toorn et al., 1996). Possible explanations for this difference are the slower time course of changes in α and the fact that the decrease in α during SE is only moderate (about 30%) in comparison with the 65–70% reduction in α seen in experimental models of ischemia (Homola et al., 2006; van der Toorn et al., 1996; Vorisek and Sykova, 1997). It has been shown that a significant increase in tortuosity occurs during the experimental application of K^+ or glutamate agonists only if the concentration of K^+ exceeds 20 mM, which evokes alterations in glial cell morphology, especially in the cell processes, which form diffusion barriers (Sykova et al., 1999; Vargova et al., 2001). However, $[K^+]_e$ during SE reached only about 13 mM, which might not be sufficient to evoke an increase in diffusion barriers formed by glial processes and thus to an increase in tortuosity.

To monitor changes in cerebral energy metabolism during SE, we used microdialysis. During the initial stadium of SE, our results show that glucose levels in the extracellular space increase. These results are supported by another microdialysis study of Darbin et al. (2005), who showed an increase in extracellular glucose concentration in the rat striatum after maximal electroshock. The decrease of ECS space volume is possibly a factor contributing to the transient increase of glucose concentration. However, as seizures continue, high cerebral metabolic rates (Fernandes et al., 1999) caused by increased uptake and glycolysis during increased neuronal activity in SE (Fray et al., 1997) could be the cause of the subsequent decrease in glucose concentration starting 1 h after pilocarpine administration and continuing until the end of our experiments.

Increased glycolysis results in the consumption of glucose and the production of lactate, which is transported into the extracellular space. This is supported by our results, in which a decrease in glucose is accompanied by an increase in lactate levels. An increase in lactate levels in selected brain regions during seizures was also seen previously (Darbin et al., 2005; During et al., 1994; Fornai et al., 2000; Kuhr and Korf, 1988a,b). These studies demonstrated that epileptic activity increases the levels of lactic acid in those areas that are recruited during seizure propagation. This is in agreement with our results, which show an increase in lactate concentrations during SE. We also found that with decreasing amplitude of the ictal discharges, elevated lactate levels recovered to initial values. In activated brain areas the increase in energy demands exceeds the glucose supply (Adachi et al., 1995). Under these conditions the increased lactate levels might be utilized by neurons as an alternative energy supply (Schurr et al., 1999, 1997, 1988). This normalization must represent the uptake and utilization of lactate by neurons and astrocytes, because no significant transport of lactate across the blood–brain barrier has been found (Kuhr et al., 1988). The increase of ECS volume in the last 2 h of our experiments is another possible contribution to the normalization of extracellular lactate concentrations during the same time period.

In addition to lactate levels as a marker for anaerobic metabolism, the tissue-specific Lactate/Pyruvate ratio is an excellent indicator of cellular hypoxia, since it is closely correlated with

the redox potential (Kuhr et al., 1988; Zoremba et al., 2007). In this study, we have found an increase in the Lactate/Pyruvate ratio during SE, indicating an increase in anaerobic glycolysis. The extracellular space volume did not affect the changes that were seen in the Lactate/Pyruvate ratio in any way, since the ratio between two extracellular substances that are subject to the same correction coefficient clearly remains unaffected by the value of that coefficient, and the diffusion coefficients of these substances are nearly equal.

Increased glutamatergic transmission is regarded as one of the possible causes of seizure origination (Bradford, 1995). In vivo microdialysis data have shown increases in extracellular glutamate concentrations during epileptic seizures in the hippocampus (Pena and Tapia, 1999; Slezia et al., 2004) and striatum (Kovacs et al., 2003) of 4-aminopyridine-treated rats and in the hippocampus of kainic acid- (Liu et al., 1997) and pilocarpine- (Khan et al., 1999; Smolders et al., 1997) treated rats. Many experiments have supported the view that the extent of glutamate release during epileptic seizures is so great that uptake is not able to re-establish the normal glutamate concentration and the excess of glutamate spreads by diffusion, activating neurons via extra-synaptic receptors (Bradford, 1995). Most of the damage induced by seizure activity is generated by glutamatergic neurotransmission-driven excitotoxicity (Whetsell, 1996). 10–100 μM glutamate is toxic to neurons grown in culture (Choi, 1988), but neurons in vivo are less vulnerable due to the presence of highly effective uptake carriers (Bruhn et al., 1992). Elevation of the extracellular levels of endogenous glutamate per se is not sufficient for the induction of neuronal degradation. Other factors that facilitate the overactivation of excitatory amino-acid receptors, for instance hyperexcitation present during seizures, seem to be necessary to induce neuronal damage. Sustained activation of the NMDA receptor as a result of excess extracellular glutamate would allow the additional entry of Ca^{2+} into the neuron which, in conjunction with the sustained repetitive depolarization of the neurons by the seizure, could allow free Ca^{2+} levels in the neuron to build up to toxic amounts and produce the subsequent neuropathology. The maximum increase in extracellular glutamate levels was observed over the same time interval as the maximum decrease in ECS volume fraction. Thus, we suggest that a substantial amount of this increase in glutamate was caused by the shrinkage of the ECS.

Taken together, our results show changes in the extracellular space diffusion parameters, $[K^+]_e$, energy-related metabolites and glutamate during the initiation and first hours of the propagation of pilocarpine-induced SE. Our results also show that the first minutes after a pilocarpine injection are followed by an increase in $[K^+]_e$ and a decrease in ECS volume, together with an increase in extracellular glucose concentration. Following a delay of 40–50 min, when α starts to reach minimal values, high amplitude epileptic discharges appear. The shrinkage of the ECS could contribute to an increase in extracellular metabolite concentrations, with all its deleterious consequences, leading to the start of epileptic discharges. With the increasing amplitude of local field potentials, the extracellular concentrations of lactate, glutamate and $[K^+]_e$ increase, reaching maximal values 80–100 min after pilocarpine application. At this time glucose concentrations decrease, and the consequent deficit in cell energy reserves is a possible reason for the discharge reduction, resulting in the progressive attenuation of SE and the normalization of all measured parameters.

We have shown that the results of DWI MR measurements are in agreement with the diffusion parameter values determined by the TMA ion-selective microelectrode method. The application of the noninvasive DW MRI technique in human epilepsy research can thus increase our understanding of the pathophysiology of seizure initiation and epileptogenesis.

Acknowledgments

This study was supported by a grant from the Academy of Sciences of the Czech Republic AV0Z50390512, by grants from the Ministry of Education, Youth and Sports of the Czech Republic 1M0538, MSM0021622404 and LC554, and by the EC-FP6-project DiMI (LSHB-CT-2005-512146).

References

Adachi, K., Cruz, N.F., Sokoloff, L., Dienel, G.A., 1995. Labeling of metabolic pools by [6–14C]glucose during K(+)-induced stimulation of glucose utilization in rat brain. J. Cereb. Blood Flow Metab. 15, 97–110.

Agnati, L.F., Zoli, M., Stromberg, I., Fuxe, K., 1995. Intercellular communication in the brain: wiring versus volume transmission. Neuroscience 69, 711–726.

Bradford, H.F., 1995. Glutamate, GABA and epilepsy. Prog. Neurobiol. 47, 477–511.

Bruhn, T., Cobo, M., Berg, M., Diemer, N.H., 1992. Limbic seizure-induced changes in extracellular amino acid levels in the hippocampal formation: a microdialysis study of freely moving rats. Acta Neurol. Scand. 86, 455–461.

Choi, D.W., 1988. Glutamate neurotoxicity and diseases of the nervous system. Neuron 1, 623–634.

Darbin, O., Risso, J.J., Carre, F., Lonjon, M., Naritoku, D.K., 2005. Metabolic changes in rat striatum following convulsive seizures. Brain Res. 1050, 124–129.

During, M.J., Fried, I., Leone, P., Katz, A., Spencer, D.D., 1994. Direct measurement of extracellular lactate in the human hippocampus during spontaneous seizures. J. Neurochem. 62, 2356–2361.

Fabene, P.F., Weiczner, R., Marzola, P., Nicolato, E., Calderan, L., Andrioli, A., Farkas, E., Sule, Z., Mihaly, A., Sbarbati, A., 2006. Structural and functional MRI following 4-aminopyridine-induced seizures: a comparative imaging and anatomical study. Neurobiol. Dis. 21, 80–89.

Fernandes, M.J., Dube, C., Boyet, S., Marescaux, C., Nehlig, A., 1999. Correlation between hypermetabolism and neuronal damage during status epilepticus induced by lithium and pilocarpine in immature and adult rats. J. Cereb. Blood Flow Metab. 19, 195–209.

Fornai, F., Bassi, L., Gesi, M., Giorgi, F.S., Guerrini, R., Bonaccorsi, I., Alessandri, M.G., 2000. Similar increases in extracellular lactic acid in the limbic system during epileptic and/or olfactory stimulation. Neuroscience 97, 447–458.

Fray, A., Boutelle, E., Fillenz, M., 1997. Extracellular glucose turnover in the striatum of unanaesthetized rats measured by quantitative microdialysis. J. Physiol. 504 (Pt 3), 721–726.

Helpern, J.A., Huang, N., 1995. Diffusion-weighted imaging in epilepsy. Magn. Reson. Imaging 13, 1227–1231.

Homola, A., Zoremba, N., Slais, K., Kuhlen, R., Sykova, E., 2006. Changes in diffusion parameters, energy-related metabolites and glutamate in the rat cortex after transient hypoxia/ischemia. Neurosci. Lett. 404 (1–2), 137–142.

Khan, G.M., Smolders, I., Lindekens, H., Manil, J., Ebinger, G., Michotte, Y., 1999. Effects of diazepam on extracellular brain neurotransmitters in pilocarpine-induced seizures in rats. Eur. J. Pharmacol. 373, 153–161.

Kilb, W., Dierkes, P.W., Sykova, E., Vargova, L., Luhmann, H.J., 2006. Hypoosmolar conditions reduce extracellular volume fraction and enhance epileptiform activity in the CA3 region of the immature rat hippocampus. J. Neurosci. Res. 84, 119–129.

Kovacs, A., Mihaly, A., Komaromi, A., Gyengesi, E., Szente, M., Weiczner, R., Kriszuin-Peva, B., Szabo, G., Telegdy, G., 2003. Seizure, neurotransmitter release, and gene expression are closely related in the striatum of 4-aminopyridine-treated rats. Epilepsy Res. 55, 117–129.

Kuhr, W.G., Korf, J., 1988a. Extracellular lactic acid as an indicator of brain metabolism: continuous on-line measurement in conscious, freely moving rats with intrastriatal dialysis. J. Cereb. Blood Flow Metab. 8, 130–137.

Kuhr, W.G., Korf, J., 1988b. *N*-methyl-D-aspartate receptor involvement in lactate production following ischemia or convulsion in rats. Eur. J. Pharmacol. 155, 145–149.

Kuhr, W.G., van den Berg, C.J., Korf, J., 1988. In vivo identification and quantitative evaluation of carrier-mediated transport of lactate at the cellular level in the striatum of conscious, freely moving rats. J. Cereb. Blood Flow Metab. 8, 848–856.

Le Bihan, D., Basser, P.J., 1995. Molecular Diffusion and Nuclear Magnetic Resonance. Raven Press, New York.

Le Bihan, D., Breton, E., Lallemand, D., Grenier, P., Cabanis, E., Laval-Jeantet, M., 1986. MR imaging of intravoxel incoherent motions: application to diffusion and perfusion in neurologic disorders. Radiology 161, 401–407.

Liu, Z., Stafstrom, C.E., Sarkisian, M.R., Yang, Y., Hori, A., Tandon, P., Holmes, G.L., 1997. Seizure-induced glutamate release in mature and immature animals: an in vivo microdialysis study. Neuroreport 8, 2019–2023.

Macias, W., Carlson, R., Rajadhyaksha, A., Barczak, A., Konradi, C., 2001. Potassium chloride depolarization mediates CREB phosphorylation in striatal neurons in an NMDA receptor-dependent manner. Brain Res. 890, 222–232.

McDonough Jr., J.H., Shih, T.M., 1997. Neuropharmacological mechanisms of nerve agent-induced seizure and neuropathology. Neurosci. Biobehav. Rev. 21, 559–579.

Muller, M., 2002. Science, medicine, and the future: microdialysis. BMJ 324, 588–591.

Nicholson, C., 1992. Quantitative analysis of extracellular space using the method of TMA+ iontophoresis and the issue of TMA+ uptake. Can. J. Physiol. Pharm. 70 Suppl, S314–S322.

Nicholson, C., Phillips, J.M., 1981. Ion diffusion modified by tortuosity and volume fraction in the extracellular microenvironment of the rat cerebellum. J. Physiol. 321, 225–257.

Nicholson, C., Sykova, E., 1998. Extracellular space structure revealed by diffusion analysis. Trends Neurosci. 21, 207–215.

Nicholson, C., Tao, L., 1993. Hindered diffusion of high molecular weight compounds in brain extracellular microenvironment measured with integrative optical imaging. Biophys. J. 65, 2277–2290.

Ormandy, G.C., Song, L., Jope, R.S., 1991. Analysis of the convulsant-potentiating effects of lithium in rats. Exp. Neurol. 111, 356–361.

Paxinos, G., Watson, C., 1998. The Rat Brain In Stereotaxic Coordinates. Academic Press, San Diego.

Pena, F., Tapia, R., 1999. Relationships among seizures, extracellular amino acid changes, and neurodegeneration induced by 4-aminopyridine in rat hippocampus: a microdialysis and electroencephalographic study. J. Neurochem. 72, 2006–2014.

Righini, A., Pierpaoli, C., Alger, J.R., Di Chiro, G., 1994. Brain parenchyma apparent diffusion coefficient alterations associated with experimental complex partial status epilepticus. Magn. Reson. Imaging 12, 865–871.

Schurr, A., West, C.A., Rigor, B.M., 1988. Lactate-supported synaptic function in the rat hippocampal slice preparation. Science 240, 1326–1328.

Schurr, A., Payne, R.S., Miller, J.J., Rigor, B.M., 1997. Brain lactate, not glucose, fuels the recovery of synaptic function from hypoxia upon reoxygenation: an in vitro study. Brain Res. 744, 105–111.

Schurr, A., Miller, J.J., Payne, R.S., Rigor, B.M., 1999. An increase in lactate output by brain tissue serves to meet the energy needs of glutamate-activated neurons. J. Neurosci. 19, 34–39.

Slezia, A., Kekesi, A.K., Szikra, T., Papp, A.M., Nagy, K., Szente, M., Magloczky, Z., Freund, T.F., Juhasz, G., 2004. Uridine release during aminopyridine-induced epilepsy. Neurobiol. Dis. 16, 490–499.

Smolders, I., Khan, G.M., Manil, J., Ebinger, G., Michotte, Y., 1997. NMDA receptor-mediated pilocarpine-induced seizures: characterization in freely moving rats by microdialysis. Br. J. Pharmacol. 121, 1171–1179.

Stringer, J.L., Lothman, E.W., 1996. During afterdischarges in the young rat in vivo extracellular potassium is not elevated above adult levels. Brain Res. Dev. Brain Res. 91, 136–139.

Stringer, J.L., Sowell, K.L., 1994. Kainic acid, bicuculline, pentylenetetrazol and pilocarpine elicit maximal dentate activation in the anesthetized rat. Epilepsy Res. 18, 11–21.

Svoboda, J., Sykova, E., 1991. Extracellular space volume changes in the rat spinal cord produced by nerve stimulation and peripheral injury. Brain Res. 560, 216–224.

Sykova, E., 1997. Extracellular space volume and geometry of the rat brain after ischemia and central injury. Adv. Neurol. 73, 121–135.

Sykova, E., 2004. Extrasynaptic volume transmission and diffusion parameters of the extracellular space. Neuroscience 129, 861–876.

Sykova, E., 2005. Glia and volume transmission during physiological and pathological states. J. Neural Transm. 112, 137–147.

Sykova, E., Svoboda, J., Polak, J., Chvatal, A., 1994. Extracellular volume fraction and diffusion characteristics during progressive ischemia and terminal anoxia in the spinal cord of the rat. J. Cereb. Blood Flow Metab. 14, 301–311.

Sykova, E., Vargova, L., Prokopova, S., Simonova, Z., 1999. Glial swelling and astrogliosis produce diffusion barriers in the rat spinal cord. Glia 25, 56–70.

Sykova, E., Mazel, T., Vargova, L., Vorisek, I., Prokopova-Kubinova, S., 2000. Extracellular space diffusion and pathological states. Prog. Brain Res. 125, 155–178.

Sykova, E., Vargova, L., Kubinova, S., Jendelova, P., Chvatal, A., 2003. The relationship between changes in intrinsic optical signals and cell swelling in rat spinal cord slices. Neuroimage 18, 214–230.

Sykova, E., Vorisek, I., Antonova, T., Mazel, T., Meyer-Luehmann, M., Jucker, M., Hajek, M., Ort, M., Bures, J., 2005. Changes in extracellular space size and geometry in APP23 transgenic mice: a model of Alzheimer's disease. Proc. Natl. Acad. Sci. U. S. A. 102, 479–484.

Turski, W.A., Cavalheiro, E.A., Schwarz, M., Czuczwar, S.J., Kleinrok, Z., Turski, L., 1983. Limbic seizures produced by pilocarpine in rats: behavioural, electroencephalographic and neuropathological study. Behav. Brain Res. 9, 315–335.

Ungerstedt, U., 1991. Microdialysis—principles and applications for studies in animals and man. J. Intern. Med. 230, 365–373.

van der Toorn, A., Sykova, E., Dijkhuizen, R.M., Vorisek, I., Vargova, L., Skobisova, E., van Lookeren Campagne, M., Reese, T., Nicolay, K., 1996. Dynamic changes in water ADC, energy metabolism, extracellular space volume, and tortuosity in neonatal rat brain during global ischemia. Magn. Reson. Med. 36, 52–60.

van Eijsden, P., Notenboom, R.G., Wu, O., de Graan, P.N., van Nieuwenhuizen, O., Nicolay, K., Braun, K.P., 2004. In vivo 1H magnetic resonance spectroscopy, T2-weighted and diffusion-weighted MRI during lithium-pilocarpine-induced status epilepticus in the rat. Brain Res. 1030, 11–18.

Vargova, L., Jendelova, P., Chvatal, A., Sykova, E., 2001. Glutamate, NMDA, and AMPA induced changes in extracellular space volume and tortuosity in the rat spinal cord. J. Cereb. Blood Flow Metab. 21, 1077–1089.

Vorisek, I., Sykova, E., 1997. Ischemia-induced changes in the extracellular space diffusion parameters, K+, and pH in the developing rat cortex and corpus callosum. J. Cereb. Blood Flow Metab. 17, 191–203.

Wall, C.J., Kendall, E.J., Obenaus, A., 2000. Rapid alterations in diffusion-weighted images with anatomic correlates in a rodent model of status epilepticus. AJNR Am. J. Neuroradiol. 21, 1841–1852.

Wang, Y., Majors, A., Najm, I., Xue, M., Comair, Y., Modic, M., Ng, T.C., 1996. Postictal alteration of sodium content and apparent diffusion coefficient in epileptic rat brain induced by kainic acid. Epilepsia 37, 1000–1006.

Wasterlain, C.G., Fujikawa, D.G., Penix, L., Sankar, R., 1993. Pathophysiological mechanisms of brain damage from status epilepticus. Epilepsia 34 (Suppl 1), S37–S53.

Whetsell Jr., W.O., 1996. Current concepts of excitotoxicity. J. Neuropathol. Exp. Neurol. 55, 1–13.

Zhong, J., Petroff, O.A., Prichard, J.W., Gore, J.C., 1993. Changes in water diffusion and relaxation properties of rat cerebrum during status epilepticus. Magn. Reson. Med. 30, 241–246.

Zoli, M., Jansson, A., Sykova, E., Agnati, L.F., Fuxe, K., 1999. Volume transmission in the CNS and its relevance for neuropsychopharmacology. Trends Pharmacol. Sci. 20, 142–150.

Zoremba, N., Homola, A., Rossaint, R., Sykova, E., 2007. Brain metabolism and extracellular space diffusion parameters during and after transient global hypoxia in the rat cortex. Exp. Neurol. 203, 34–41.